

**BSE Public Lecture –
Hydrogen Production Using Solar or Nuclear Thermochemical Techniques on 14 January 2010**

Organized by the Department of Building Services Engineering, a CPD lecture delivered by Professor Yitung Chen on *Hydrogen Production Using Solar or Nuclear Thermochemical Techniques* was held on 14 January 2010 (Thursday).

Professor Yitung Chen holds a professorship in the Department of Mechanical Engineering at the University of Nevada Las Vegas (UNLV). He is also a Co-Director of the Centre for Energy Research (CER) at UNLV. Currently, he is the President-elect of the Chinese in America Thermal Engineering Association (CATEA). He has more than 20 years of research and program development experiences in experimental and computational aspects of momentum, heat, and mass transfer.

The current hydrogen industry is not focused on the production or use of hydrogen as an energy carrier or a fuel for energy generation. Rather, more than ten million tons of hydrogen produced each year are used mainly for chemicals, petroleum refining, metals, and electronics.

In the talk, Professor Chen discussed the use of hydrogen as an energy carrier or major fuel which requires development in several industry segments, including production, delivery, storage, conversion and end-use. He explained that each industry segment is integral to building a hydrogen-based economy, and the development of one segment relies on corresponding development of all other segments. Professor Chen also enlightened how hydrogen can be produced using traditional fossil fuels such as natural gas and coal, nuclear, biomass and other renewable energy technologies and pointed out the overall challenge to hydrogen production.

Professor Chen finished the talk with a discussion on barriers to Nuclear Thermochemical Water-Splitting and Research Opportunities.



Talk delivered by Prof. YT Chen



Souviner presented to Prof. YT Chen by Prof. WK Chow

[Powerpoint file of the CPD lecture](#)

Hydrogen Production Using Solar or Nuclear Thermochemical Techniques

Yi-Tung Chen

**Department of Mechanical Engineering
University of Nevada, Las Vegas**

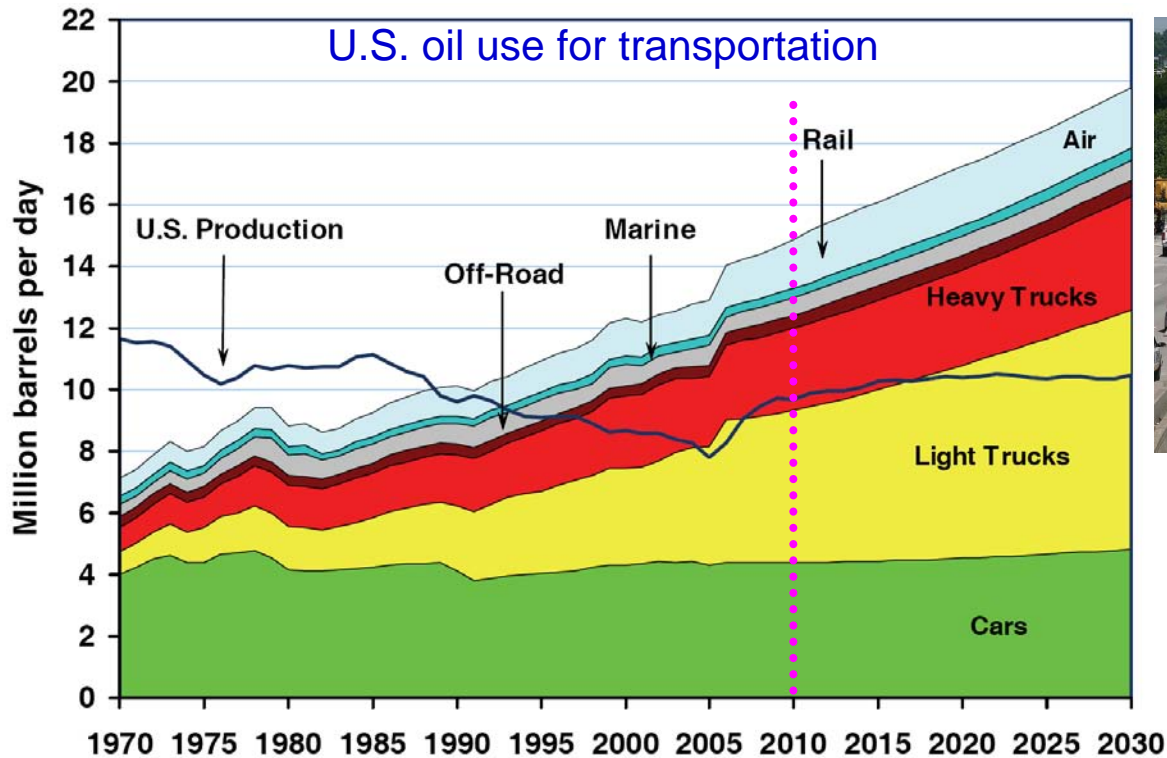
January 14, 2010

The Hong Kong Polytechnic University

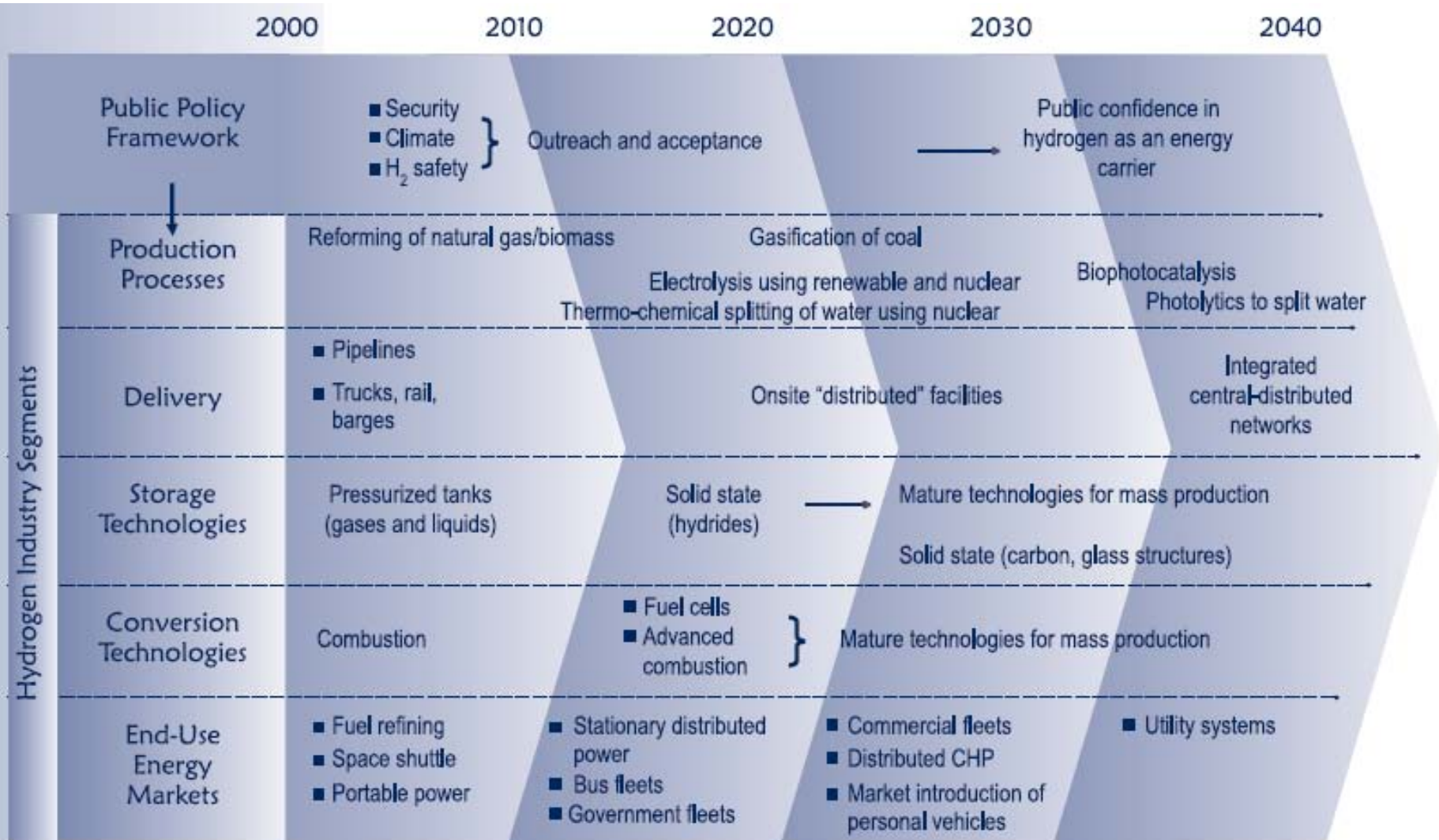
Hydrogen: an International Initiative

Hydrogen - a future solution to world's energy needs

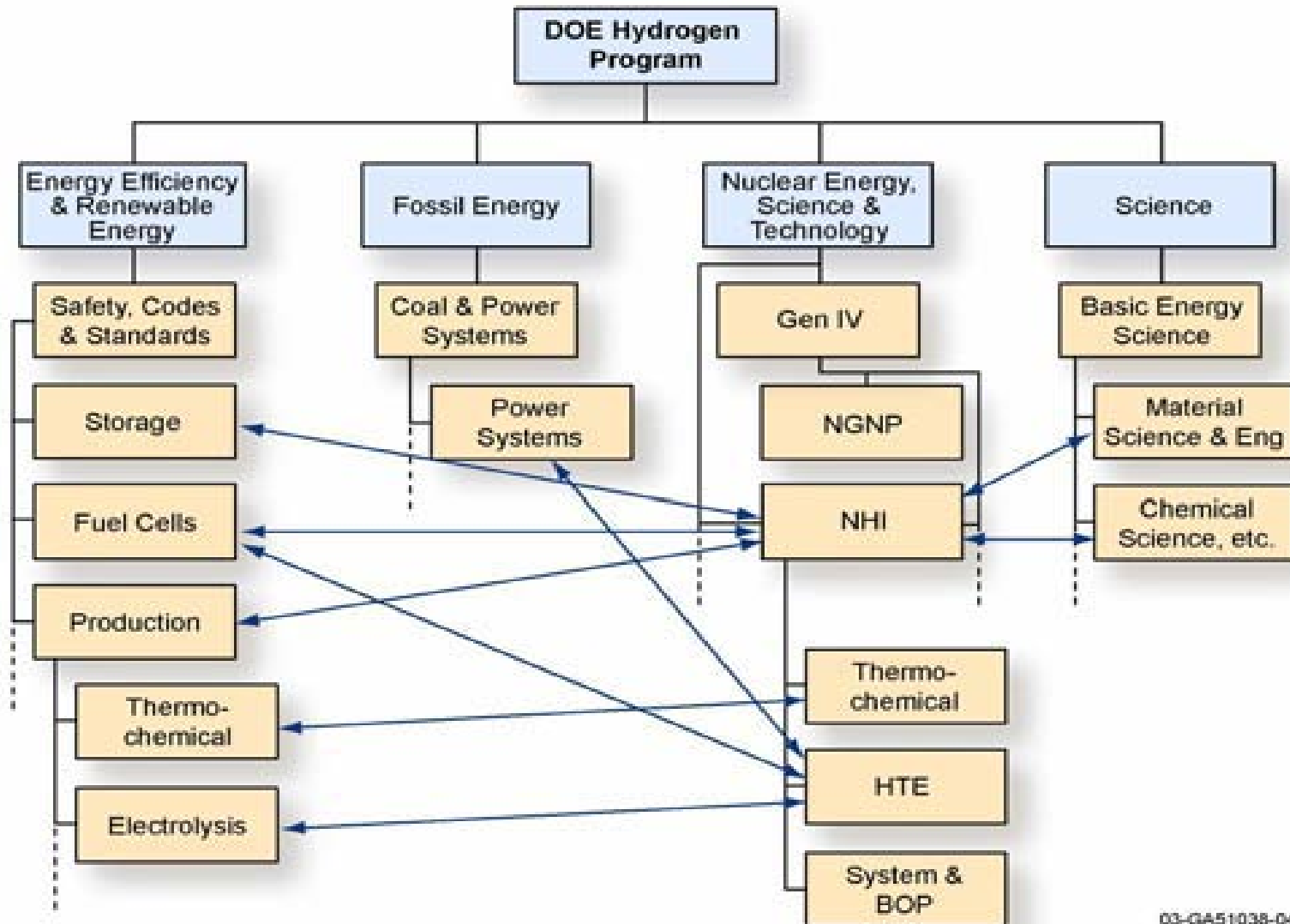
- To reduce dependence on petroleum imports
- To reduce pollution and greenhouse gas emissions



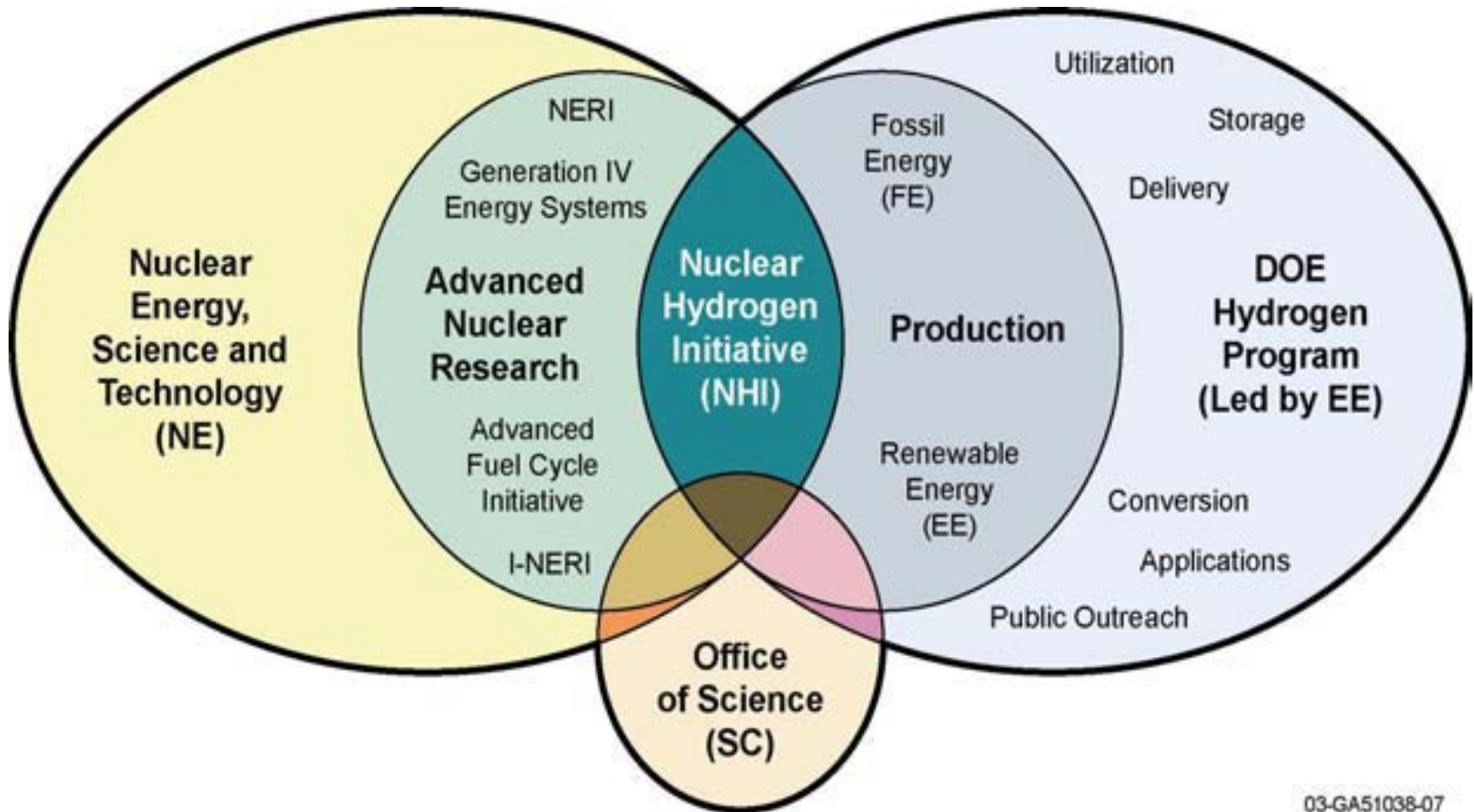
Overview of the Transition to the Hydrogen Economy



U.S. DOE Hydrogen Program Elements/Structure



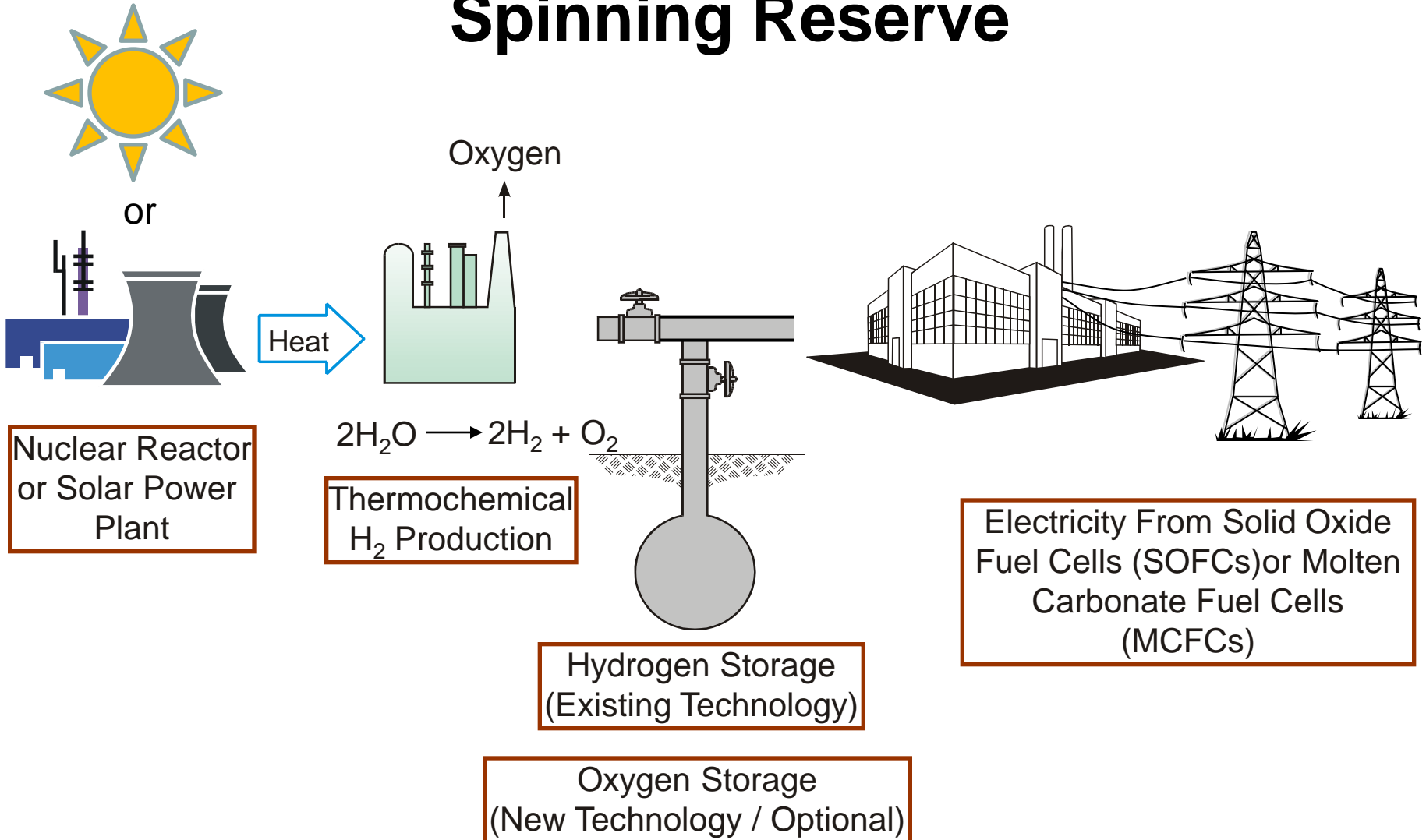
An Integrated DOE Program to Develop Technologies for Nuclear Hydrogen Production



Hydrogen Production Requires Energy

- Hydrogen is an **energy carrier**, not an **energy source**; its production requires energy
- A **Hydrogen Economy** only makes sense if hydrogen is produced with **sustainable, non-fossil, non-greenhouse gas energy**
 - Solar and Nuclear (fission and in the long term fusion)
- Hydrogen can be produced from water using thermal energy
 - **Electric power generation → Electrolysis**
 - Proven technology
 - Overall efficiency ~24% (LWR), ~36% (Hi T Reactors)
(efficiency of electric power generation x efficiency of electrolysis)
 - **Heat → Thermochemical water-splitting**
 - Net plant efficiencies of up to ~50%
 - Developing technology
 - **Electricity + Heat → High temperature electrolysis or Hybrid cycles**

Using Solar or Nuclear Hydrogen To Meet Peak Electric Power Demands and Provide Spinning Reserve



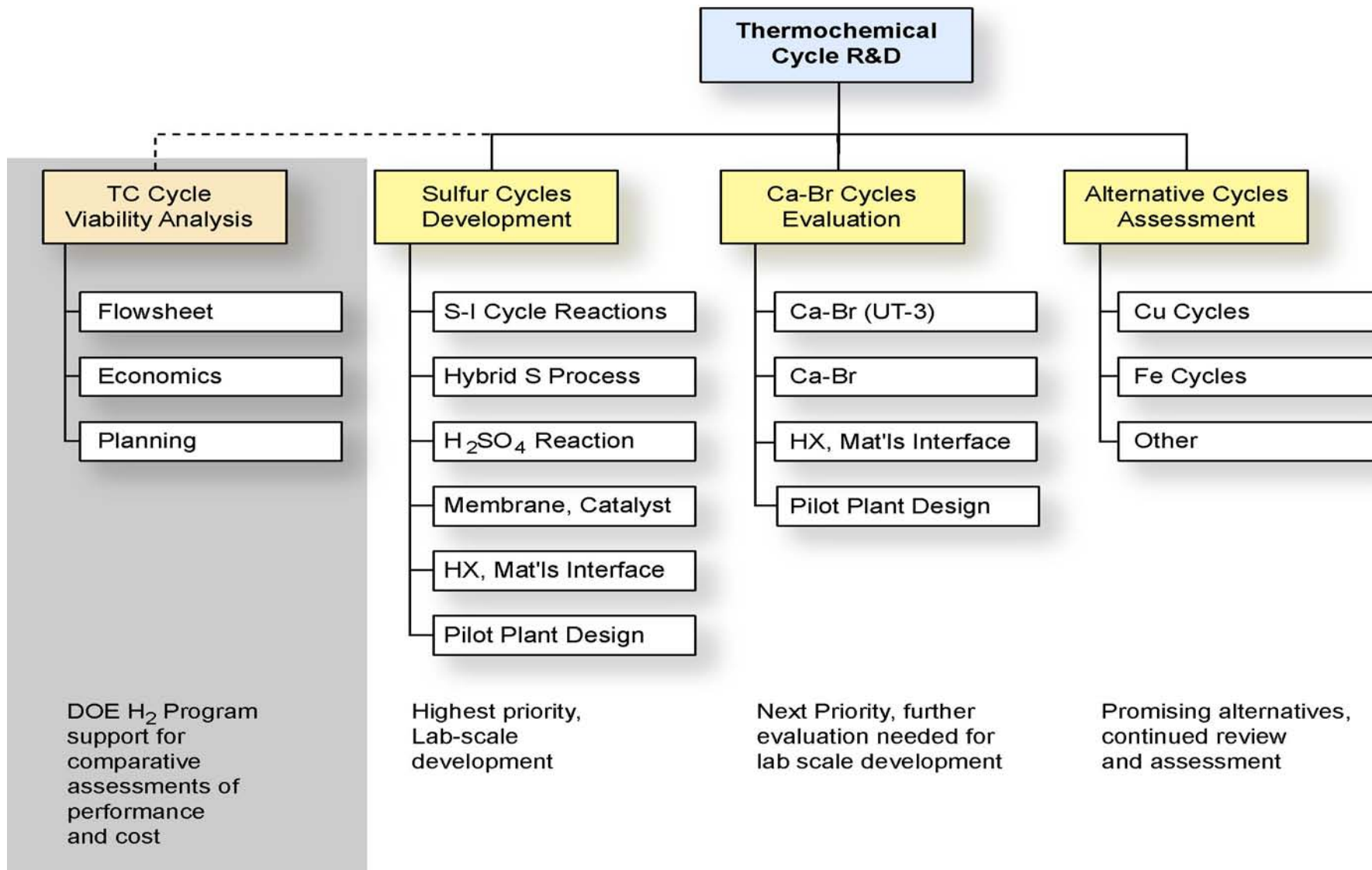
Current Hydrogen Production Processes

- Steam methane reforming (SMR)
- Natural gas reforming
- Coal reforming
- Electrolysis
- High temperature electrolysis (HTE)
- Photoelectrochemical (PEC) processes
- Biological and photobiological processes
- Thermochemical (TC) water-splitting

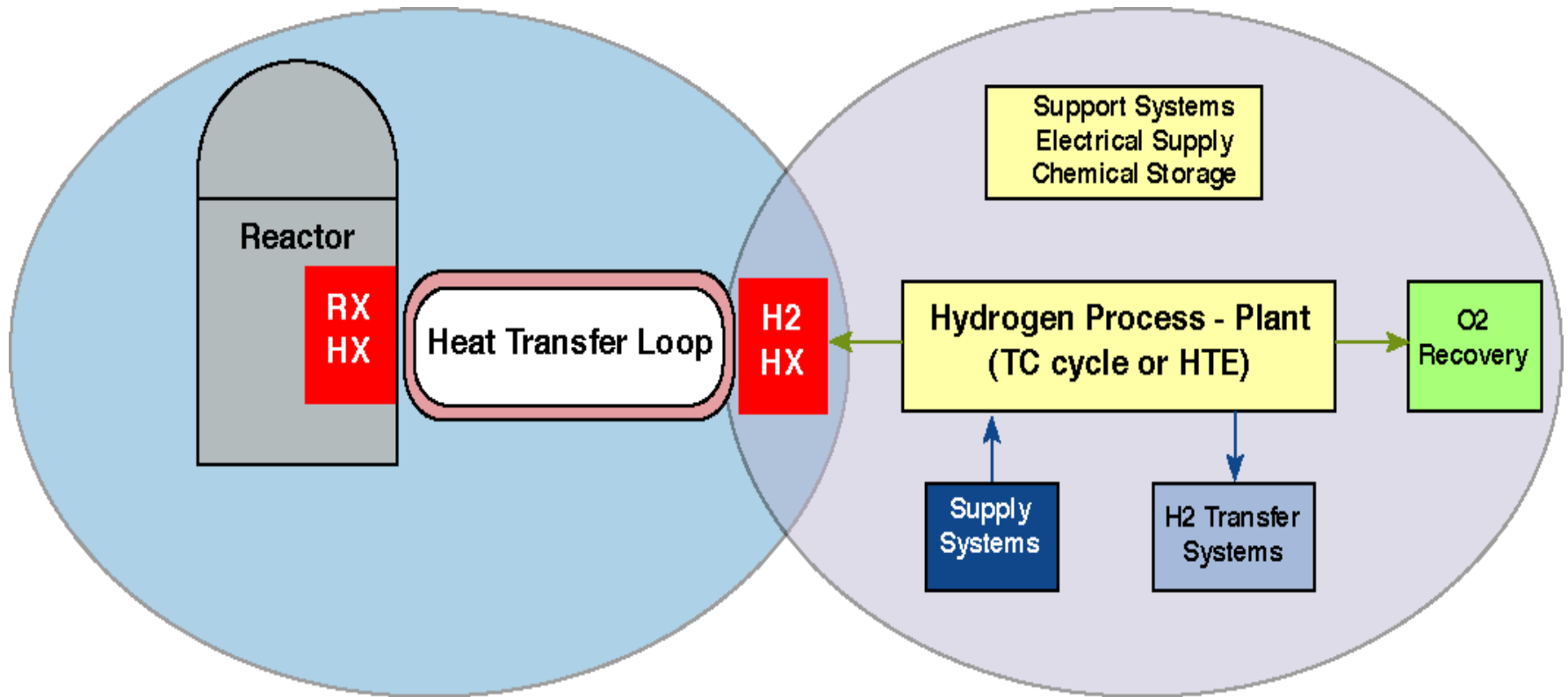
Thermochemical Water-splitting

- A set of coupled, thermally-driven chemical reactions that sum to the decomposition of water into H_2 and O_2
 - All reagents returned within the cycle and recycled
 - Only high temperature heat and water are input, only low temperature heat, H_2 and O_2 are output
- High efficiency is possible – at high temperature
- A developing technology
 - Explored extensively in the 1970s
 - Numerous possible cycles identified and explored
 - Not commercialized yet

Thermochemical Processes



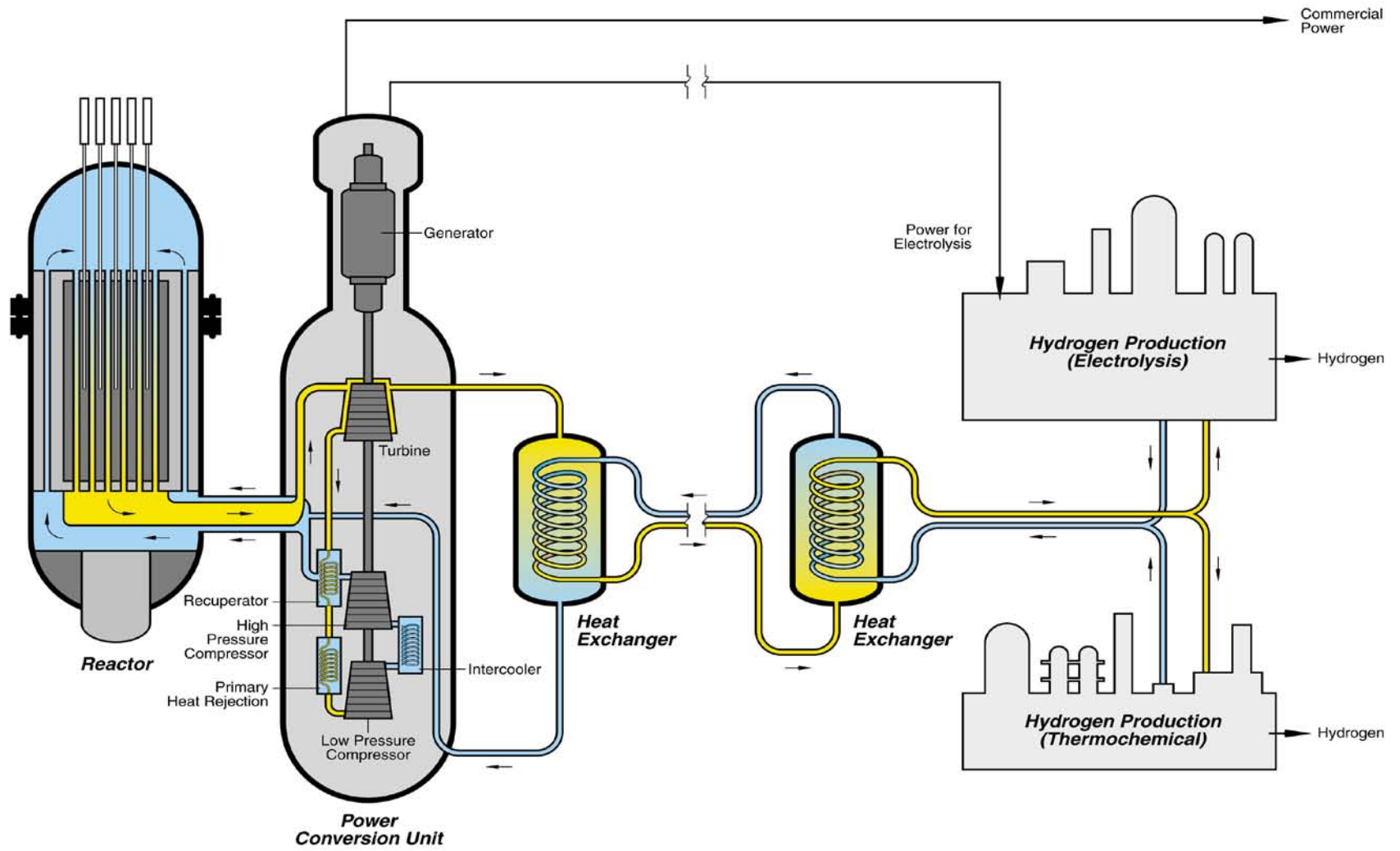
Gen IV Coupled with NHI for Hydrogen Production



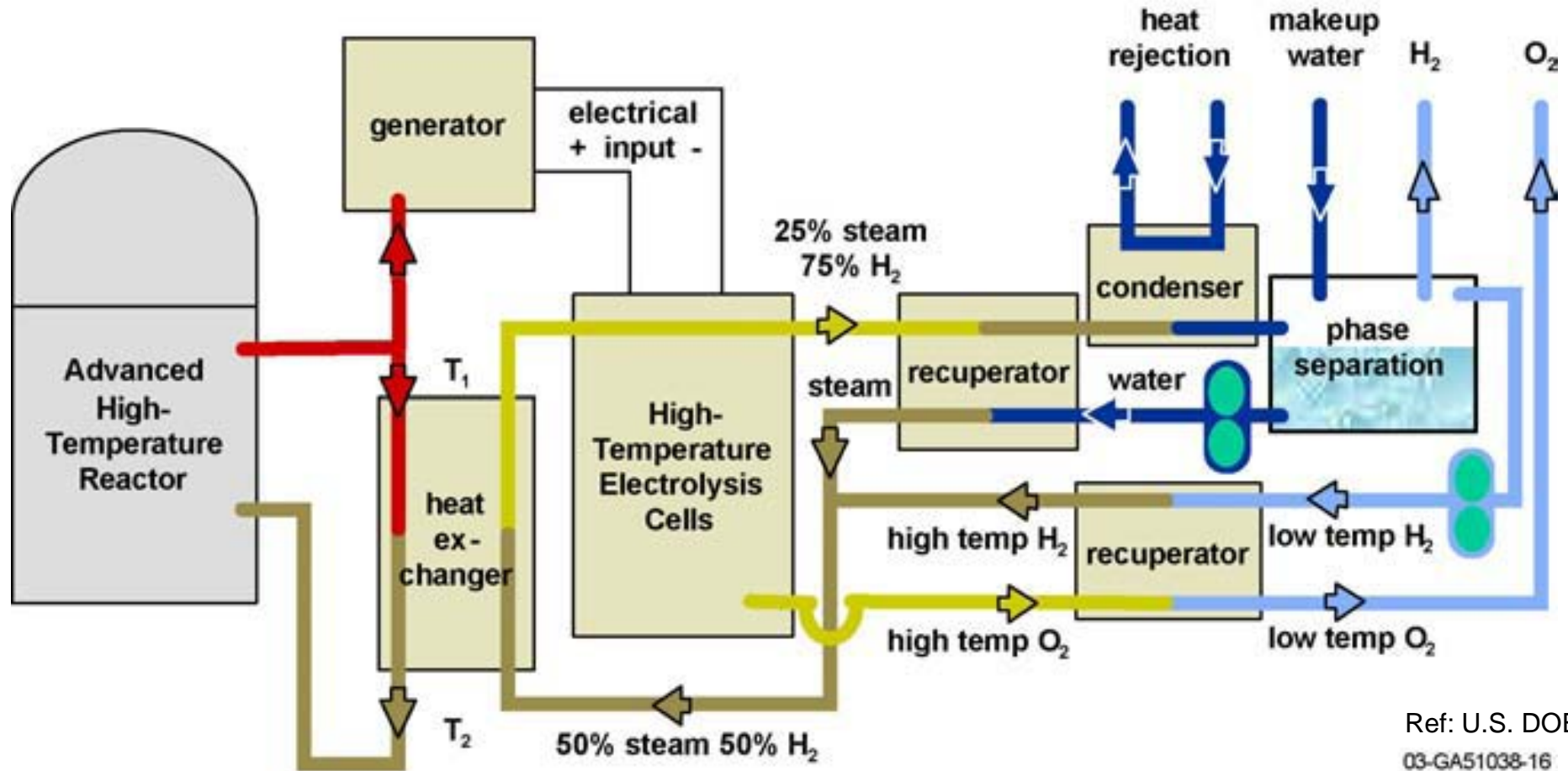
Very High Temperature Reactor
(Gen IV)

Hydrogen Plant Systems
(NHI)

Gen IV Nuclear Power Plant Concept



Major Components of a Conceptual Nuclear High-temperature Electrolysis Plant

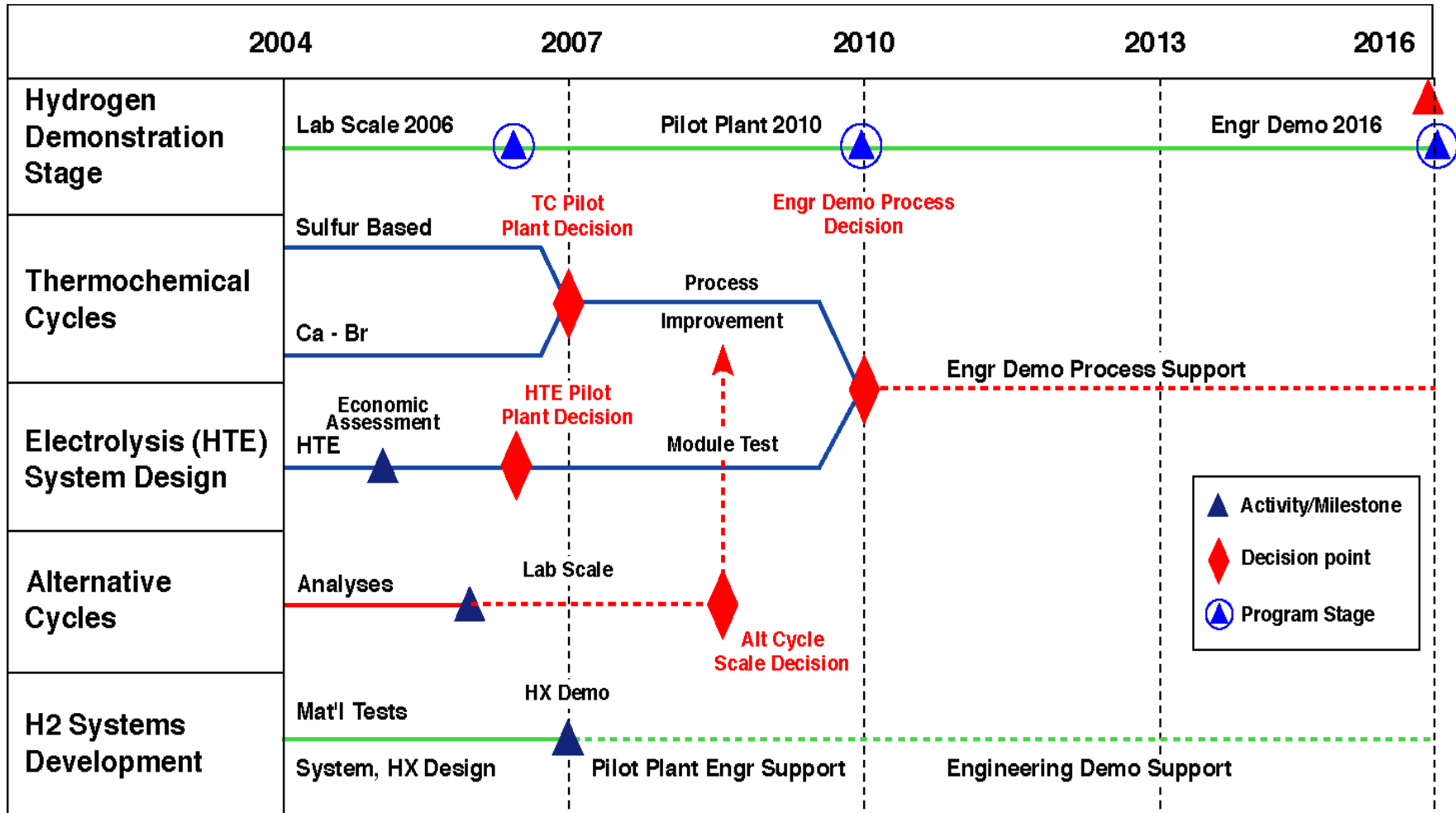


Ref: U.S. DOE
03-GA51038-16

Systems Interface and Balance of Plant Areas Nuclear Hydrogen Initiative

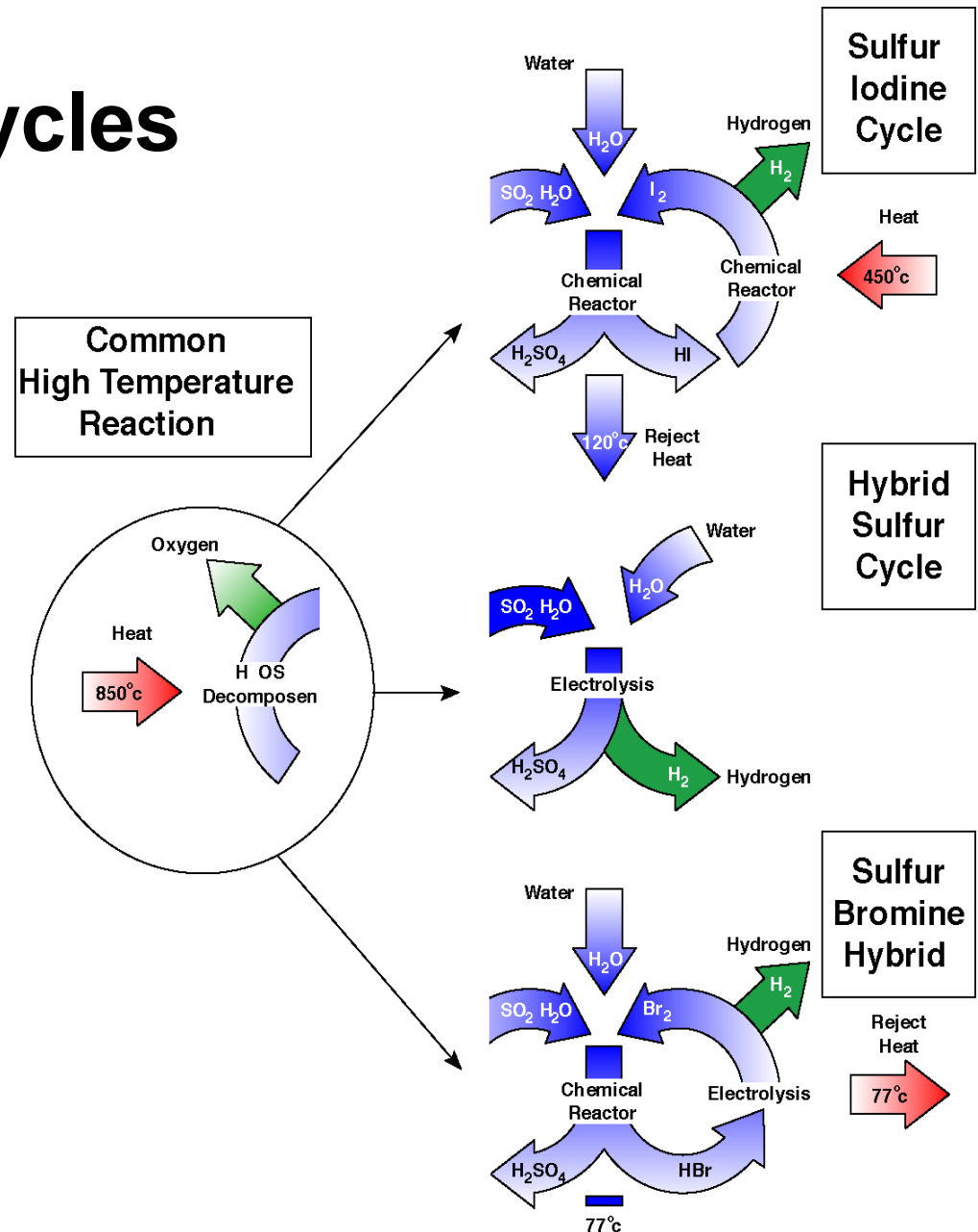
- Thermal Systems Analyses – requirements
 - Reactor-intermediate loop-process interface
 - Baseline cycles and HTE
- Heat Exchangers
 - Designs, range of conditions
 - Materials – options, testing
- Intermediate loop materials, conditions
- Supporting systems

Nuclear Hydrogen R&D Schedule



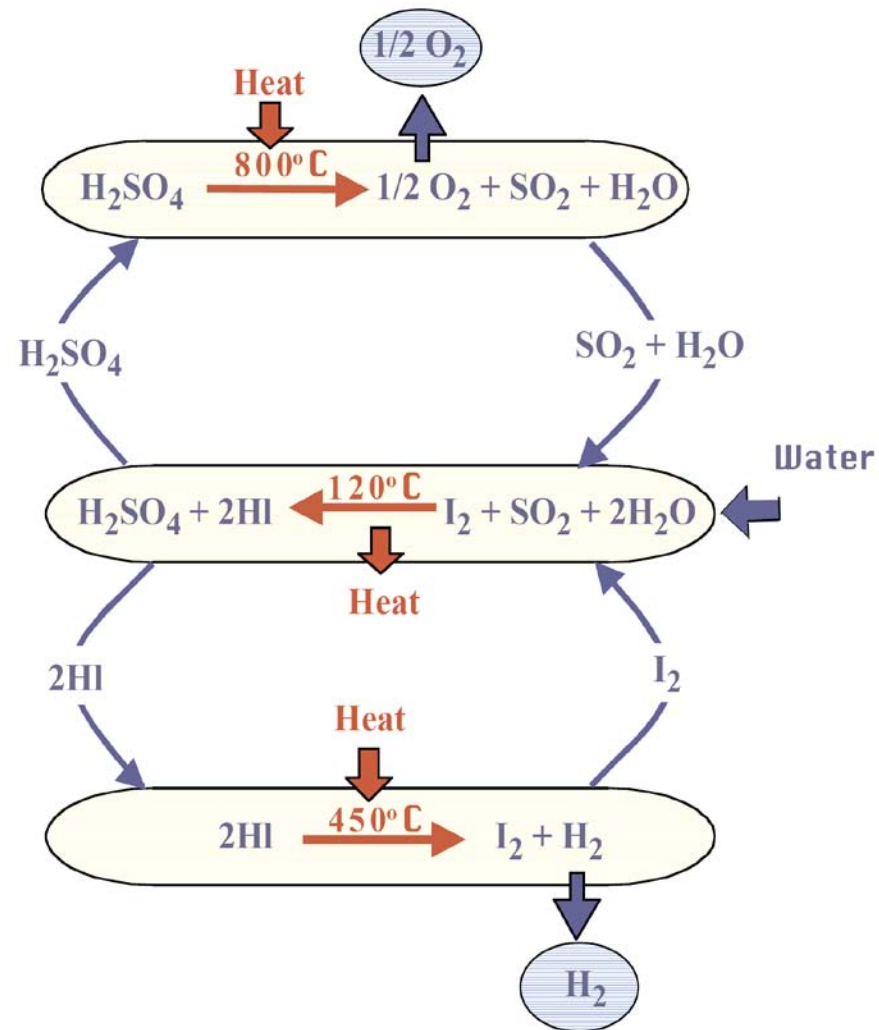
Sulfur Based Thermochemical Cycles

- Identified as a **baseline process**
- High overall efficiencies
- Most extensively demonstrated thermochemical process
- Least complex system
- Increased viability based on number of process options



The Sulfur-Iodine Cycle is One of the Best Suited to Nuclear Production of H₂

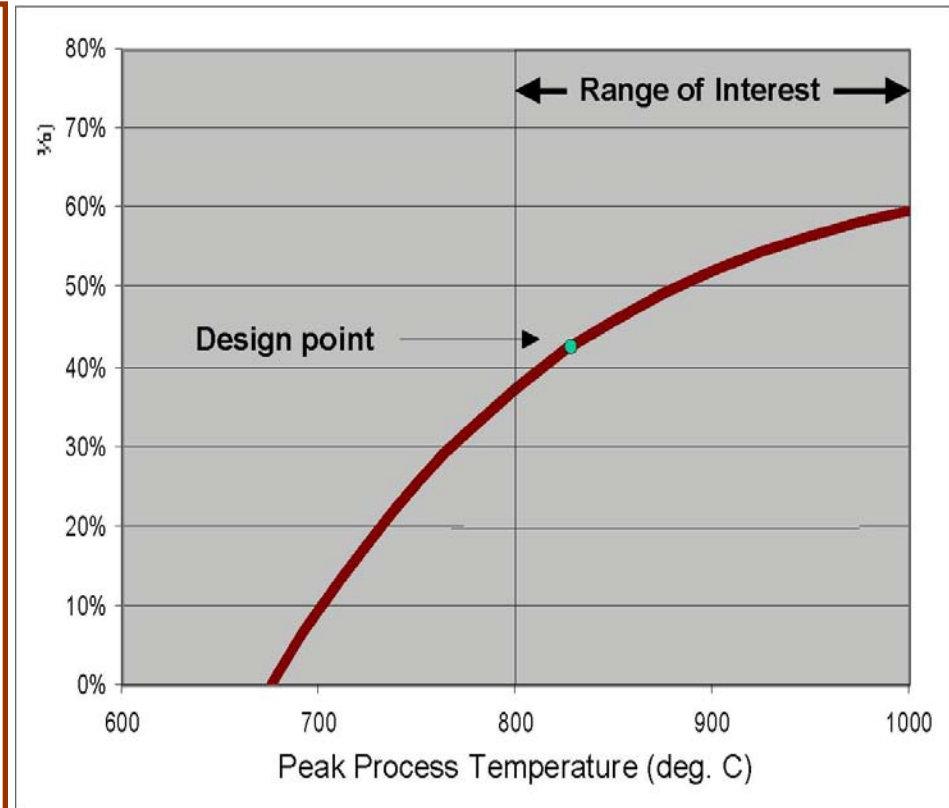
- **Invented at GA in 1970s**
 - Serious investigations for nuclear and solar
 - Chemistry reactions all demonstrated
 - Materials candidates selected and tested
- **Advantages:**
 - All fluid continuous process, chemicals all recycled; no effluents
 - H₂ produced at high pressure – 22 - 84 atm.
 - Highest cited projected efficiency, ~50%
- **Challenges:**
 - Requires high temperature, ≥800°C
 - Must be demonstrated as a closed loop under prototypical conditions



High Temperature Increases Efficiency

Estimated S-I process thermal-to-hydrogen energy efficiency (HHV)

- Process is coupled to nuclear heat source by an intermediate loop with 2 heat exchangers $\sim 50^{\circ}\text{C}$ ΔT
- Earlier studies used 827°C , achieved 42% efficiency
- $>50\%$ efficiency requires $>900^{\circ}\text{C}$ peak process T
- Reactor outlet $T \geq 950^{\circ}\text{C}$ desired



GA Completed the S-I process Design

- Used chemical process design code **Aspen Plus**
- Designed the three main chemical process systems
 - **Prime or Bunsen reaction (CEA)**

$$(2\text{H}_2\text{O} + \text{SO}_2 + \text{I}_2 \rightarrow \text{H}_2\text{SO}_4 + 2\text{HI})$$
 - **Sulfuric acid decomposition (SNL and UNLV)**

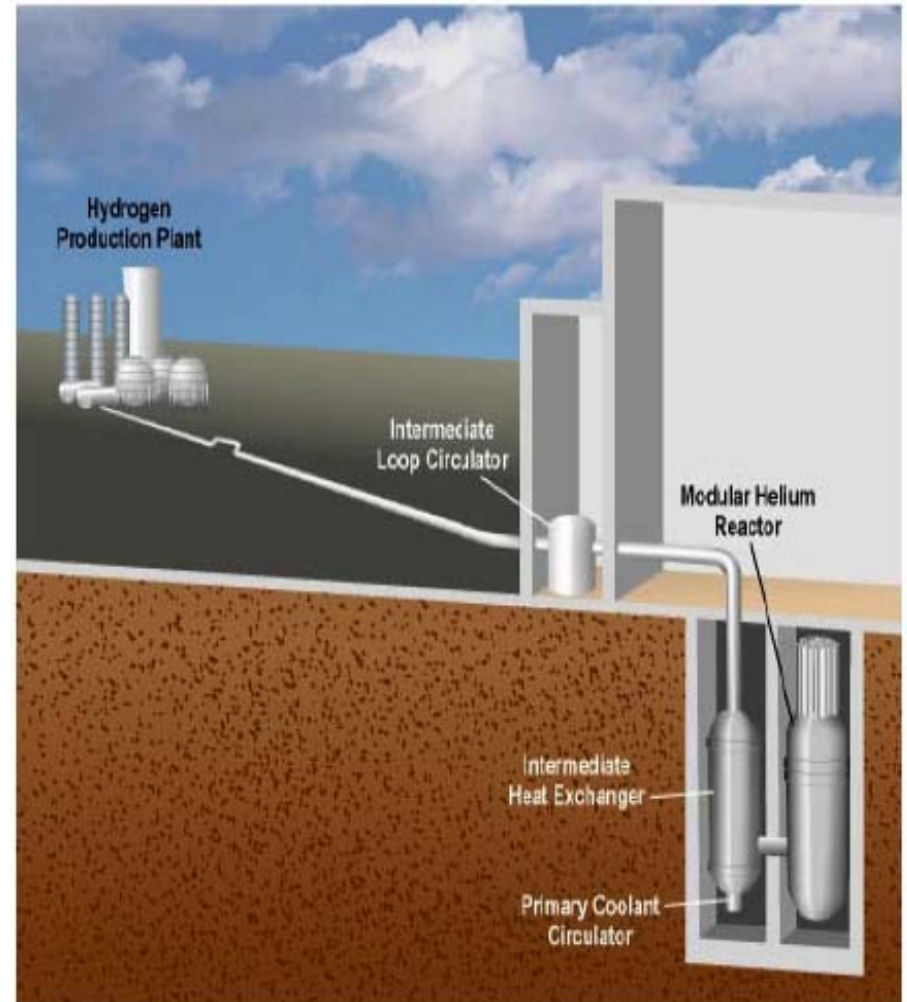
$$(2\text{H}_2\text{SO}_4 \rightarrow 2\text{SO}_2 + 2\text{H}_2\text{O} + \text{O}_2)$$
 - **Hydrogen iodide decomposition (GA)**

$$(2\text{HI} \rightarrow \text{I}_2 + \text{H}_2)$$
- They estimate high efficiency (**52% at 900°C**) and reasonable cost (**~\$250/kWt**)
 - Benefit of high reactor outlet temperature important
- **Experimental verification is needed**
 - HI, H2O, I2 Vapor-Liquid Equilibrium data needed
 - Confirmation of HI Reactive Distillation analysis important, may allow further cost savings

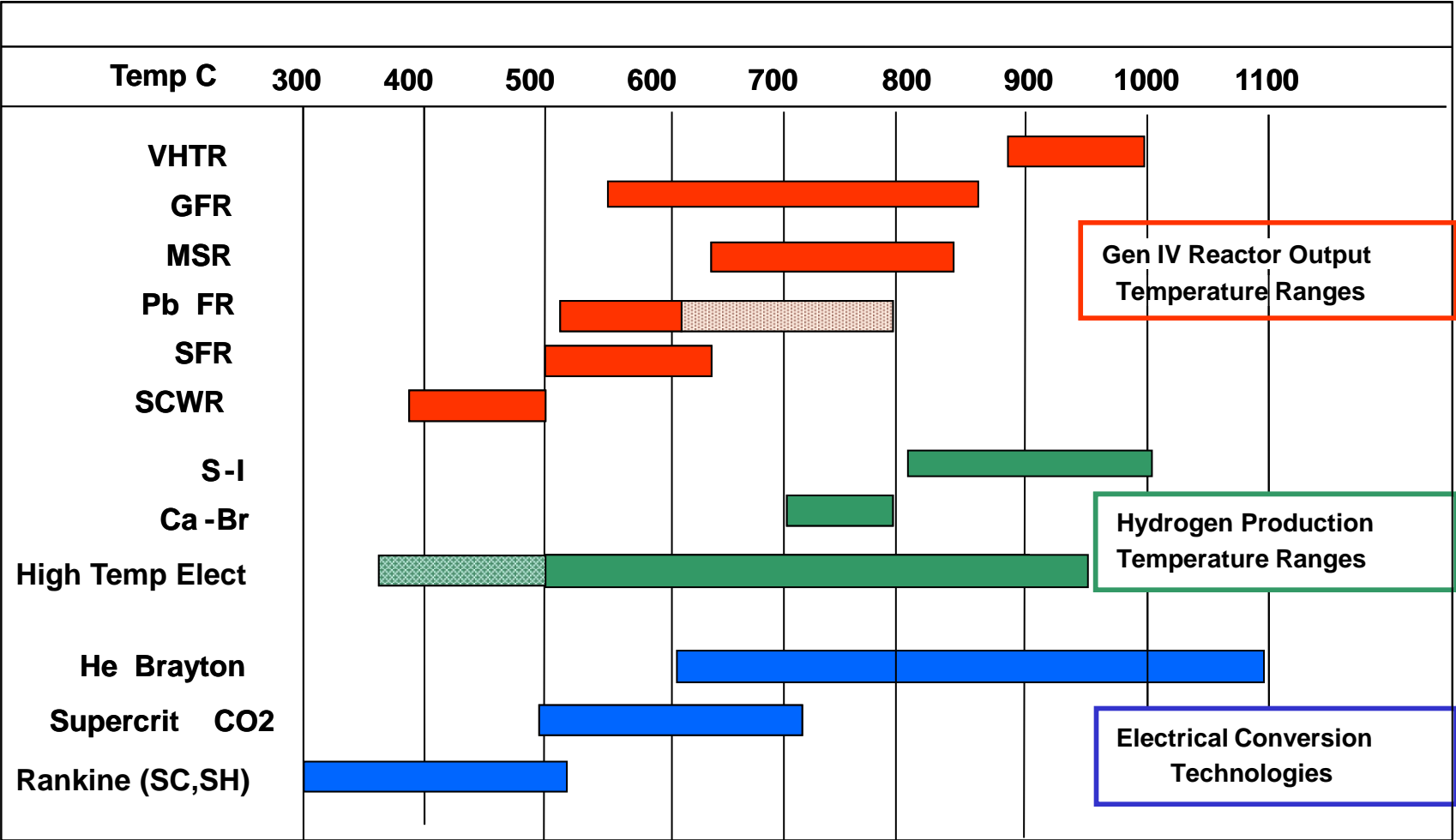
600 MWt H2-MHR Process Parameters		
Material	Flow rate tons/day	Inventory tons
H2	200	2
H2O	1,800	40
H2SO4	9,800	100
I2	203,200	2,120

SNL Evaluated Candidate Nuclear Reactors for Thermochemical Water-splitting

- **SNL evaluated 9 categories:**
 - PWR, BWR, Organic, Alkali metal, Heavy metal, Gas-cooled, Molten salt, Liquid-core and Gas-core
 - Assessed reactor features, development requirements
- **Current commercial reactors are too low temperature**
- **Helium, heavy metal, molten salt rated well; helium gas-cooled most developed**
- **Selected Modular Helium Reactor (MHR) as best suited for thermochemical production of hydrogen**



Gen IV Reactor Outlet Temperatures Electrical / Hydrogen Requirements

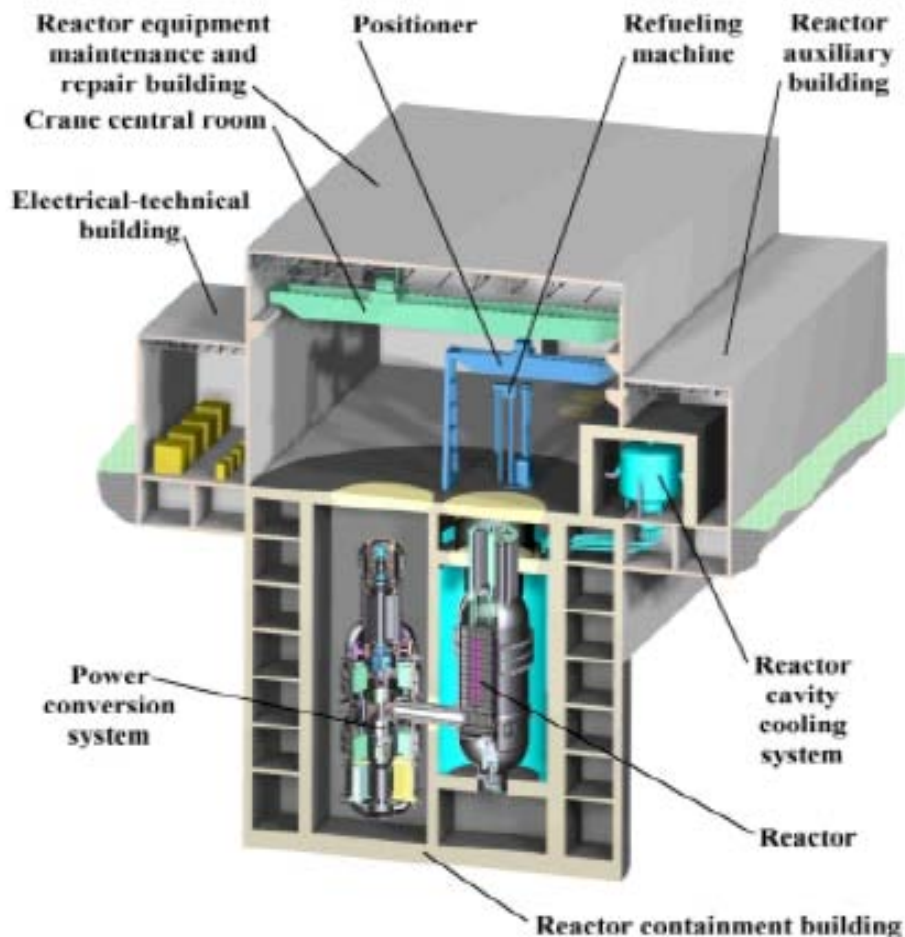


The Modular Helium Reactor Solves the Problems of First Generation Reactors

- High temperature all-ceramic fuel is passively safe
- Allows high coolant temperatures – 850 - 950°C
- Coupled to gas turbine at 850°C: GT-MHR, 48% efficiency
- Coupled to S-I water-splitting at 950°C: Hydrogen at 52% efficiency
- Reduces cost and minimizes waste
- Proliferation resistant

... Opens a new opportunity for nuclear power

Inherent Reactor Characteristics Provide Passive Safety



Ref.: General Atomics

- Helium gas coolant (inert)
- Refractory fuel (high temperature capability)
- Graphite reactor core (high temperature stability)
- Low power density, modular size (slow thermal response)
- Demonstrated technologies from 7 prototypes world-wide over 40 years

**... EFFICIENT
PERFORMANCE WITH
PASSIVE SAFETY**

Hydrogen Production Research Groups (Academic and National Lab)

Research emphases	Universities/National Labs
Production (solar powered thermo-chemical production, natural gas cracking, steam reforming, electrolyzer, biomass, nuclear)	UNLV , Arizona State, Iowa State, MIT, Ohio State, UC Berkeley, UC Davis, UC Santa Barbara, Univ. Central Florida, Univ. Colorado, Univ. Hawaii, Univ. Kentucky, Univ. Nevada-Reno ANL, INL, NERL, ORNL, SNL, SRNL, PNNL

Center of Energy Research (CER) at UNLV: Solar powered thermo-chemical production, high-temperature heat exchanger development, high-efficiency high-pressure proton exchange membrane electrolyzer

Hydrogen Storage Research Groups (Academic and National Lab)

Research emphases	Universities/National Labs
Storage (metal hydride, hydrogen sorption, chemical hydrogen storage, new materials & concepts)	<p>UNLV, Caltech, Duke University, Northern Arizona Univ., Penn State, Rice Univ., Stanford, Univ. Alabama, UC Berkeley, UC Davis, UCLA, UC Santa Barbara, Univ. Connecticut, University of Hawaii, Univ, Illinois Urbana-Champaign, Univ. Michigan, Univ. Pennsylvania, Univ. Utah, Univ. Washington</p> <p>ANL, LANL, LLNL, NIST, NREL, ORNL, PNNL, Sandia-Livermore</p>

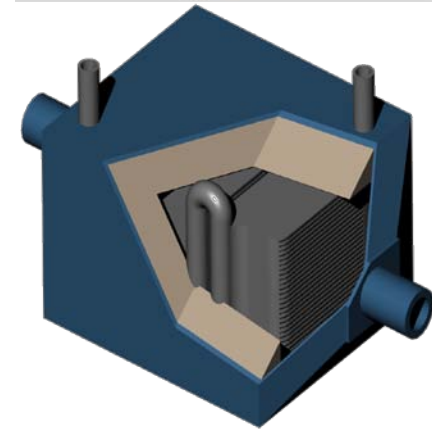
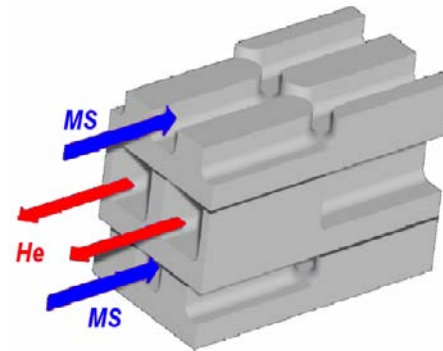
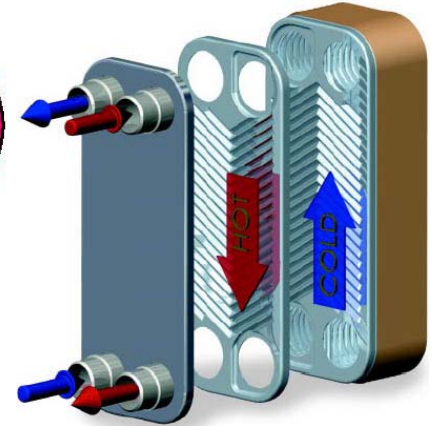
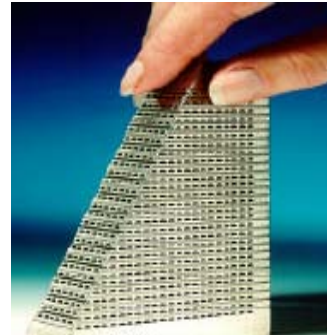
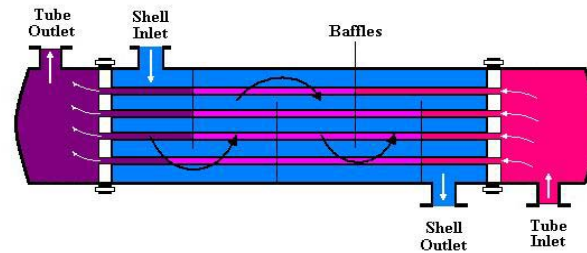
Hydrogen Utilization Research Groups (Academic and National Lab)

Research emphases	Institutes/National Labs
Utilization (membrane, catalyst, system analysis, electrode, transport phenomena, combustion, hydrogen filling station)	UNLV , Arizona State, Case Western Reserve Univ., Clemson, Colorado School of Mines, Penn State, Univ. Central Florida, Univ. Tennessee, Univ. South Carolina, Univ. South Mississippi, Virginia Tech ANL, LASNL, NIST, ORNL, SNL, PNNL

Center of Energy Research (CER) at UNLV: hydrogen filling station, PEM fuel cell, hydrogen-powered vehicles, HICE

NHI Identification of Intermediate Heat Exchanger Design Concepts

- Shell and Tube Heat Exchangers
- Flat Plate Heat Exchangers
- Printed Circuit Heat Exchangers
- Offset Fin Plate Heat Exchangers Catalyst-Packed Shell and Tube Heat Exchangers
- Catalyst-Coated Printed Circuit Heat Exchangers



U.S. National Hydrogen Initiative (NHI) Participants

- **UNLV** – *High temperature heat exchanger and decomposer design*
- **SNL** – *Sulfuric acid decomposition*
- **GA** – *Sulfur-iodine flowsheet analysis, HI decomposition and Bunsen reactor*
- **ANL** – *Ca-Br and Cu-Cl cycles, interface issues, SI&SS overview and infrastructure*
- **ORNL** – *Materials and membrane*
- **INL** – *Membrane and catalyst research, safety analysis, thermal hydraulics, materials, loop heat exchanger*
- **SRNL** – *Hybrid sulfur cycle*

High Temperature Heat Exchanger Project Collaborators

- UNLV

- *Hydrodynamics and thermal performance study based on the different high temperature heat exchanger requirements*
- *Perform a baseline design for the sulfuric acid decomposition heat exchanger*
- *Thermo-chemical process analysis*
- *Evaluate candidate fluids*
- *Design concept and optimization*
- *Thermal and mechanics stress analysis*
- *Experimental measurements*
- *Development and characterization of materials for advanced HTHXs*
- *Corrosion studies of candidate structural materials in Hlx environment as functions of metallurgical variables*

High Temperature Heat Exchanger Project Collaborators (Cont.)

- UC-Berkeley
 - *Design of offset fin plate ceramic heat exchangers*
 - *Mechanical design and stress analysis of complete ceramic heat exchangers*
 - *Process heat exchanger safety analysis*
 - *Identification and characterization of candidate ceramic heat exchanger materials and processes*
 - *Identification and demonstration of candidate ceramic heat exchanger fabrication methods*

High Temperature Heat Exchanger Project Collaborators (Cont.)

- MIT

- *Material chemistry identification, alloy procurement and metallurgical characterization*
 - *Initial chemistry identification*
 - *Larger size quantity production*
 - *Powder production*
- *Catalyst effectiveness determination*
 - *Facility construction*
 - *Catalyst proof of principal*
 - *Catalyst effectiveness*
- *Mechanical properties determination*
- *Prototypic shape fabrication and testing*
 - *Compact heat exchanger application*
 - *Shell & tube application*

High Temperature Heat Exchanger Project Collaborators (Cont.)

- Ceramatec, Inc.
 - *Process design*
 - *General Atomics flow sheets*
 - *Ceramatec scope*
 - *Unit operations*
 - *Shell and plate design*
 - *Modular stacks*
 - *Plate design – primary repeat unit*
 - *Layout and gas flows*
 - *Synergy for 3 unit operations*
 - *Design variables*
 - *Analytical support*
 - *Local/feature analysis*
 - *Conjugate heat & flow, thermo-mechanical*

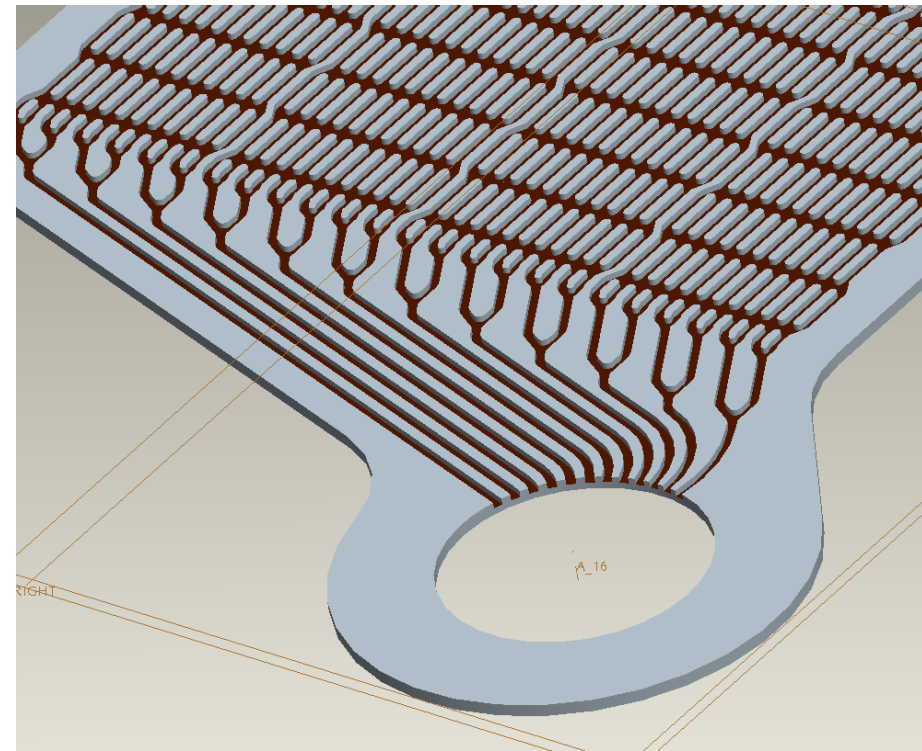
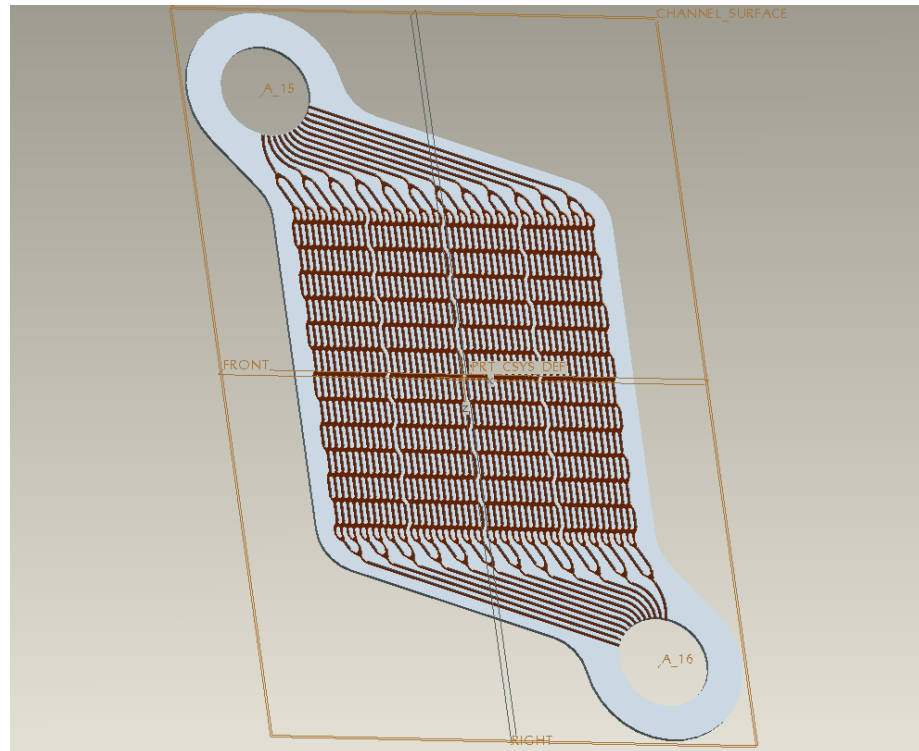
High Temperature Heat Exchanger Project Collaborators (Cont.)

- General Atomics
 - *Identify the materials of construction for HI Decomposition as part of the overall nuclear hydrogen demonstration using the sulfur-iodine thermo-chemical process*
 - *Immersion coupons*
 - *Crack initiation & growth, long term testing, cladding*
 - *S-I loop/pilot plant, testing*

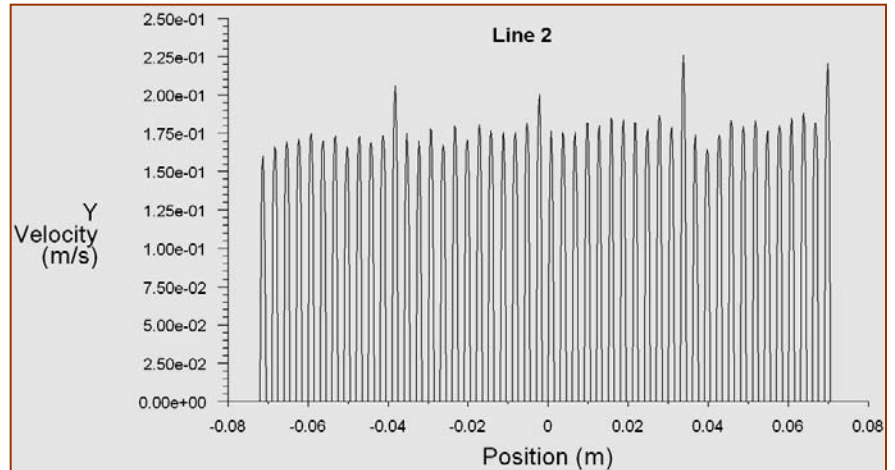
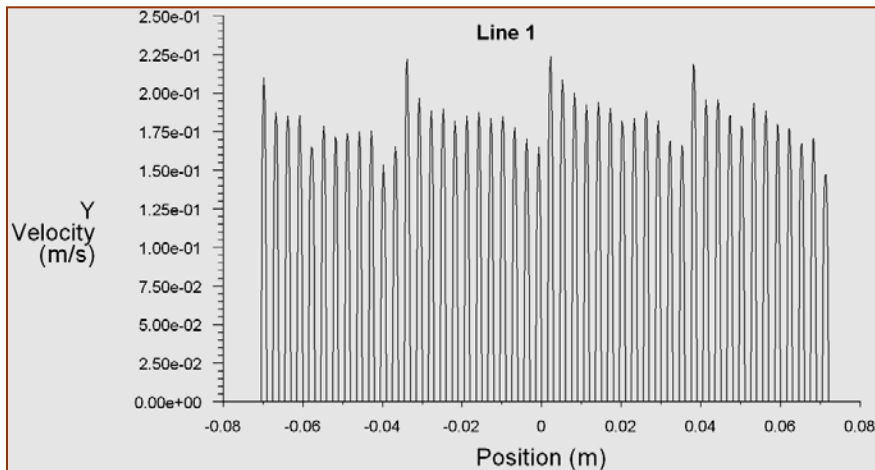
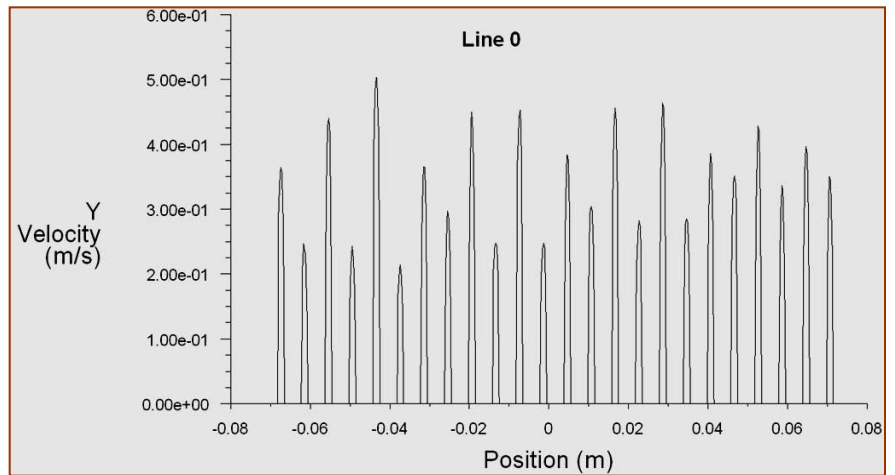
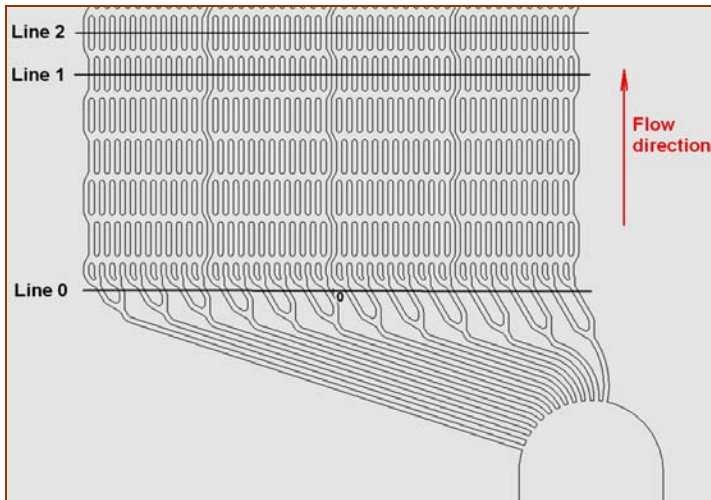
UNLV Numerical Modeling Research Approaches

- **Numerical modeling of high temperature heat exchanger and decomposer**
 - design and operating conditions
 - transport phenomena
 - chemical reactions and kinetics
 - stress analysis
 - numerical procedure
- **Validation of computational model**
 - comparison with experimental results
 - comparison with calculation results of other researchers
- **Modeling of processes in high temperature heat exchanger and decomposer (baseline design)**
 - one layer model
 - one channel model
- **Parametric studies**
 - manifold design
 - channel geometry
 - operating conditions

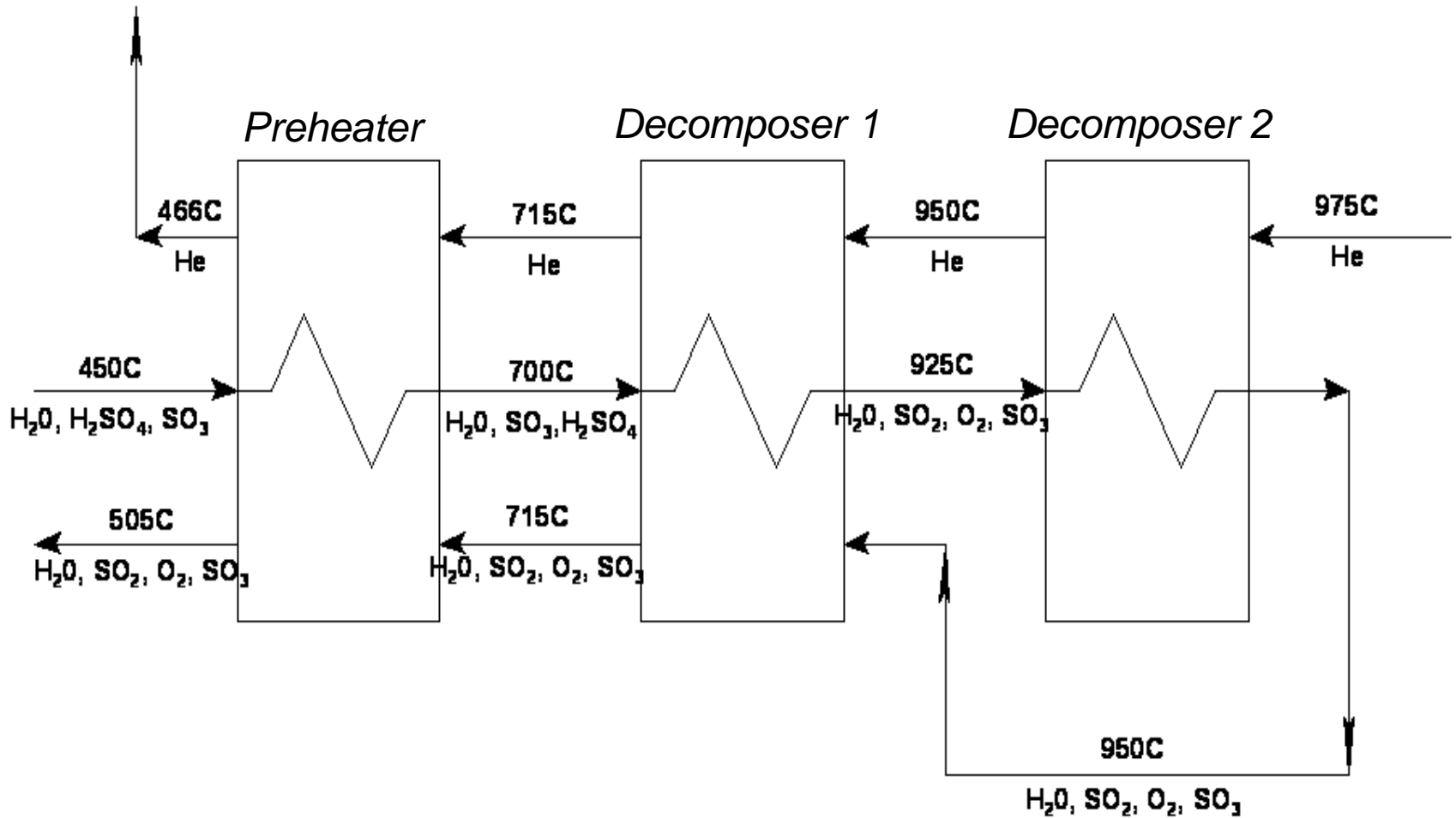
Geometry of Liquid Salt Part of the Offset Strip Fin HTHX



Velocity Distribution in Liquid Salt Part of the Offset Strip Fin HTHX



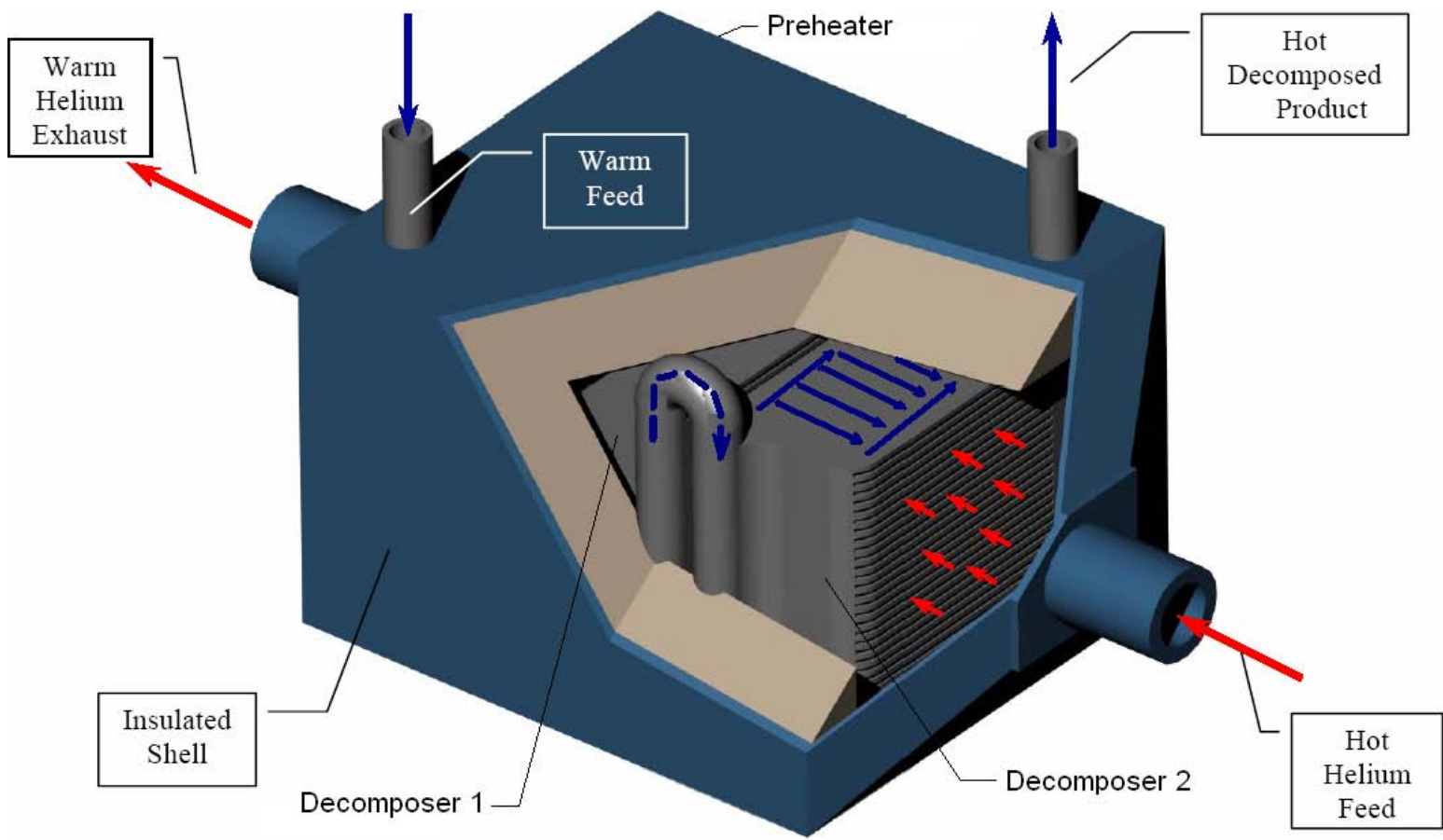
Process Design – GA Flowsheet



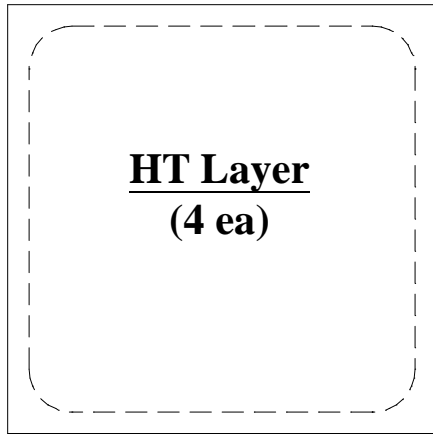
$$\dot{m}_{\text{He}} = 71 \frac{\text{kg}}{\text{hr}}; \quad \dot{m}_{\text{SI}} = 158.66 \frac{\text{kg}}{\text{hr}}$$

High Temperature Heat Exchanger for SI Process – Preheater & Decomposer (“Ceramatec, Inc.” Design)

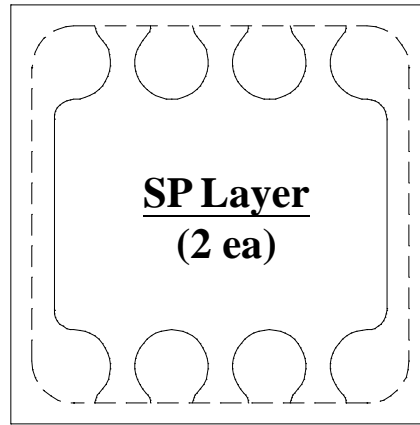
Shell and Plate Heat Exchanger



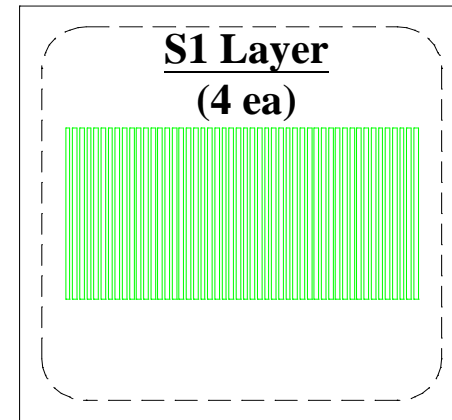
Layers – Decomposer 1 (3 Fluids)



Thickness=0.3 mm

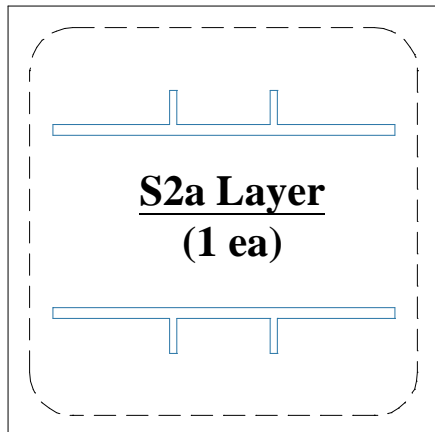


Thickness=0.85 mm



Thickness=0.424 mm

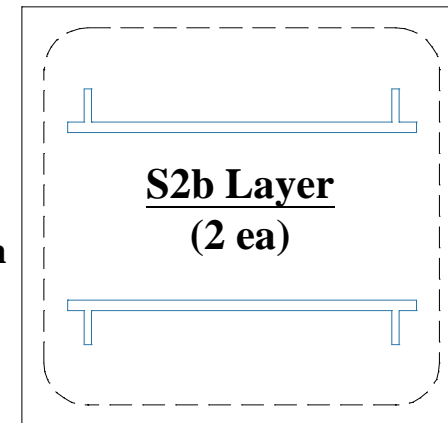
Channels
L = 52.324 mm
W = 1.27 mm
n = 50



Thickness=0.45 mm

Manifolds
L = 101 mm
W = 3.175 mm

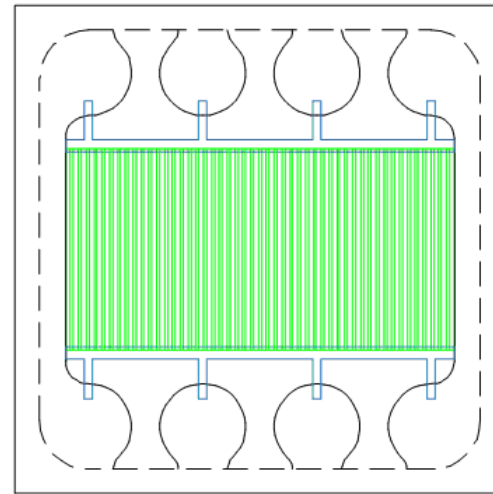
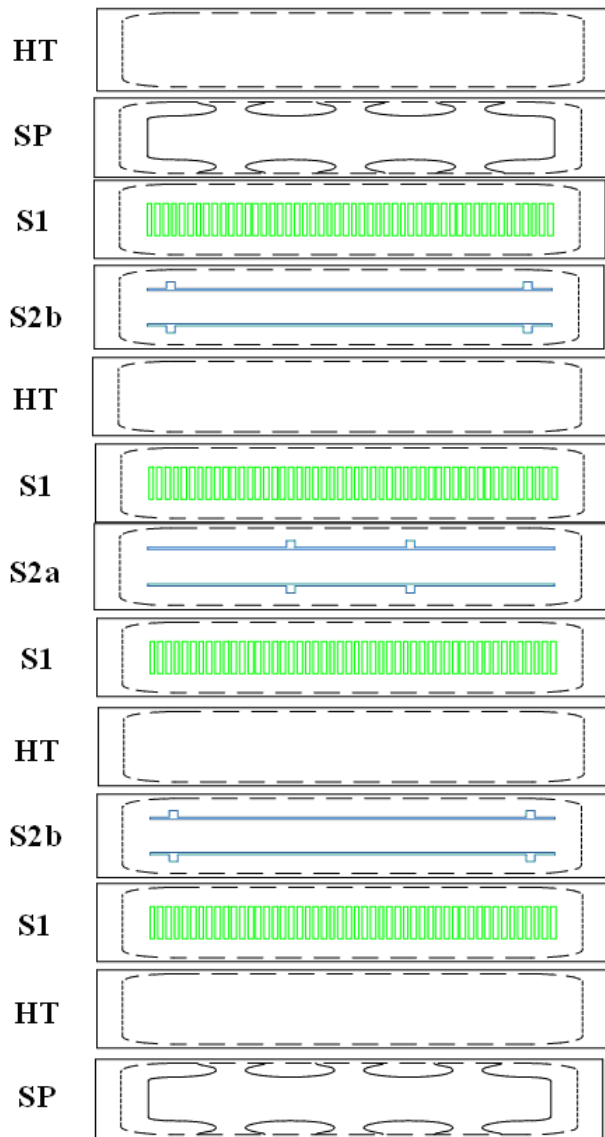
Vents
L = 10.16 mm
W = 2.032 mm



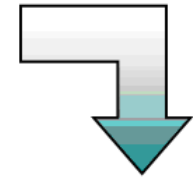
Thickness=0.45 mm

Plates size: 114.3 mm × 114.3 mm

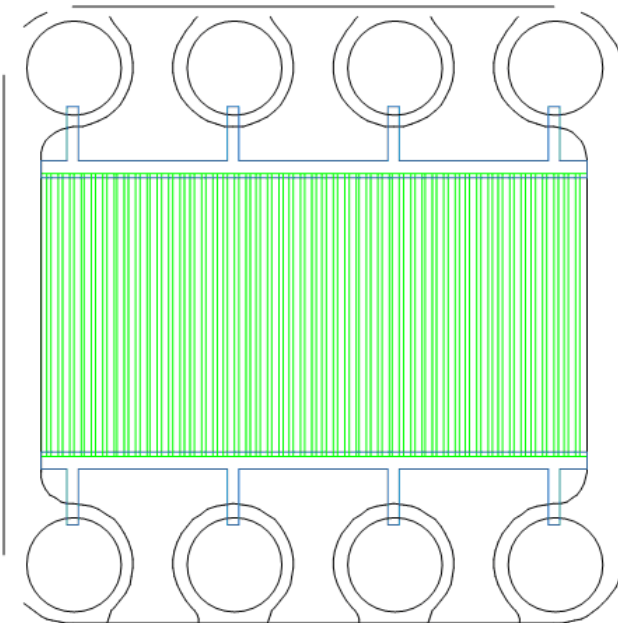
Decomposer 1 (3 Fluids)



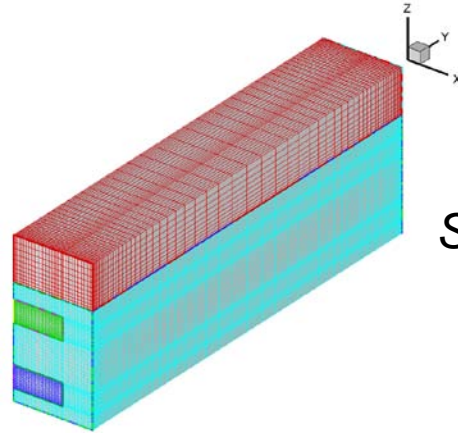
Multi-Layer Lamination



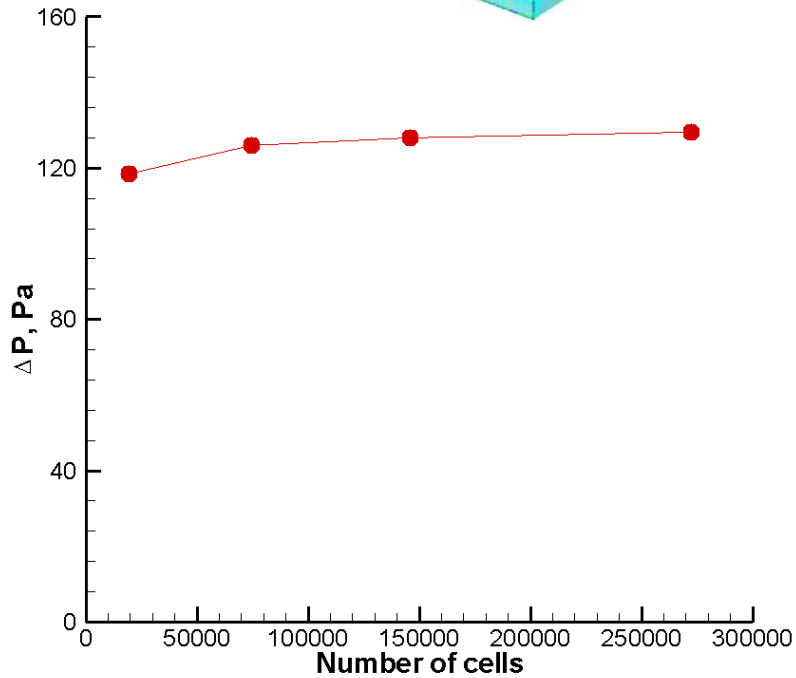
**Finish Cut of Plate Features
(Perimeter & Headers)**



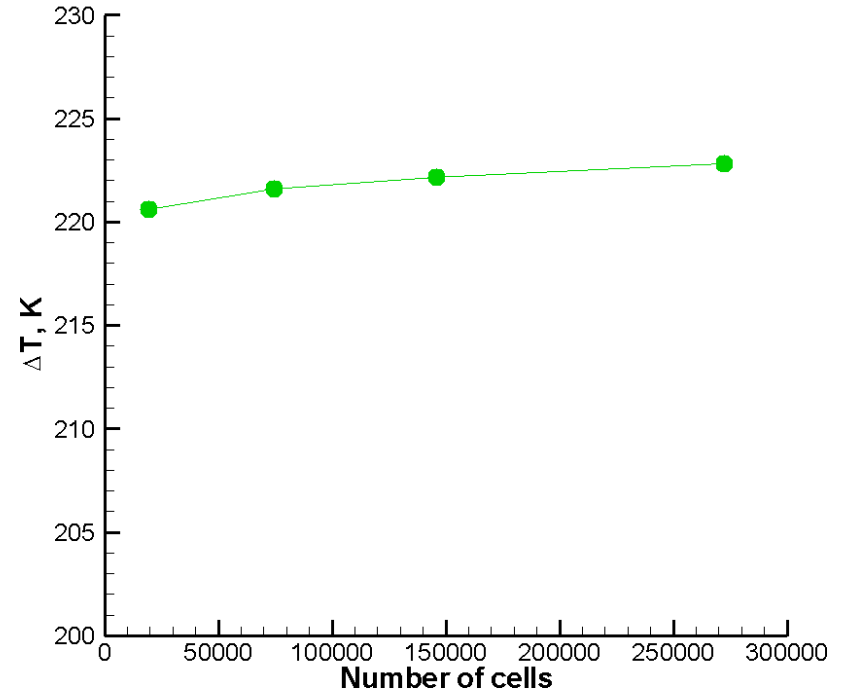
Mesh Independence Study



Single Channel Model

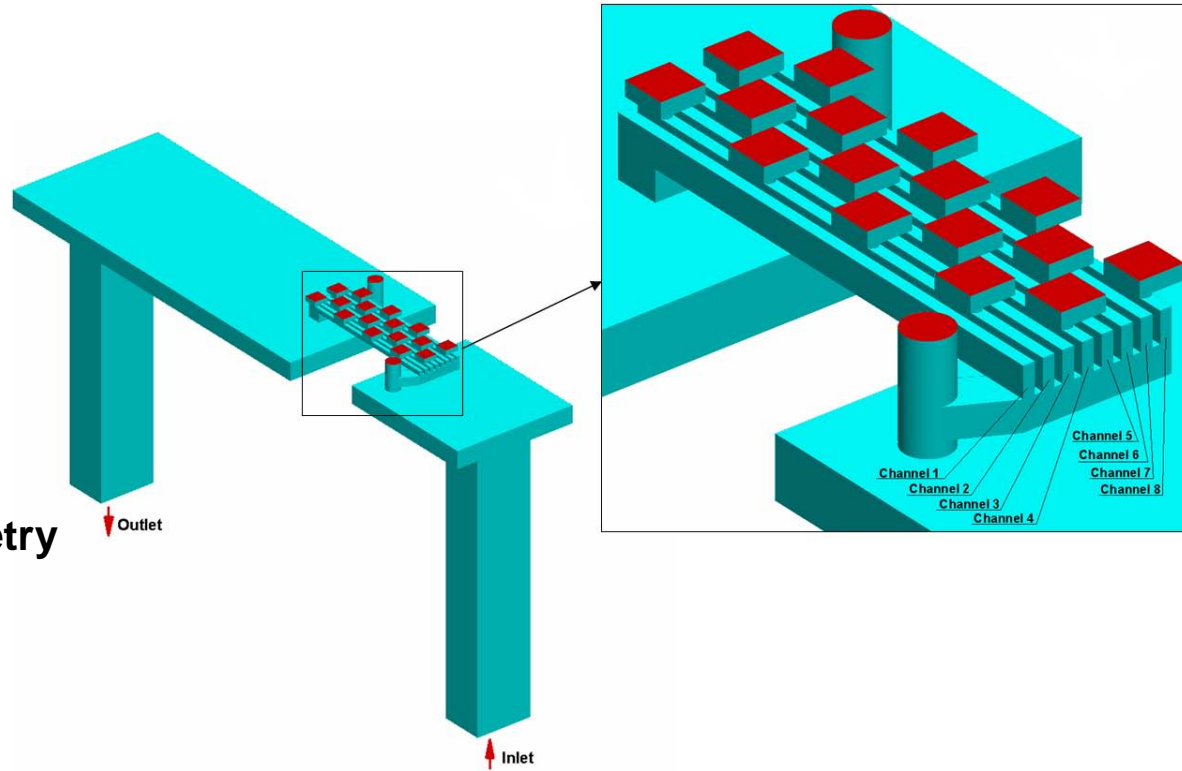
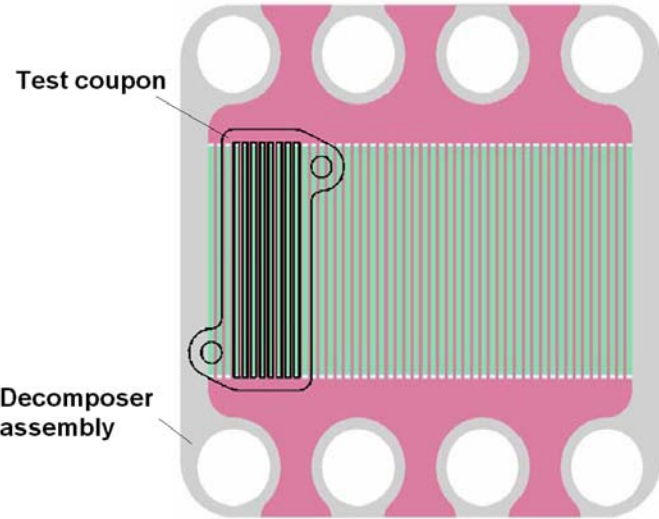


Pressure gradient in y-direction, Pa

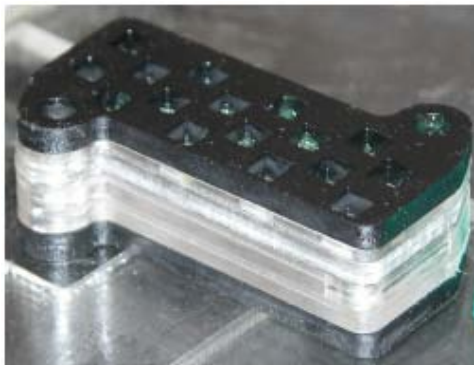


Temperature difference in y-direction, K

Validation of Fluid Flow Model



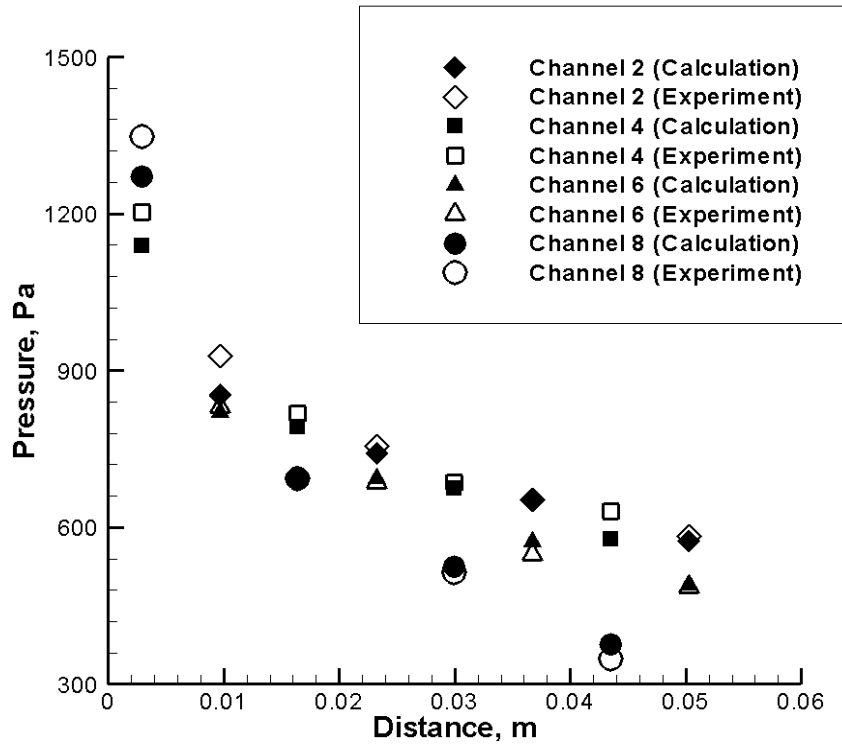
Comparison of test coupon geometry with heat exchanger assembly



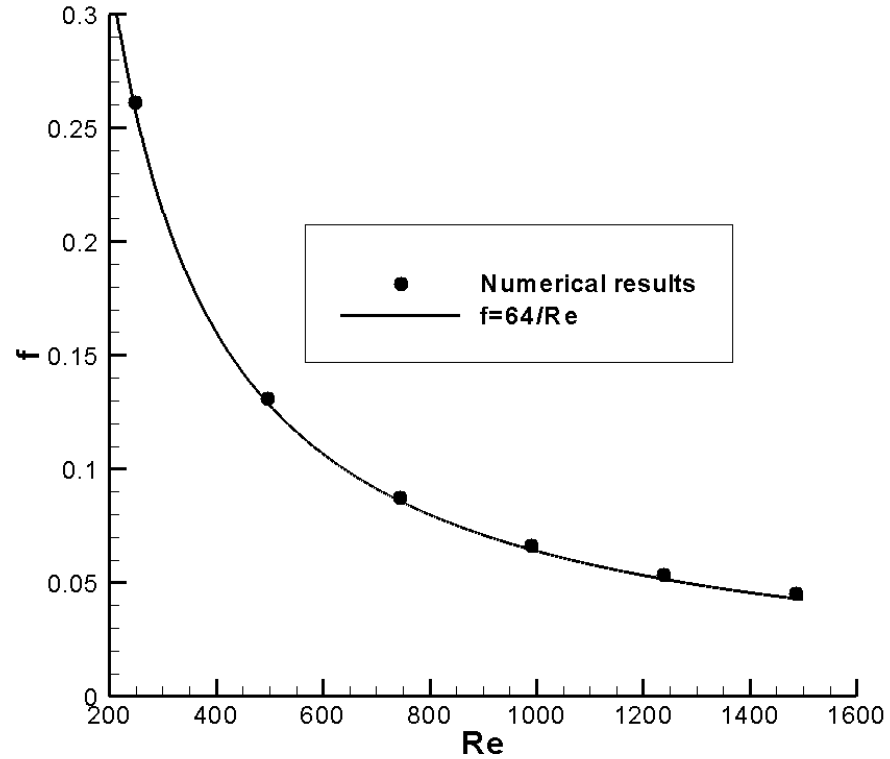
Calculation geometry and channel numbering for the test coupon model

Plexiglas test coupon (Ceramatec, Inc.)

Validation of Fluid Flow Model (Cont.)

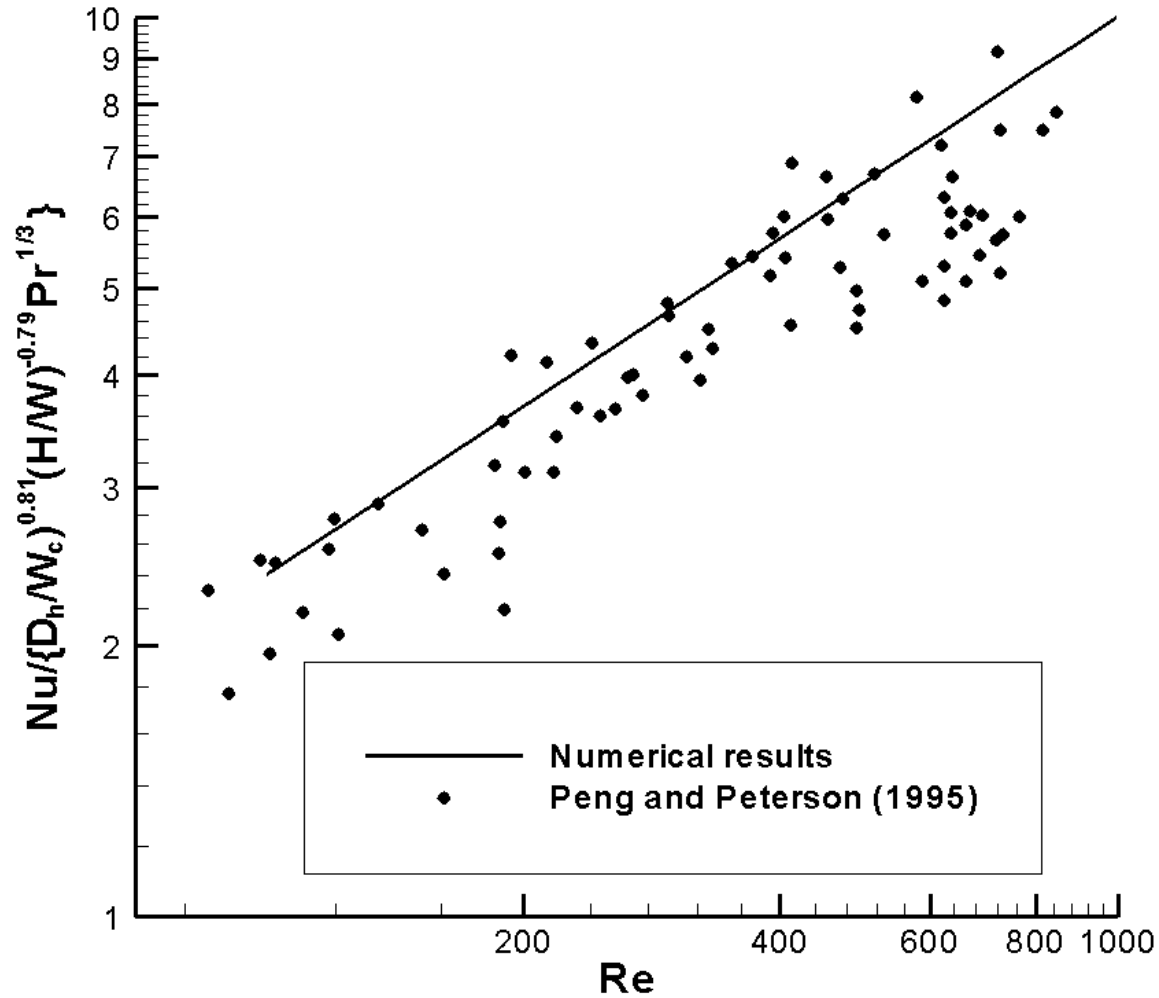


Pressures for Re=870

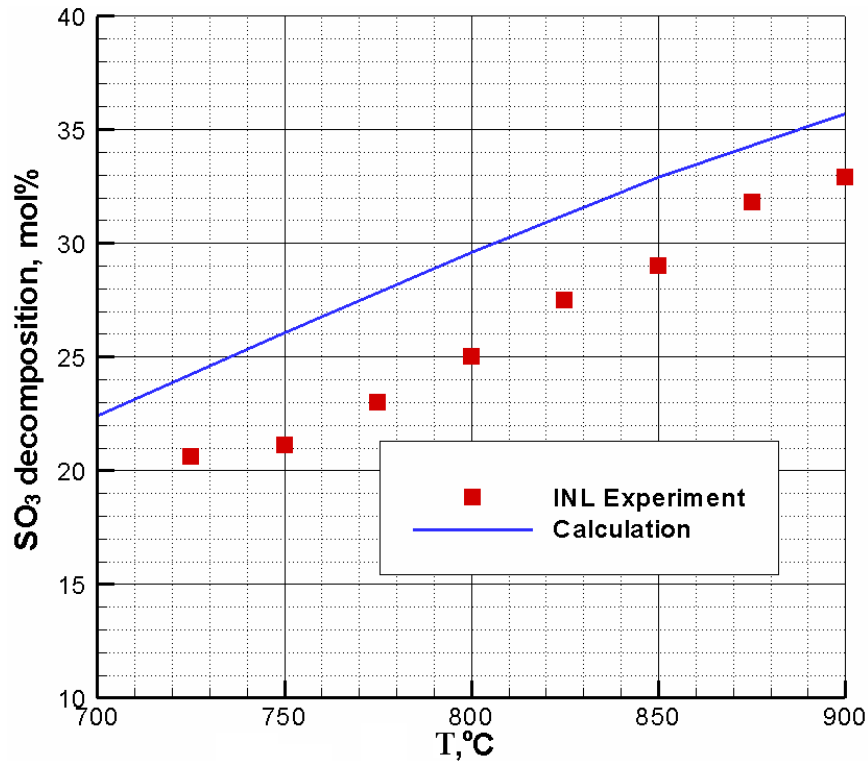


Friction factor

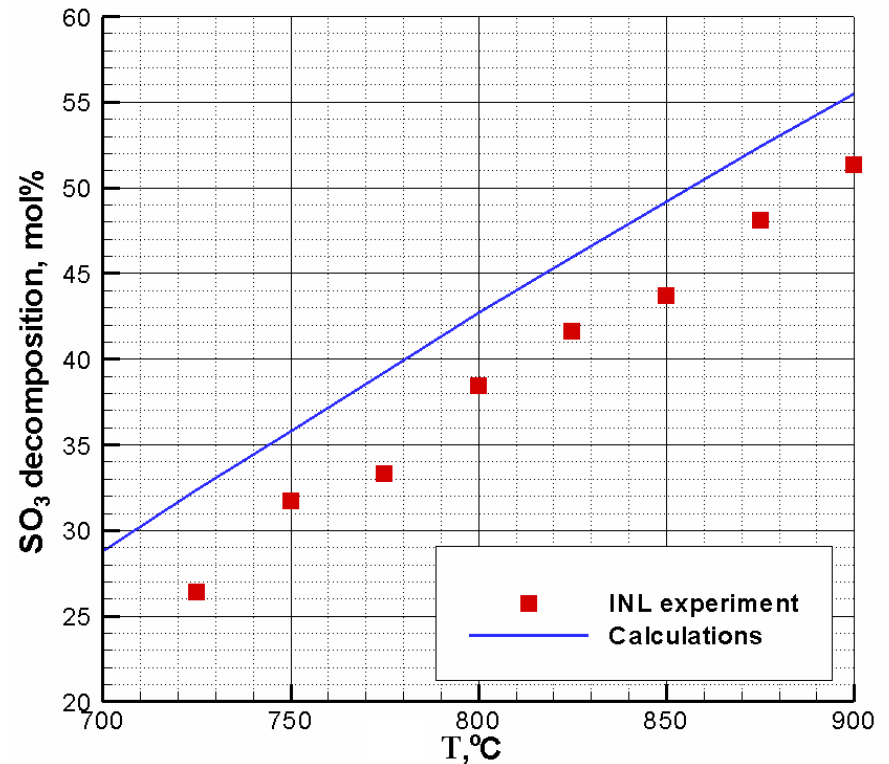
Validation of Heat Transfer Model



Validation of Chemical Reaction Model



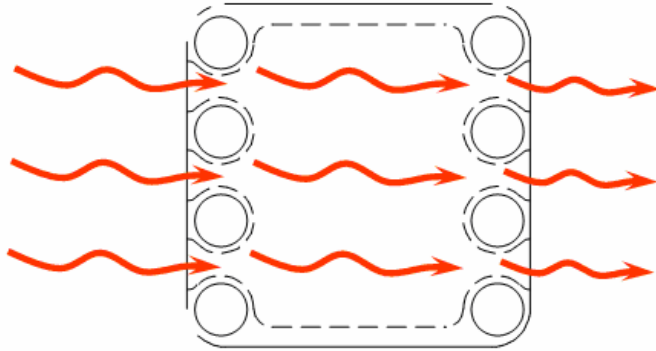
**Sulfur trioxide decomposition
for 0.1% Pt/TiO₂ catalyst**



**Sulfur trioxide decomposition
for 1% Pt/TiO₂ catalyst**

Single Layer Model

**He
Flow
(SP Layer)**

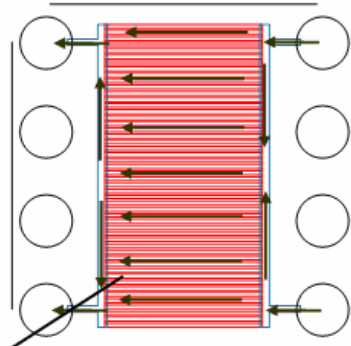


$$\dot{m} = 1.41 \cdot 10^{-4} \text{ kg / s}$$

$$\rho = 0.653 \text{ kg / m}^3$$

$$\mu = 1.99 \cdot 10^{-5} \text{ kg / (m \cdot s)}$$

**Reacting
flow
(S1 and S2b Layers)**



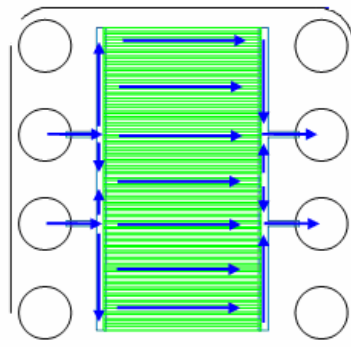
$$\dot{m} = 3.148 \cdot 10^{-4} \text{ kg / s}$$

$$\rho = 7.243 \text{ kg / m}^3$$

$$\mu = 1.5 \cdot 10^{-5} \text{ kg / (m \cdot s)}$$

Catalyst Added
to Channels

**Product
flow
(S1 and S2a Layers)**



$$\dot{m} = 3.148 \cdot 10^{-4} \text{ kg / s}$$

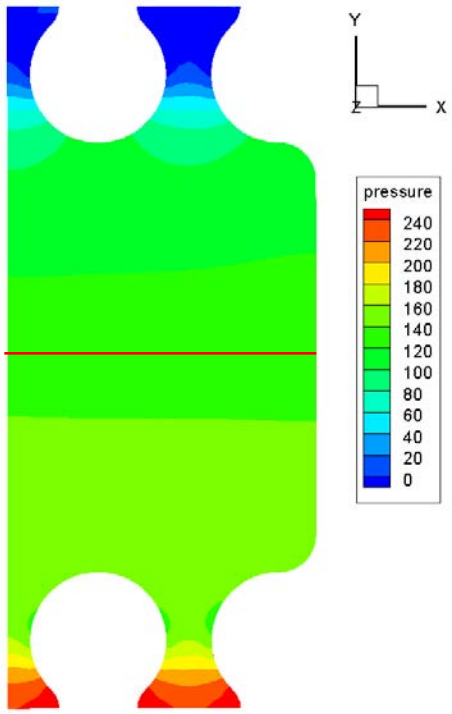
$$\rho = 6.401 \text{ kg / m}^3$$

$$\mu = 1.343 \cdot 10^{-5} \text{ kg / (m \cdot s)}$$

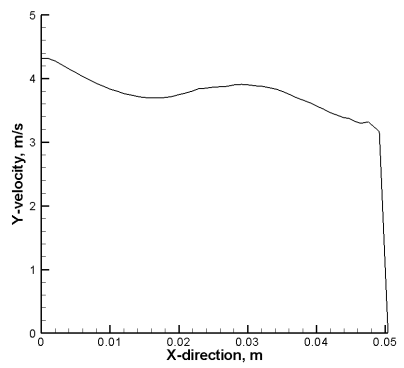
P=1.5 MPa

Calculation Results of Single Layer Model

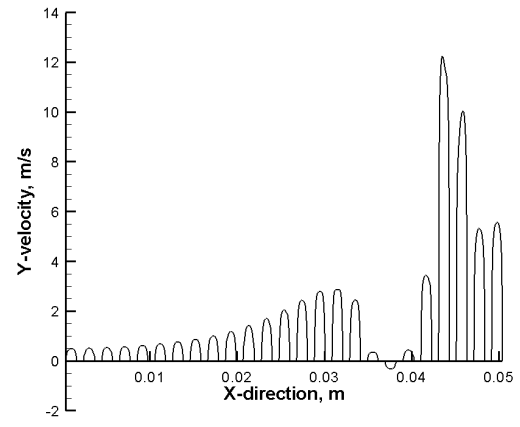
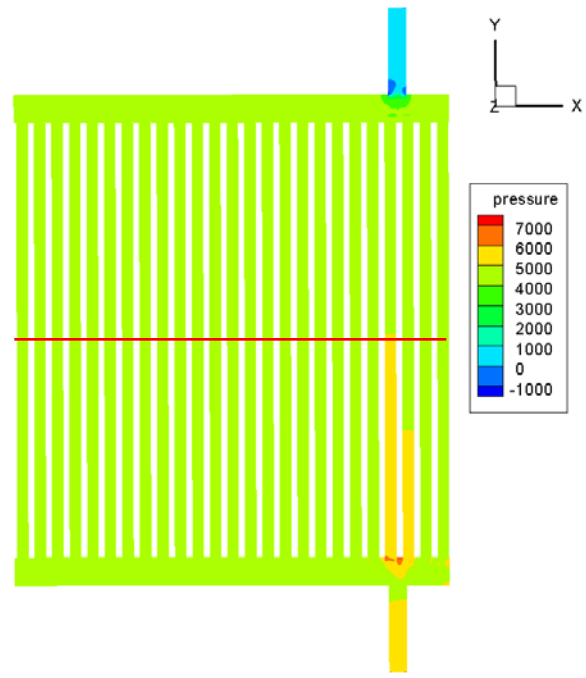
Pressure, Pa



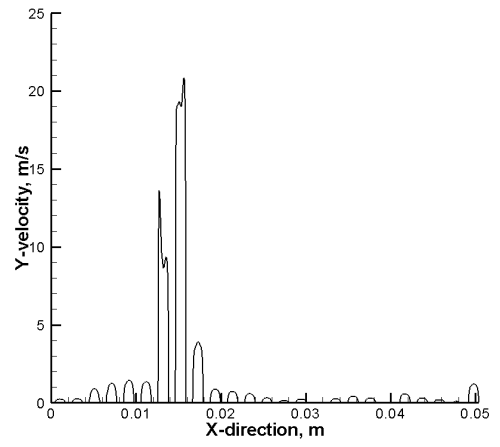
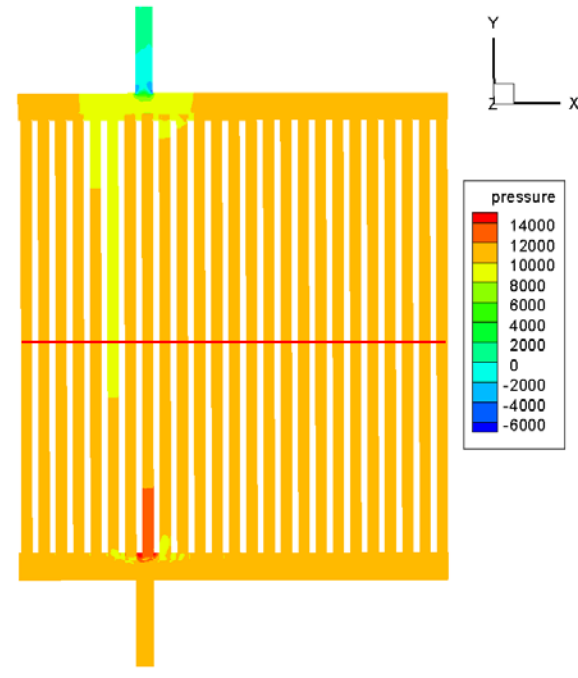
Y-velocity, m/s



He flow

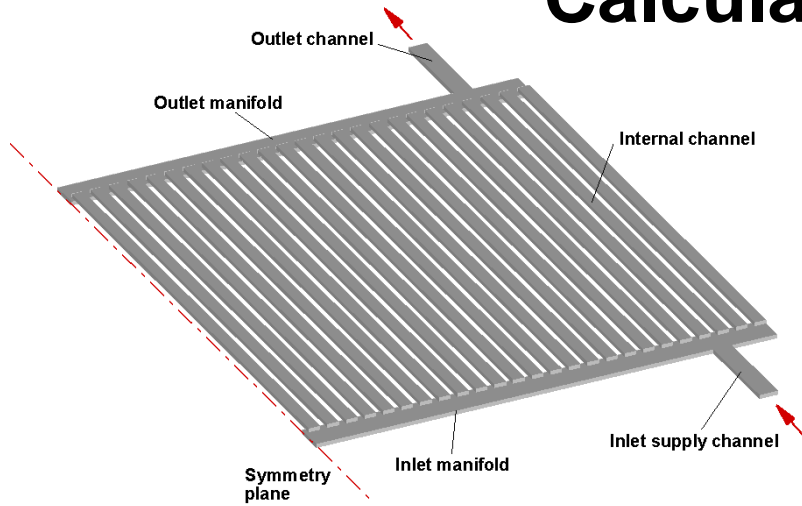


Reacting flow

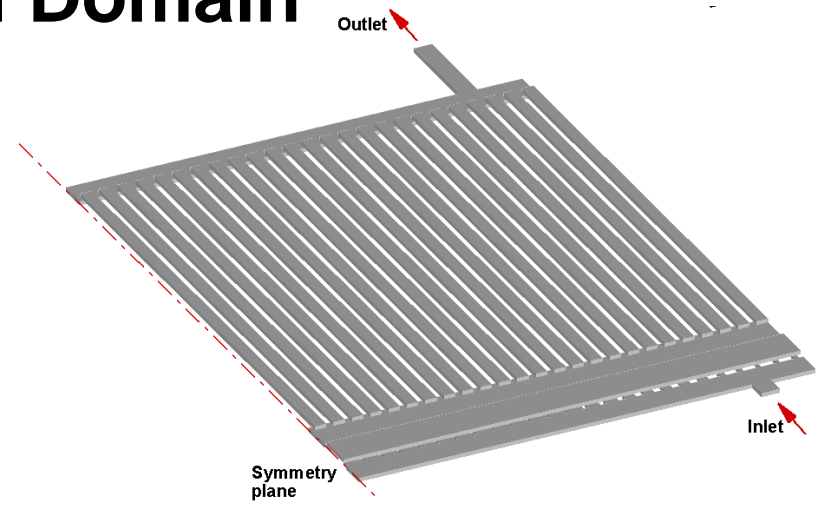


Product flow

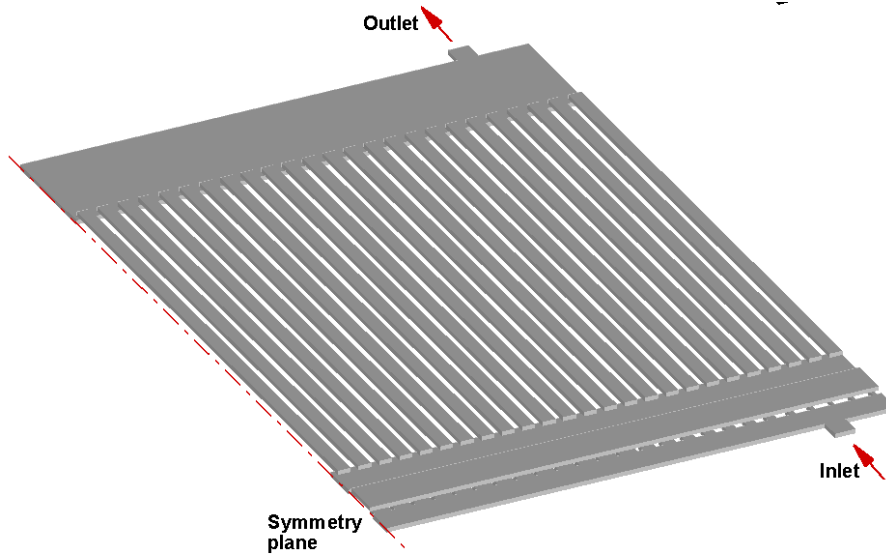
Single Layer Model - Four Different Cases of the Calculation Domain



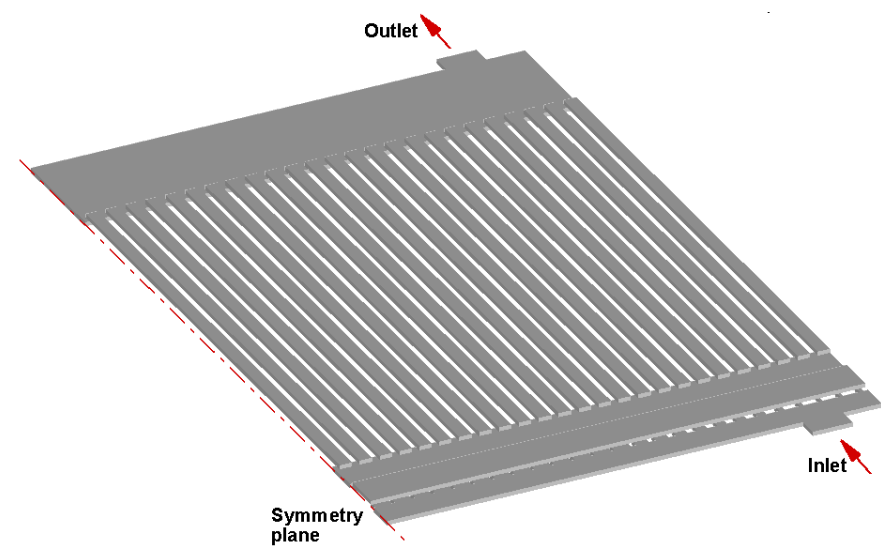
Case A (baseline design)



Case B (modified inlet manifold)

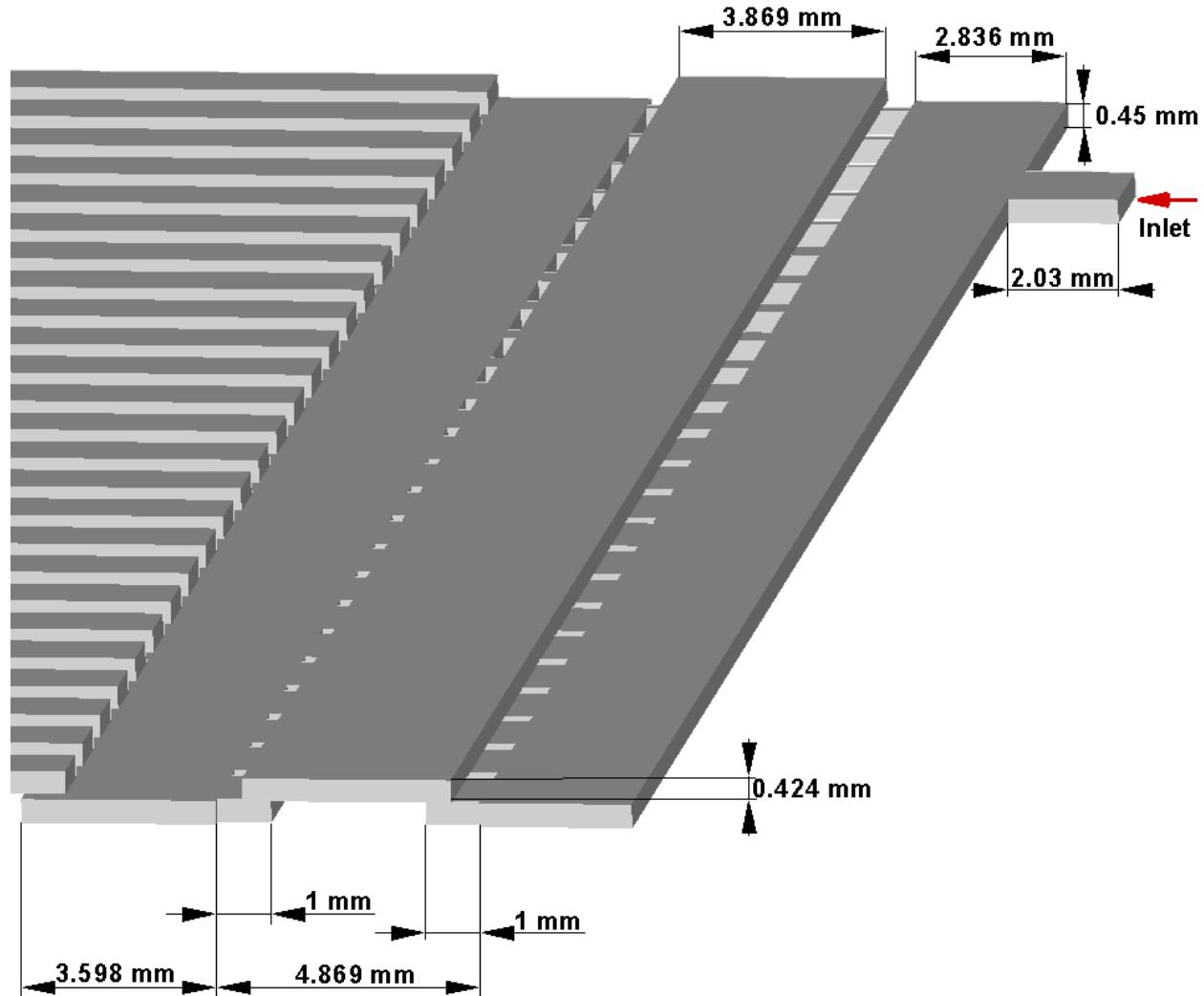


Case C (modified inlet and outlet manifold)

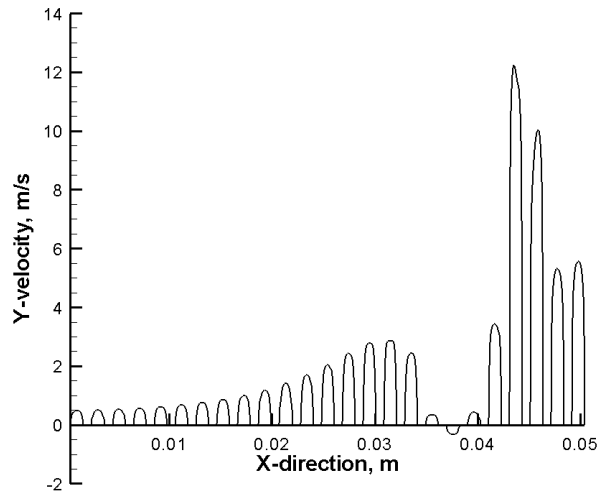


Case D (modified inlet, outlet manifold and supply channels)

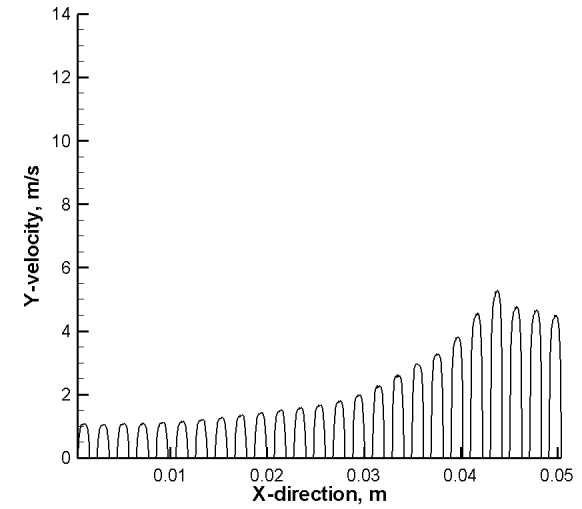
Geometry and Dimensions of the Modified Inlet Manifold



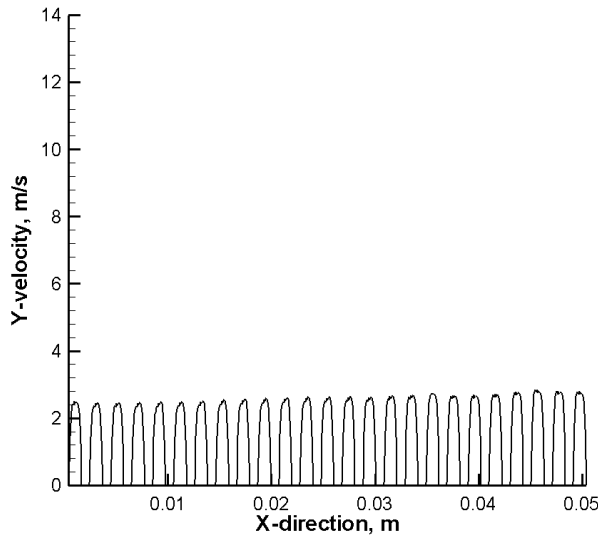
Y-velocity Distribution at the Midsection of the Channels



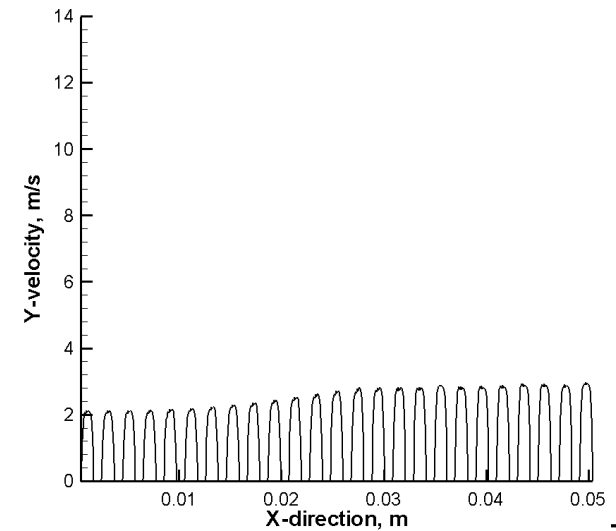
Case A (baseline design)



Case B (modified inlet manifold)

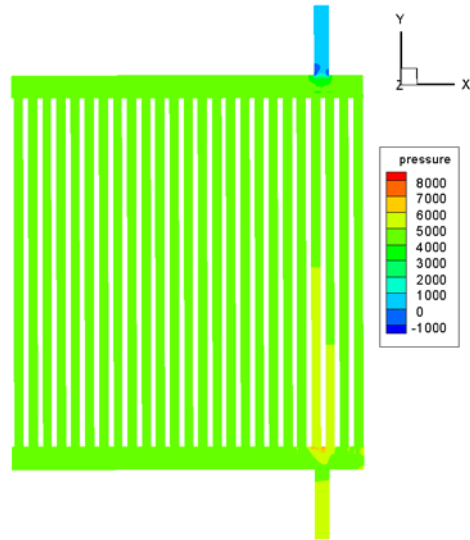


Case C (modified inlet and outlet manifold)

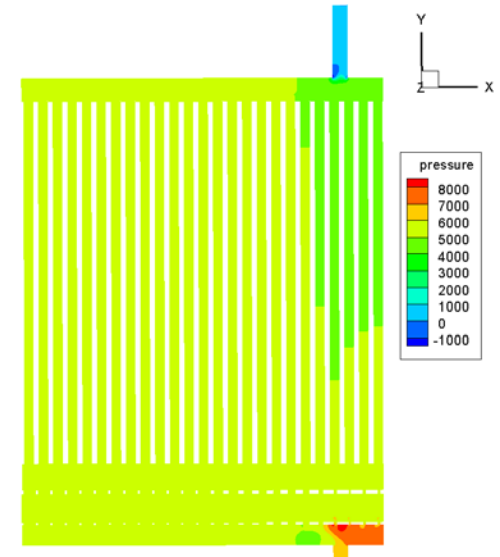


Case D (modified inlet, outlet manifold and supply channels)

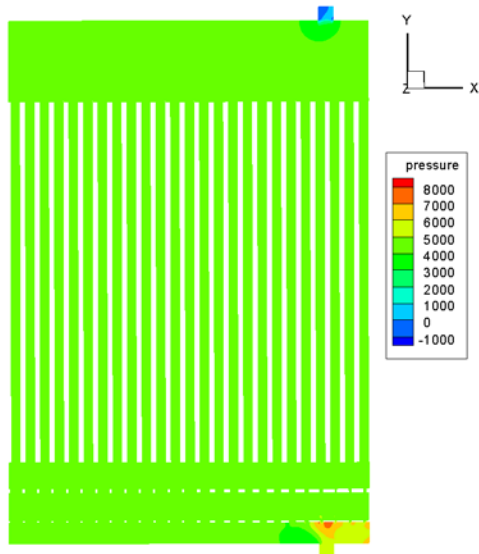
Pressure Distribution, Pa



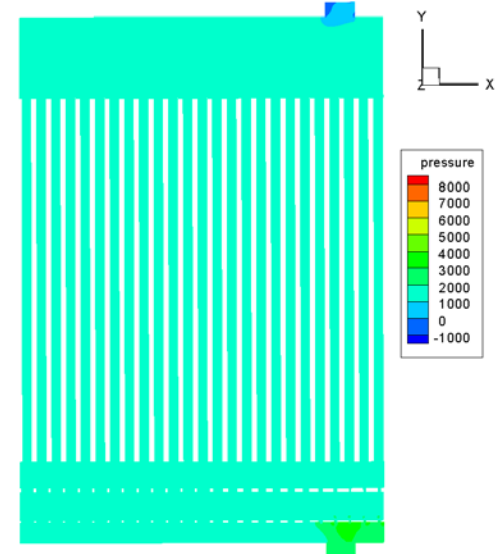
Case A (baseline design)



Case B (modified inlet manifold)

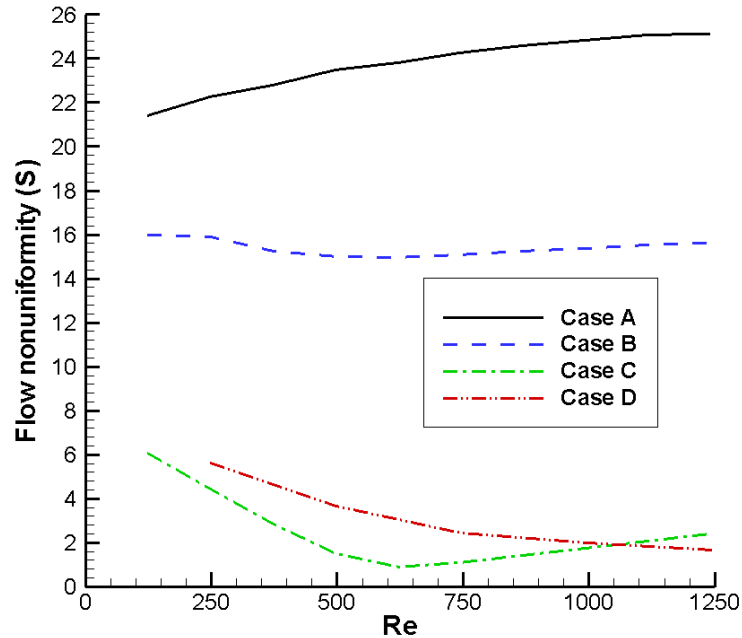


Case C (modified inlet and outlet manifold)

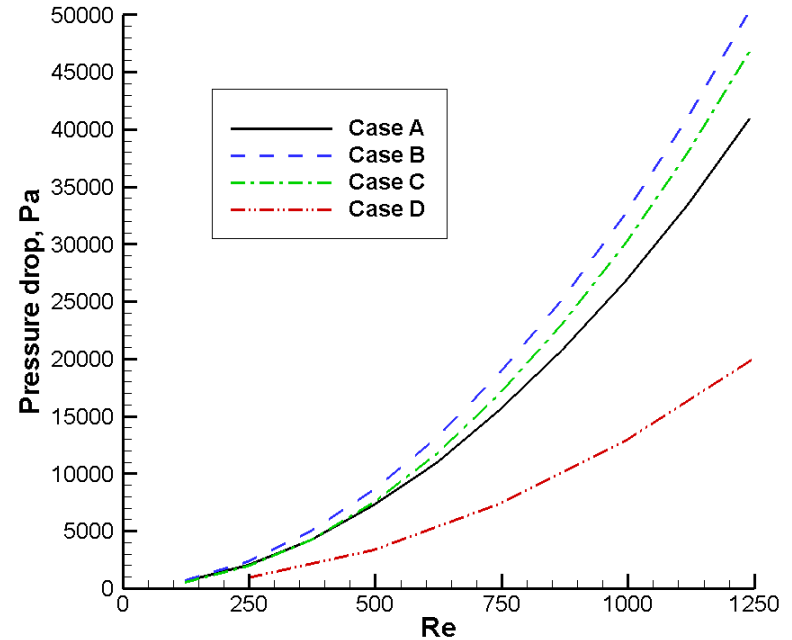


Case D (modified inlet, outlet manifold and supply channels)

Parametric Study



Flow nonuniformity parameter vs. Re



Overall pressure drop vs. Re

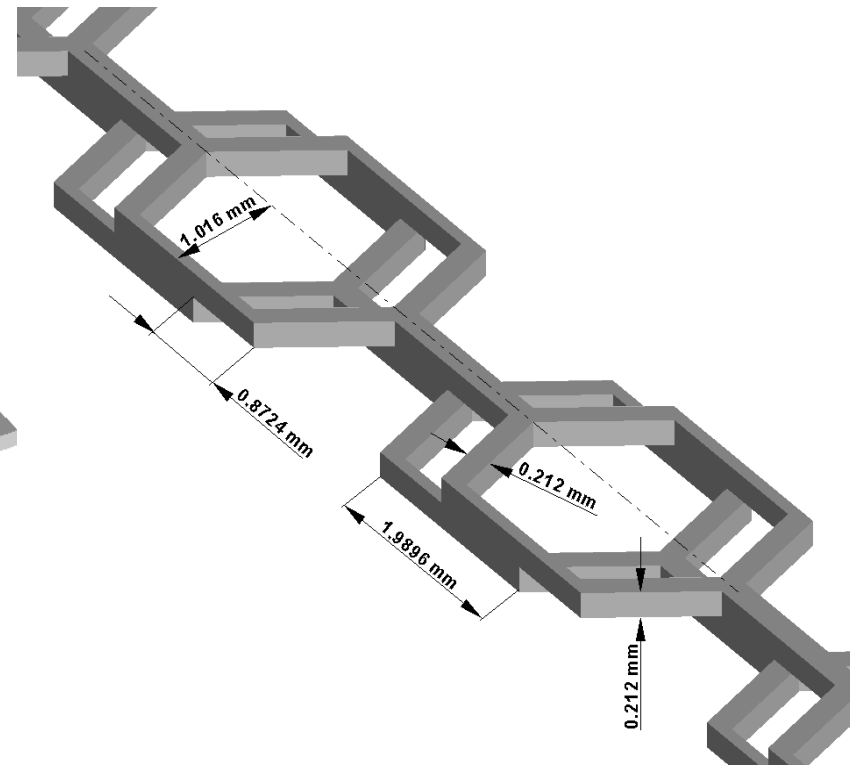
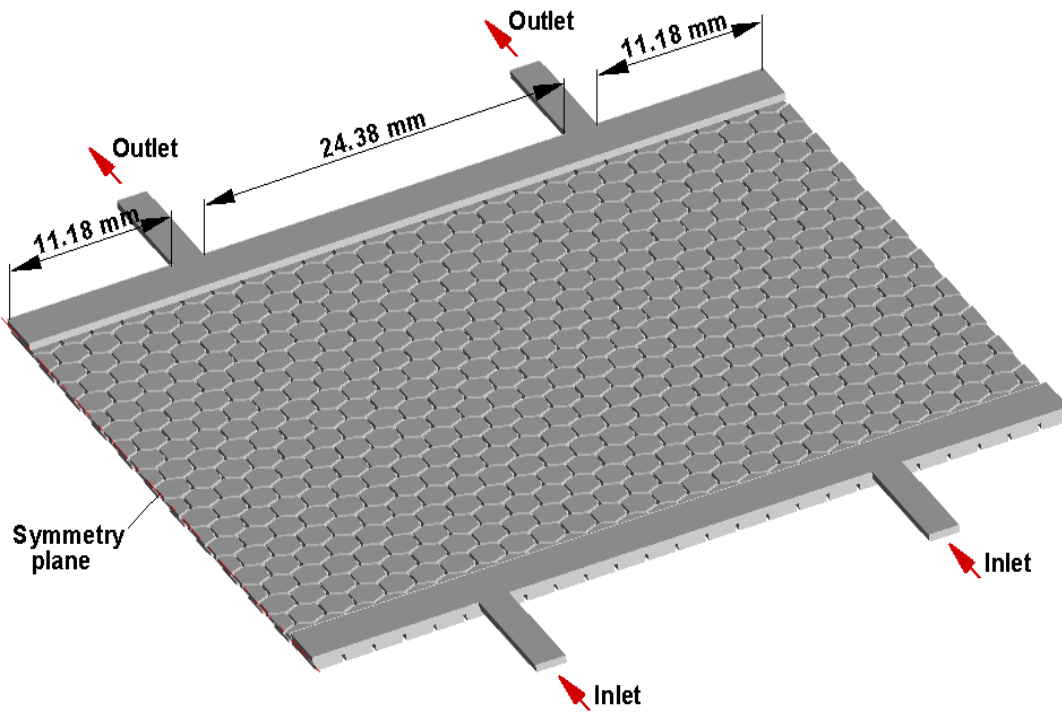
$$S_i = (g_i - g_a) / g_a$$

$$S = \sum_{i=1}^{25} |(g_i - g_a) / g_a|$$

Ref.: Zhang and Li (2003)

S_i - flow nonuniformity for individual channel
 S - sum of flow nonuniformity
 g_i - local mass flow rate for internal channel i
 g_a - mean mass flow rate for the cross-section

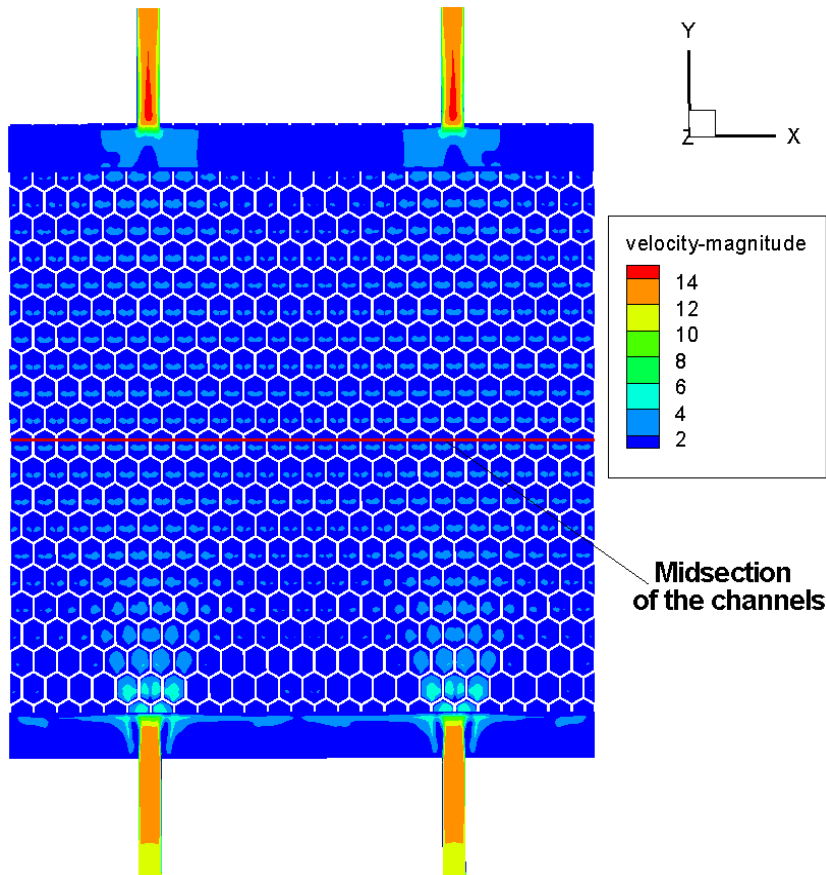
Improved Design with Hexagonal Channels



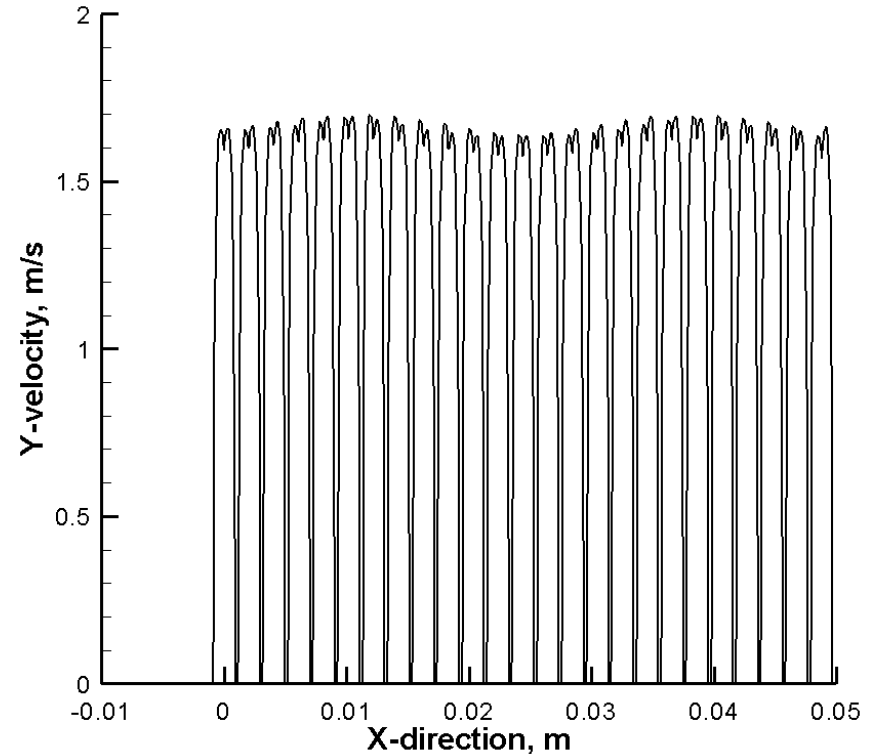
Geometry and dimensions of the single plate model with hexagonal channels

Dimensions of hexagonal channels (ceramic part)

Improved Design with Hexagonal Channels (Cont.)

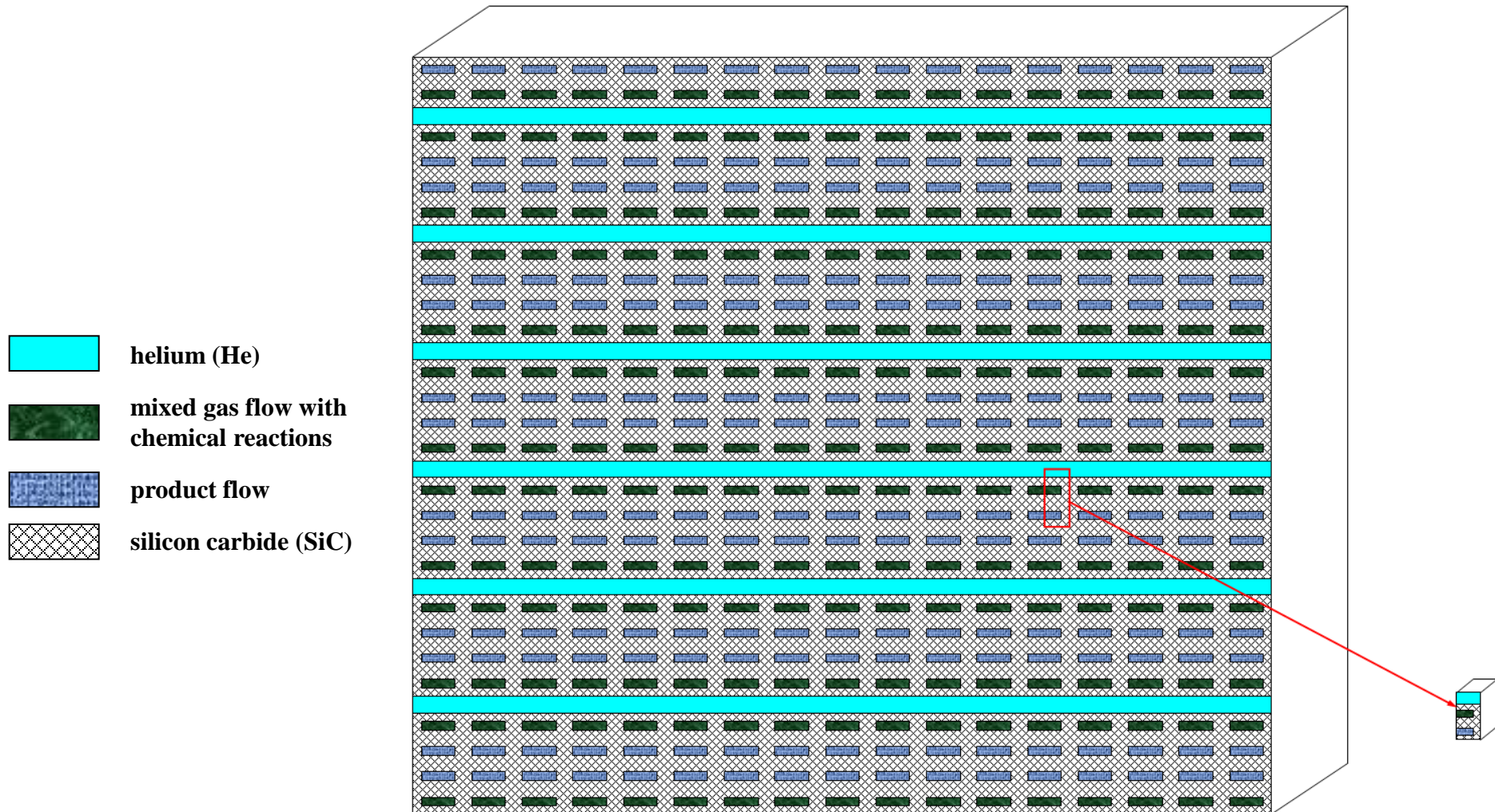


Velocity magnitude distribution for the geometry with hexagonal channels, m/s

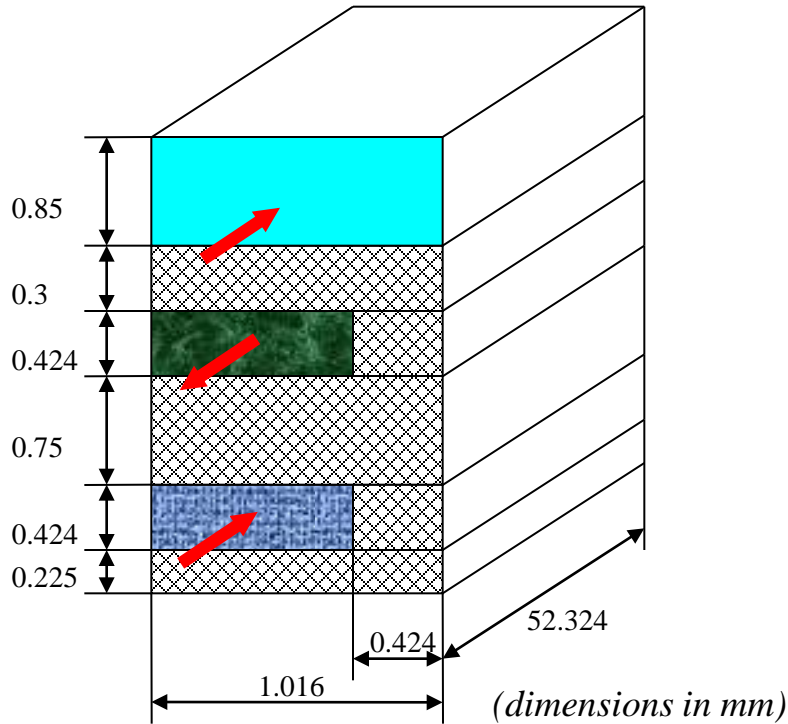


Y-velocity distribution at the midsection of the of the hexagonal channels in the lower plate, m/s

Single Channel Model - Baseline Design



Single Channel Model - Baseline Design (Cont.)



Boundary conditions

Inlet conditions for He part:

$$\dot{m} = 2.8175 \cdot 10^{-6} \text{ kg/s}; T = 1223.15 \text{ K (950}^\circ\text{C)}.$$

SI inlet for reacting flow:

$$\dot{m} = 6.296 \cdot 10^{-6} \text{ kg/s}; T = 974.9 \text{ K (701.75}^\circ\text{C)};$$





$$x_{\text{SO}_3} = 0.8163; x_{\text{SO}_2} = 0; x_{\text{O}_2} = 0; x_{\text{H}_2\text{O}} = 0.1837$$

SI inlet for reacting flow:

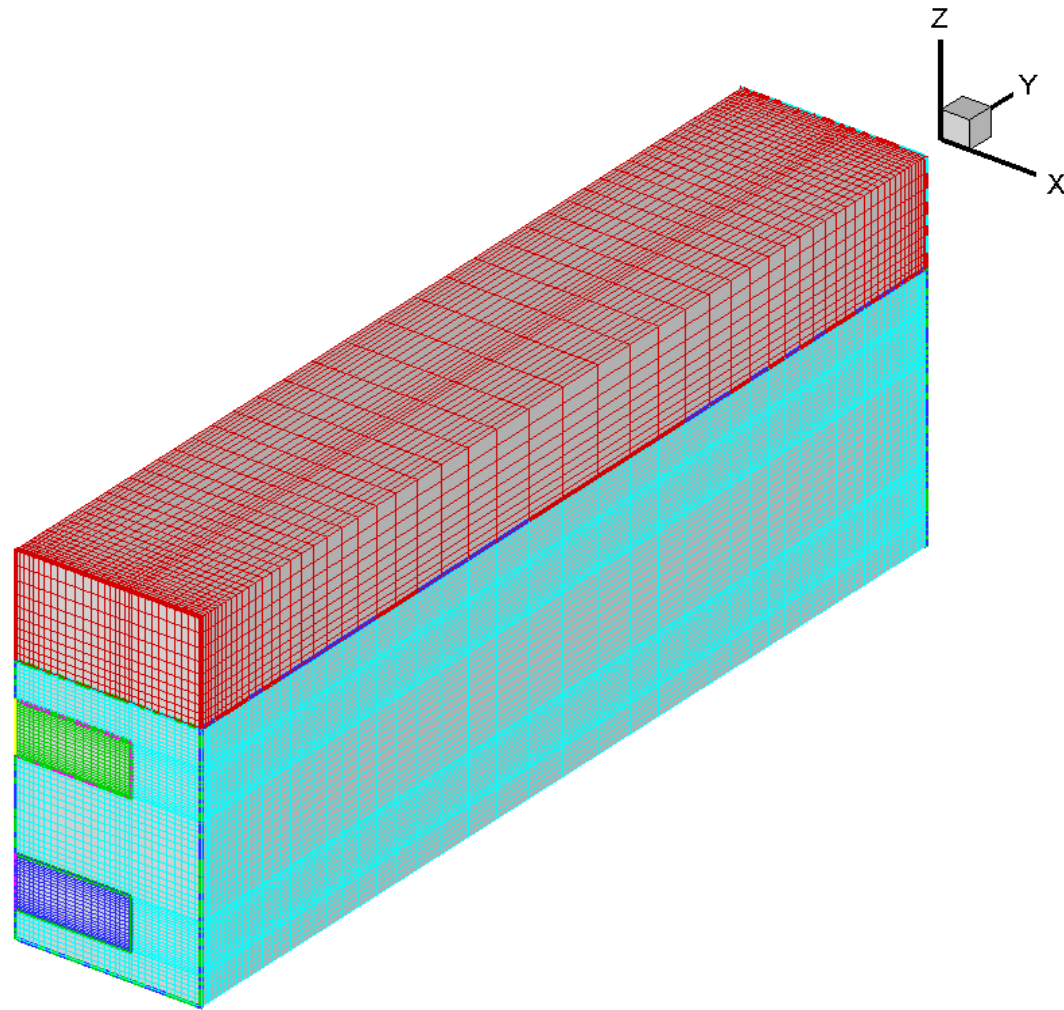
$$\dot{m} = 6.296 \cdot 10^{-6} \text{ kg/s}; T = 1223.15 \text{ K (950}^\circ\text{C)};$$

$$x_{\text{SO}_3} = 0; x_{\text{SO}_2} = 0.6532; x_{\text{O}_2} = 0.1631; x_{\text{H}_2\text{O}} = 0.1837$$

Operation pressure is 1.5 MPa

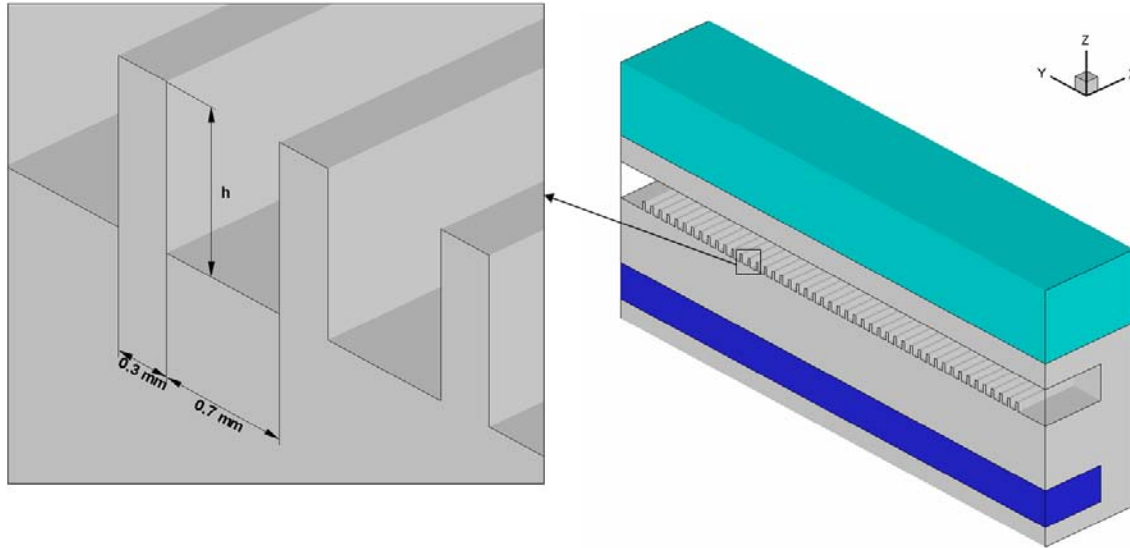
-  helium (He)
-  mixed gas flow with chemical reactions: $\text{H}_2\text{O} + \text{SO}_3 + \text{H}_2\text{SO}_4 \rightarrow \text{H}_2\text{O} + \text{SO}_2 + \text{O}_2 + \text{SO}_3$
-  mixed gas flow without chemical reactions: $\text{H}_2\text{O} + \text{SO}_2 + \text{O}_2 + \text{SO}_3$
-  silicon carbide (SiC)

Computational Mesh

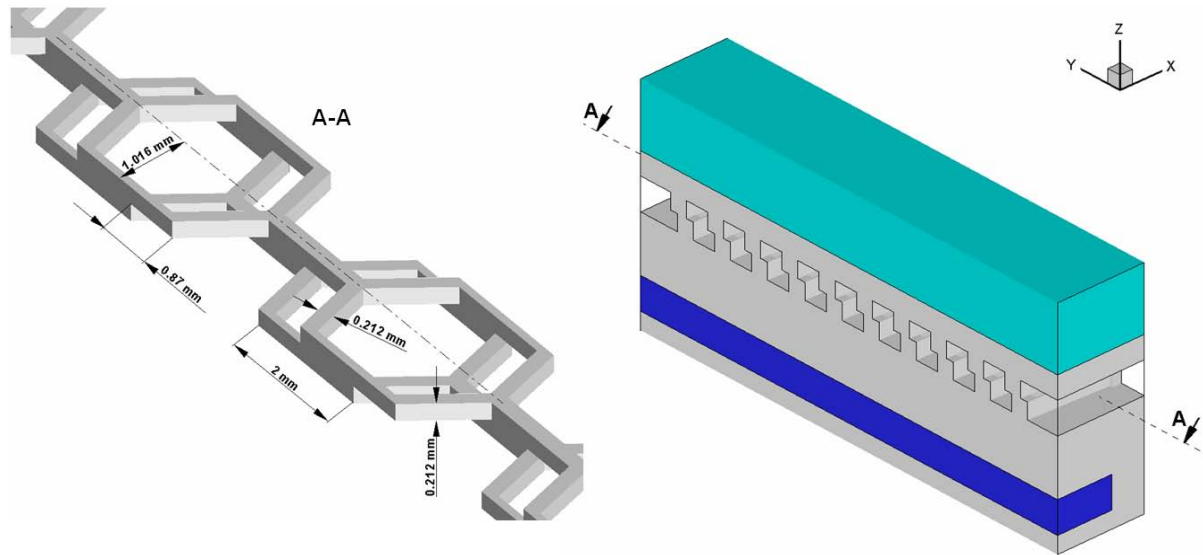


163,735 nodes 145,800 cells

Alternative Designs

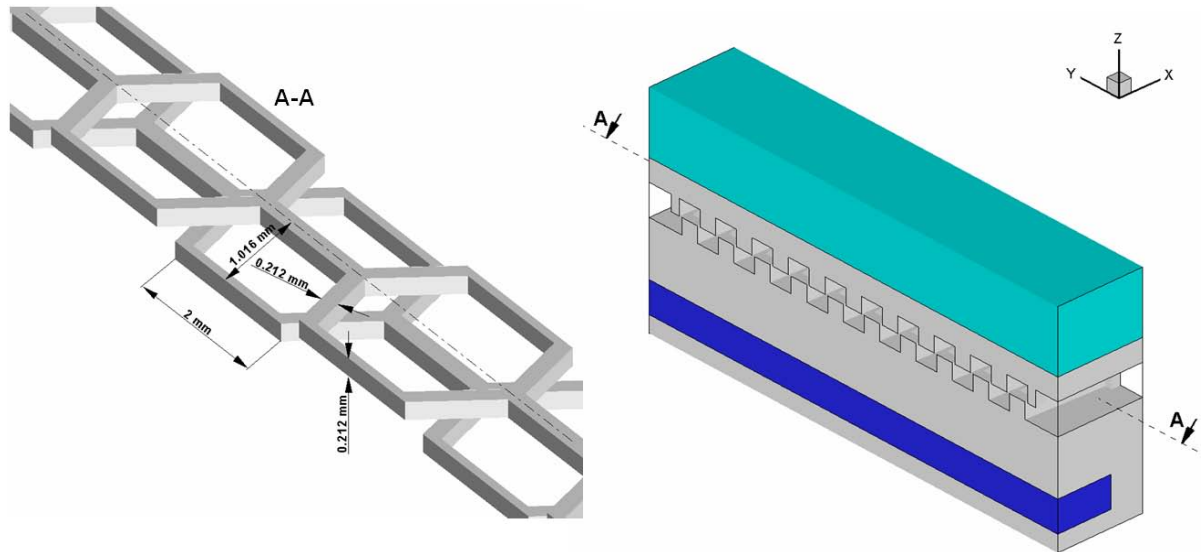


Ribbed ground channel, $h=0.1 \text{ mm}$, $h=0.2 \text{ mm}$,

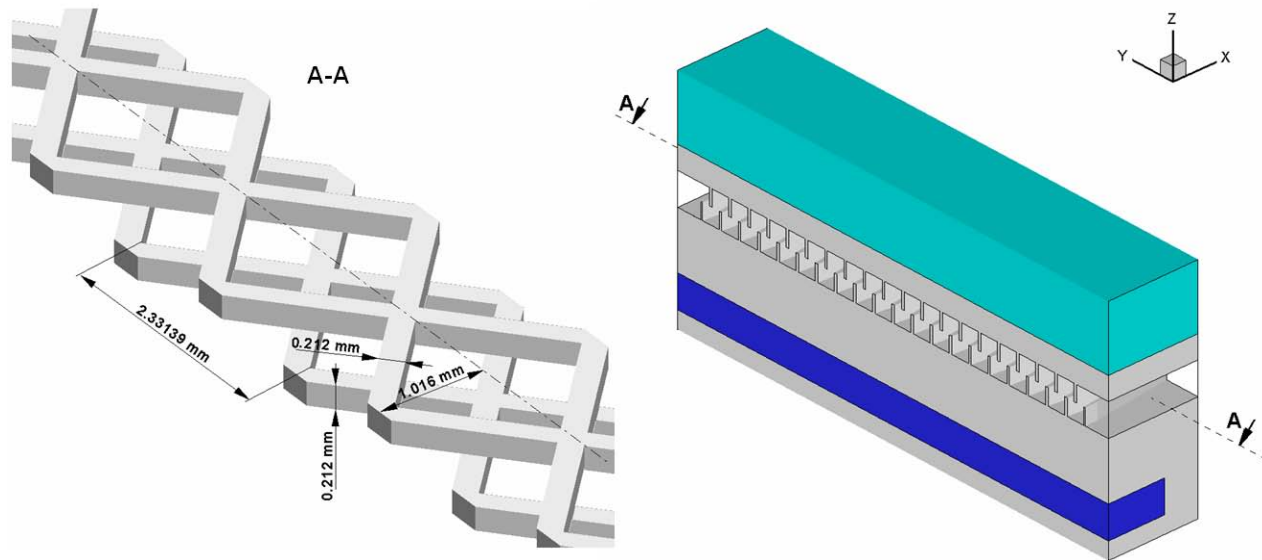


Two hexagonal layers under 50% of layers overlapping

Alternative Designs (Cont.)

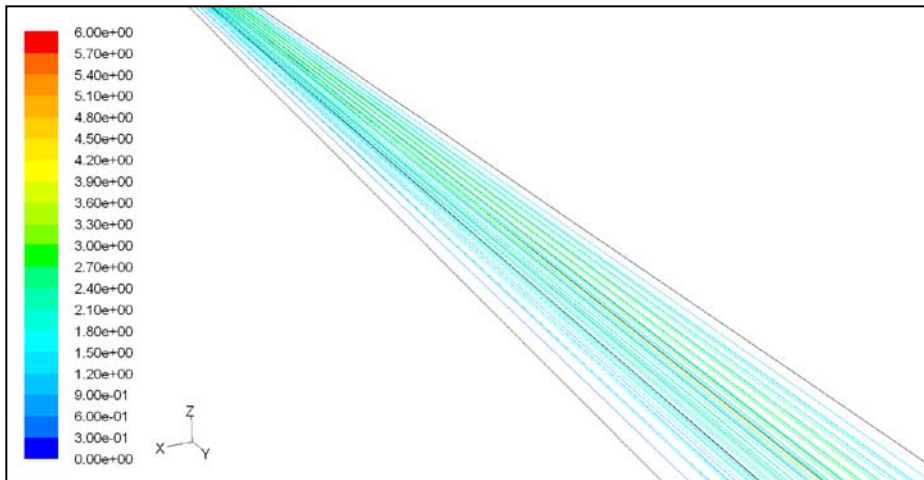


Two hexagonal layers under 100% of layers overlapping

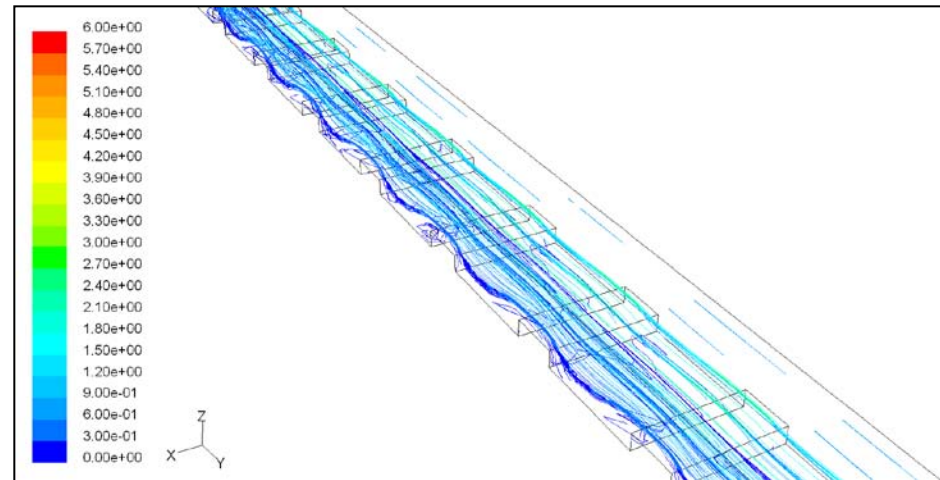


Diamond-shaped channel

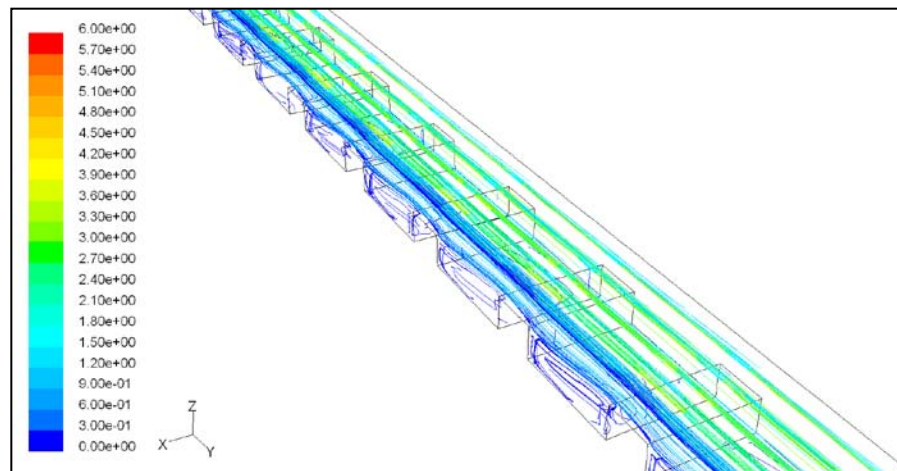
Reacting Flow Streamlines Colored by Velocity Magnitude, m/s



Baseline design

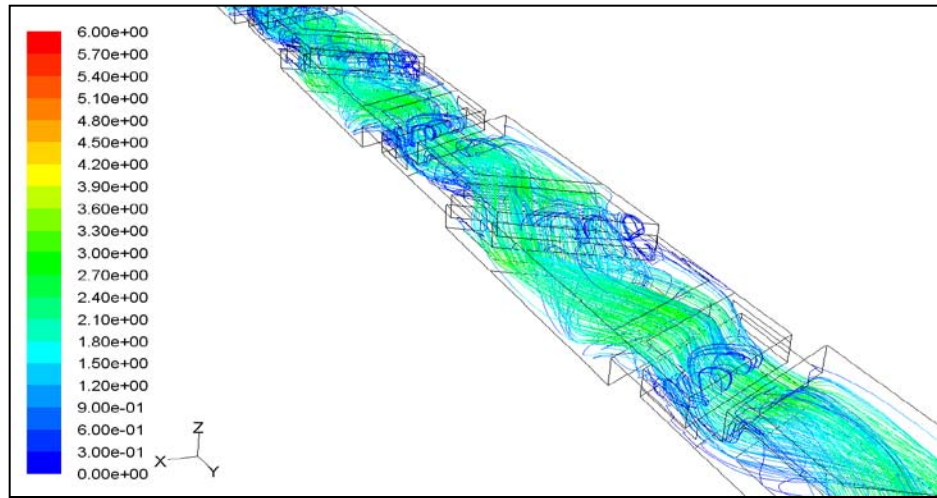


Ribbed ground channel (ribs height – 0.1mm)

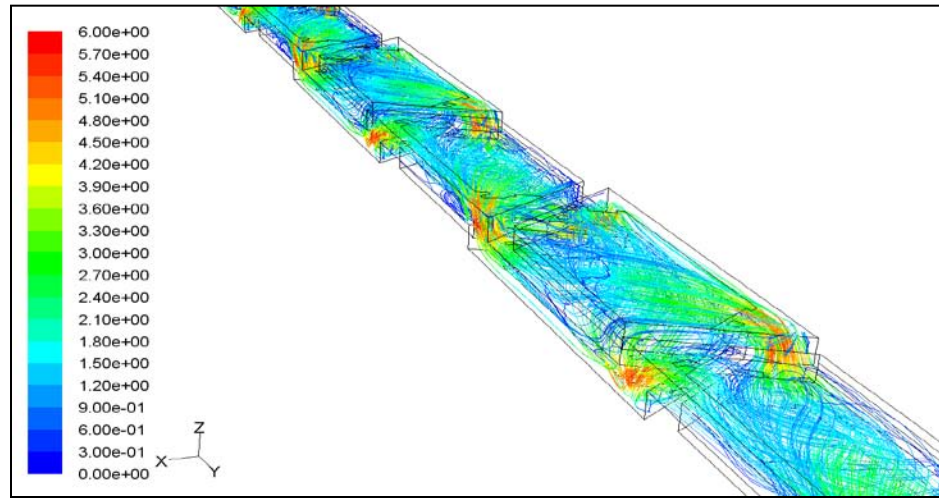


Ribbed ground channel (ribs height – 0.2mm)

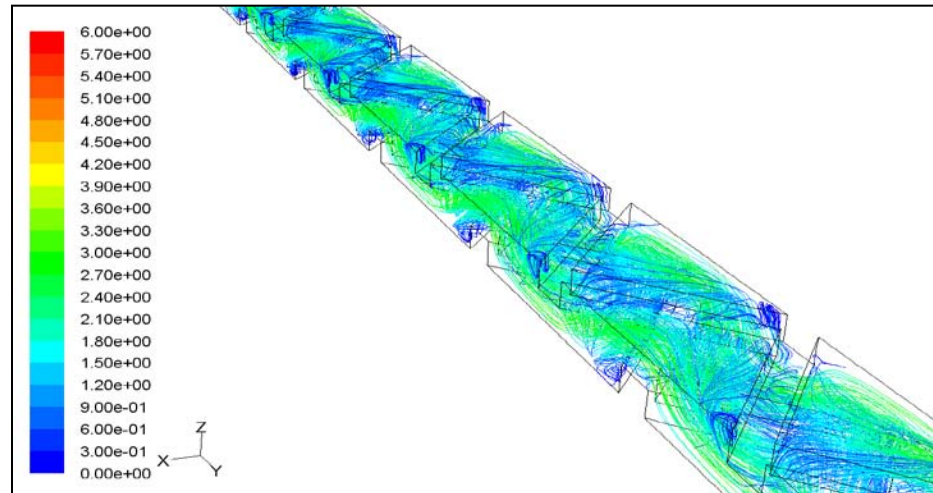
Reacting Flow Streamlines Colored by Velocity Magnitude, m/s (Cont.)



Two hexagonal layers
under 50% of layers overlapping

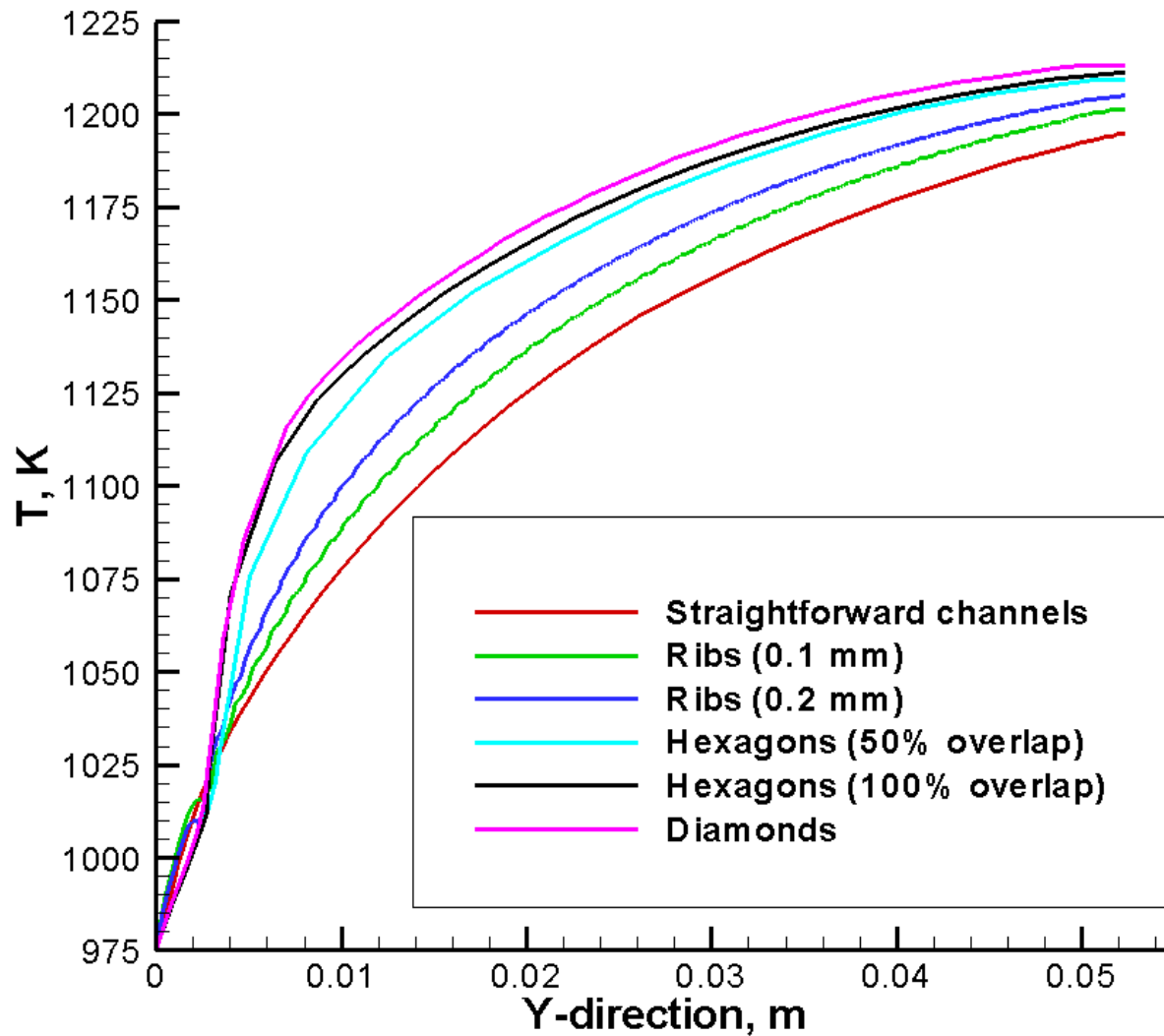


Two hexagonal layers
under 100% of layers overlapping

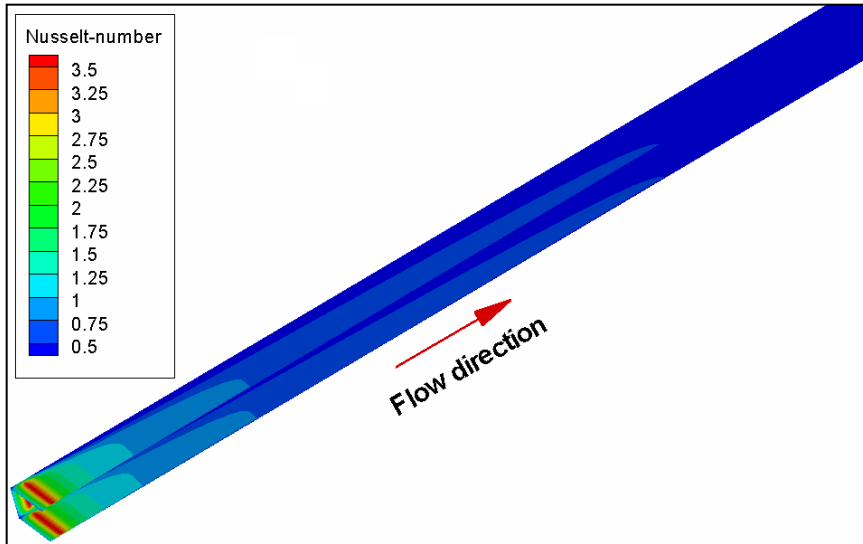


Diamond-shaped channel

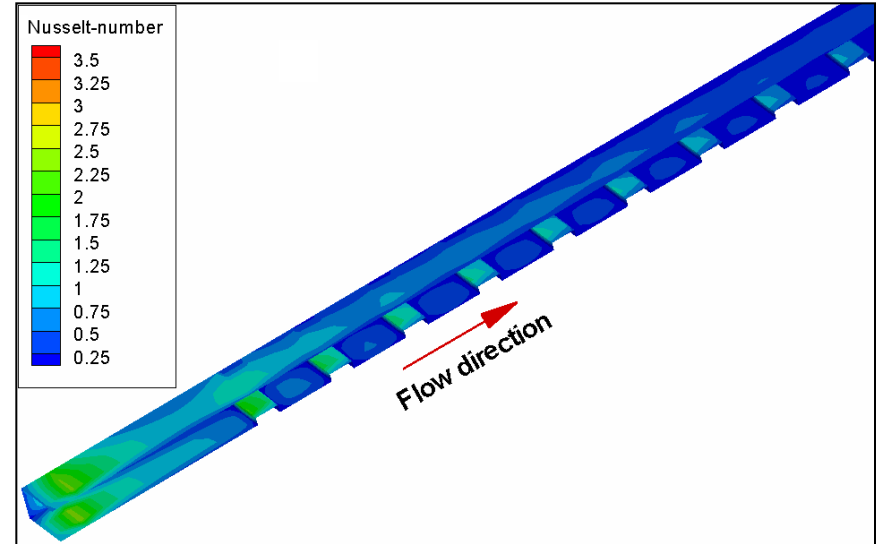
Temperature Distribution along the Reacting Flow



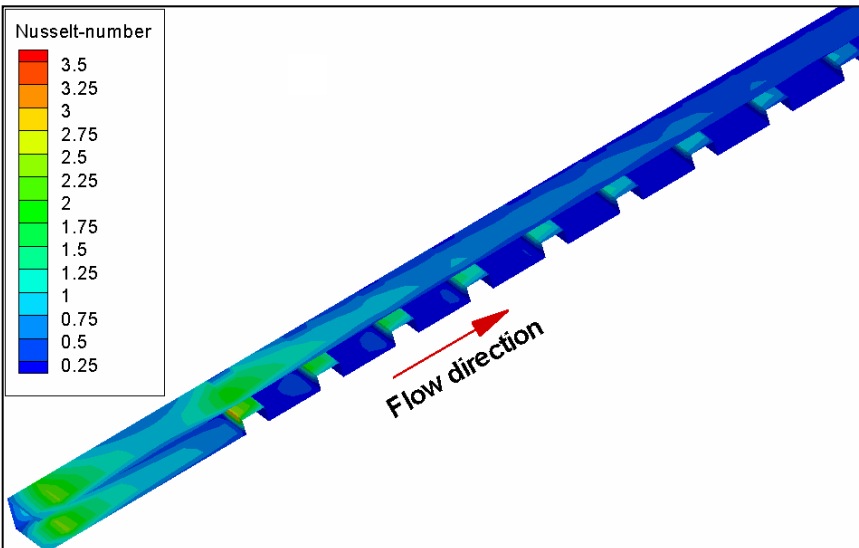
Nusselt Number Distribution along the Channel Flow Wall



Baseline design



Ribbed ground channel (ribs height – 0.1mm)



Ribbed ground channel (ribs height – 0.2mm)

$$Nu = \frac{hD_h}{k}; \quad h = \frac{q}{T_b - T_w};$$

h – heat transfer coefficient;

D_h – hydraulic diameter;

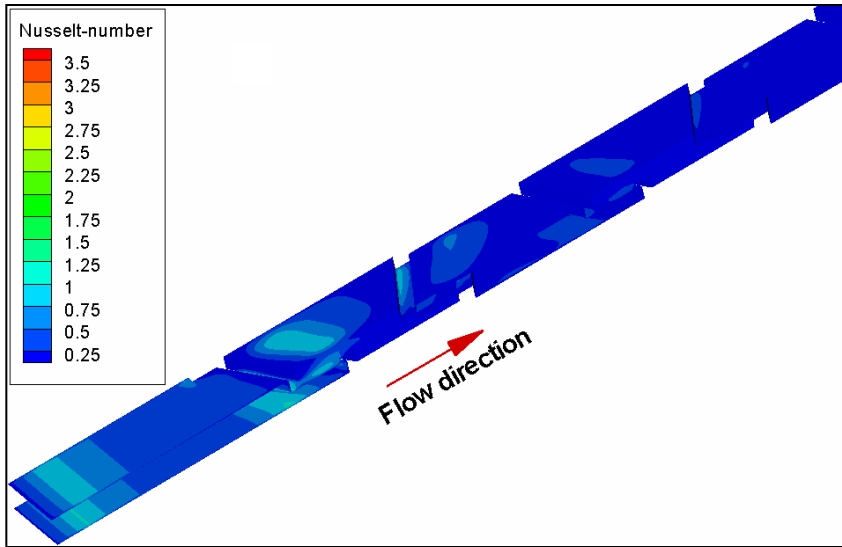
k – thermal conductivity of the fluid;

q – local wall heat flux;

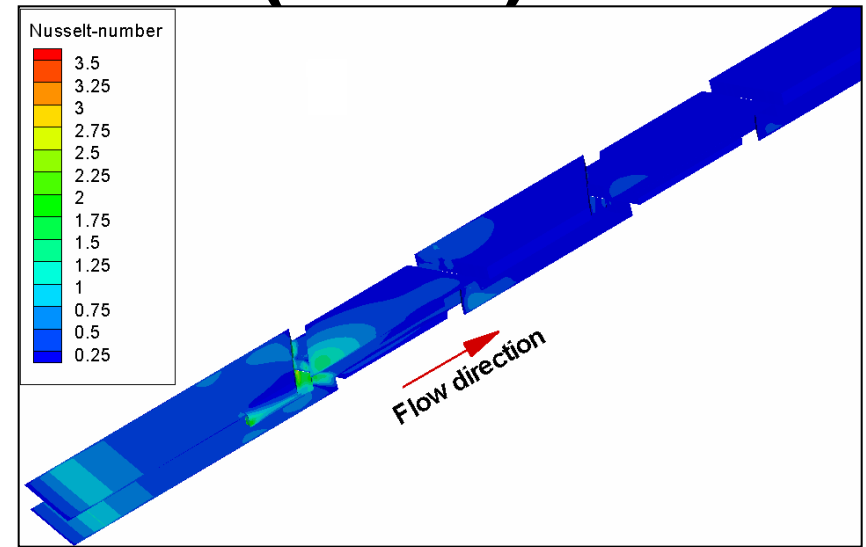
T_b – bulk temperature;

T_w – local wall temperature

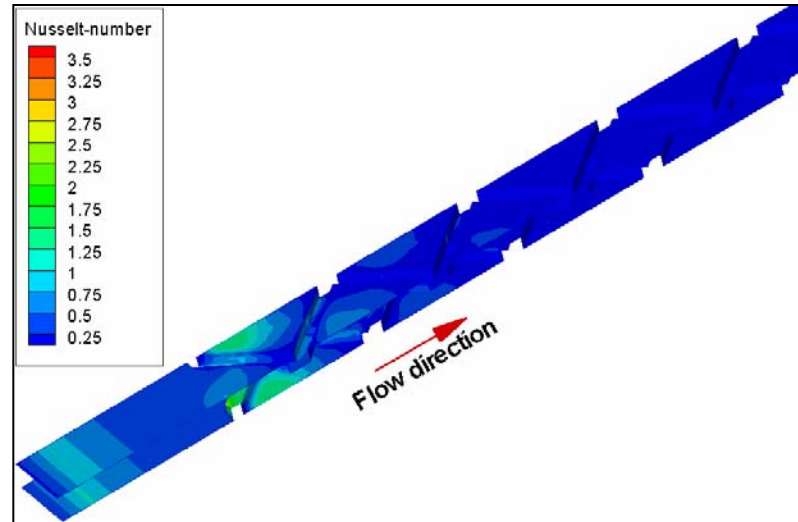
Nusselt Number Distribution along the Channel Flow Wall (Cont.)



Two hexagonal layers
under 50% of layers overlapping



Two hexagonal layers
under 100% of layers overlapping



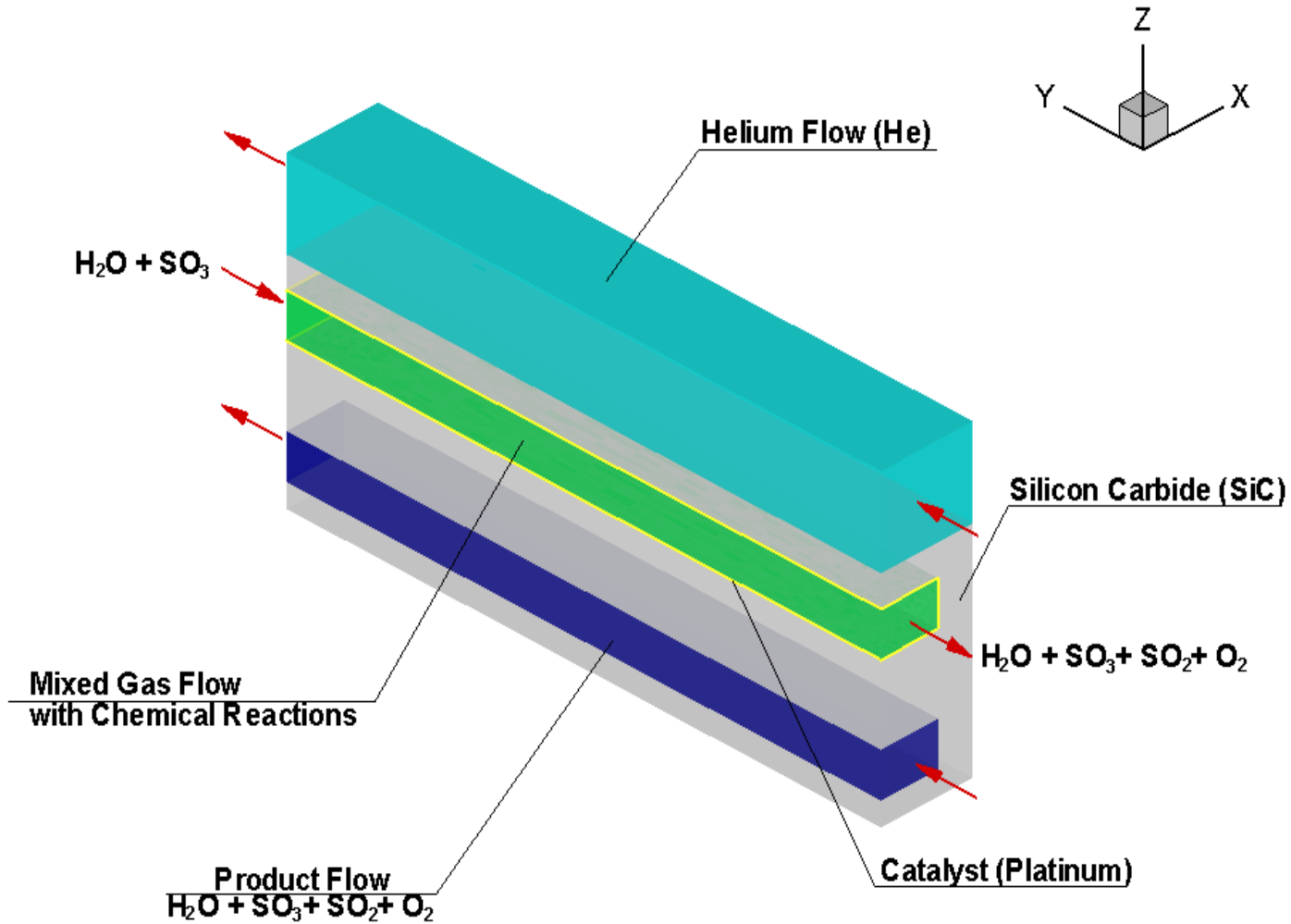
Diamond-shaped channel

Friction Factor and Effectiveness

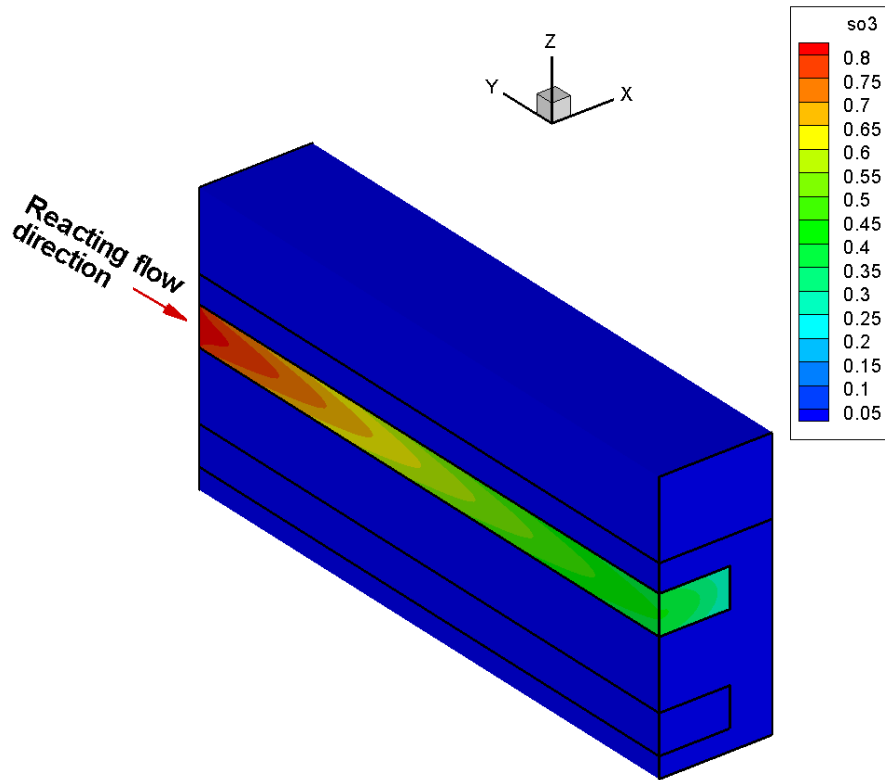
Name of case	Friction factor, f	Effectiveness, ε	Effectiveness relative to baseline case, %
Straightforward channels	0.151	0.895	-
Ribs (0.1 mm)	0.304	0.924	3.24
Ribs (0.2 mm)	0.724	0.934	4.18
Hexagons (50% overlap)	1.851	0.951	6.26
Hexagons (100% overlap)	8.824	0.953	6.48
Diamonds	3.598	0.959	7.15

$$f = \frac{-\left(\frac{\Delta p}{L}\right)d_h}{\frac{1}{2}\rho U^2} ; \quad \varepsilon = \frac{Q}{Q_{max}}$$

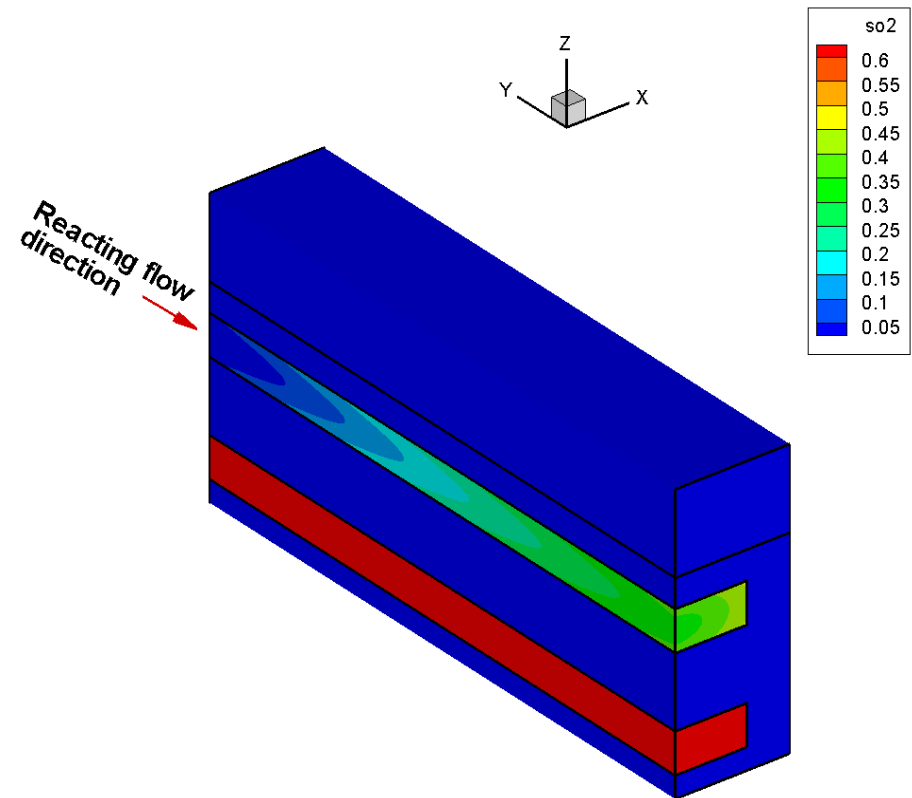
Chemical Reactions Modeling



Results of Chemical Reactions Modeling for the Baseline Case

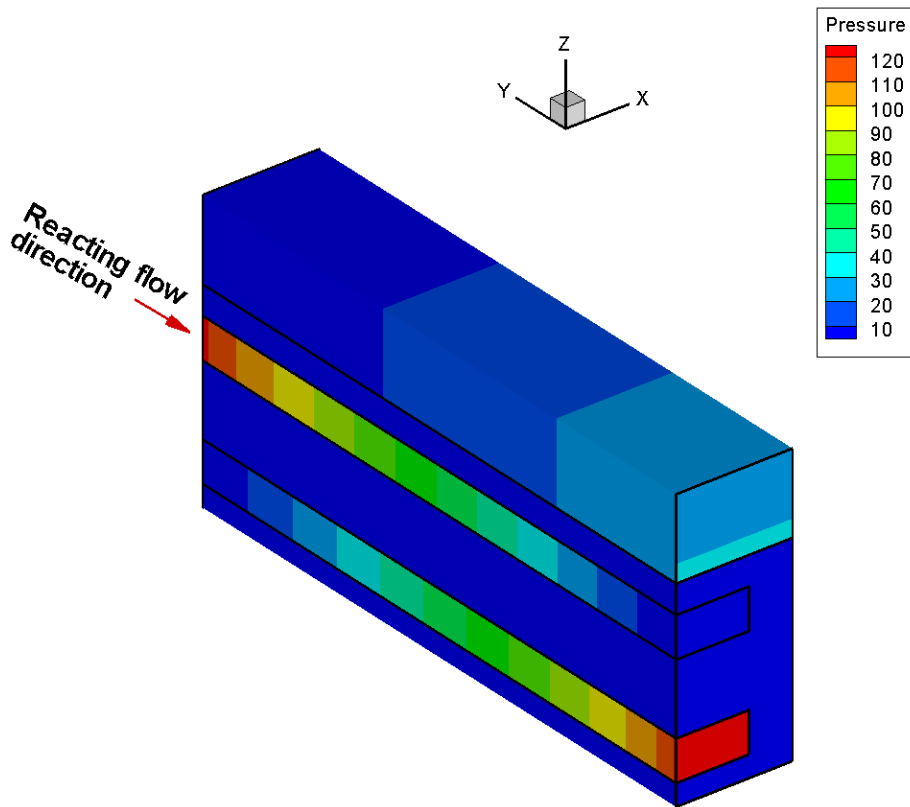


*Mass fraction of SO_3
for the channel with chemical reaction*

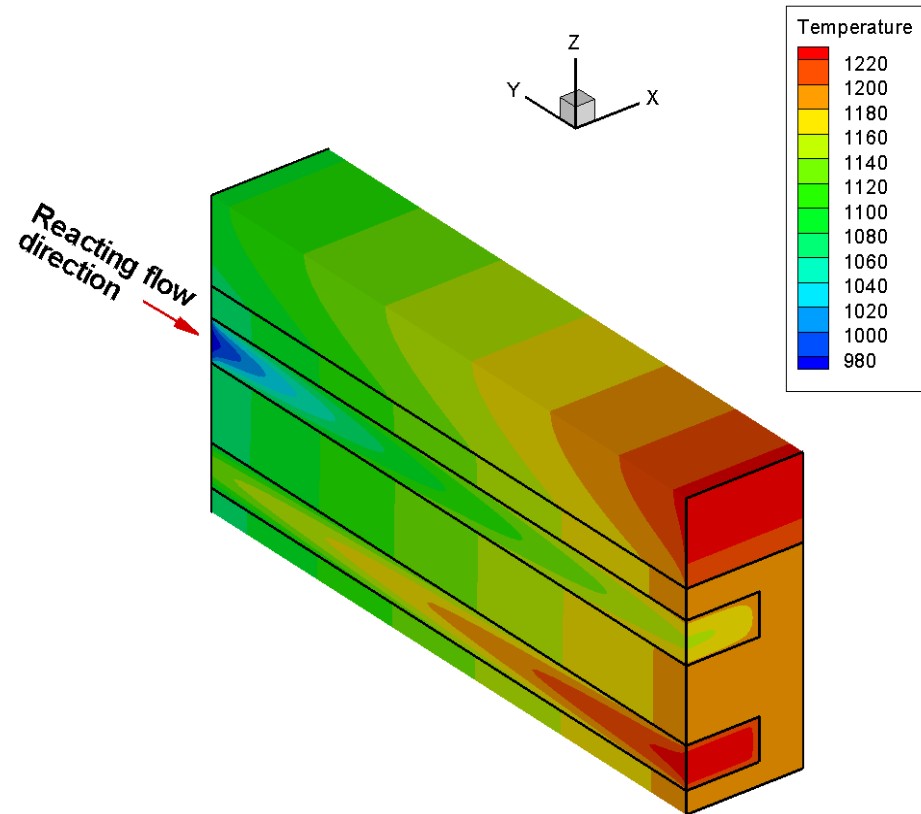


*Mass fraction of SO_2
for the channel with chemical reaction*

Results of Chemical Reactions Modeling for the Baseline Case (Cont.)

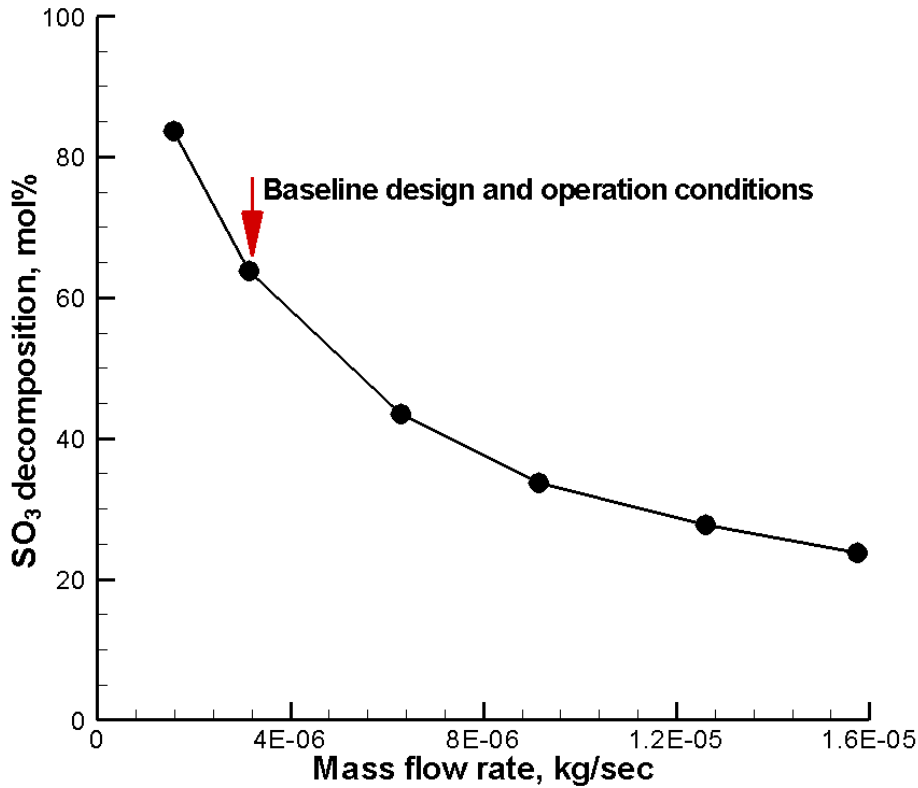


Static pressure distribution, Pa

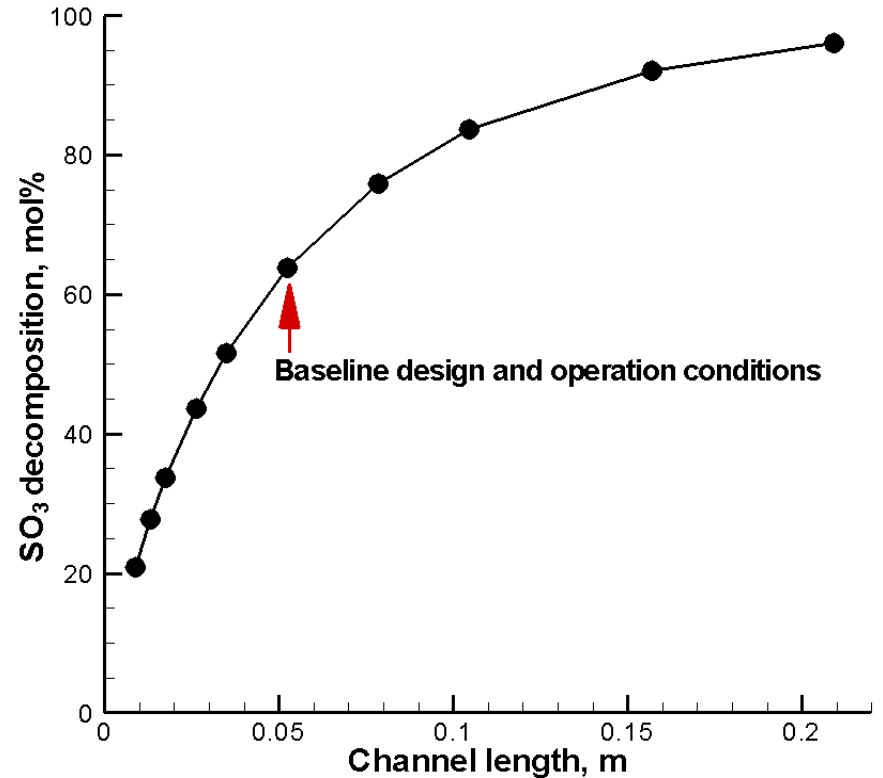


Temperature distribution, K

Parametric Study of the SI Decomposer Design

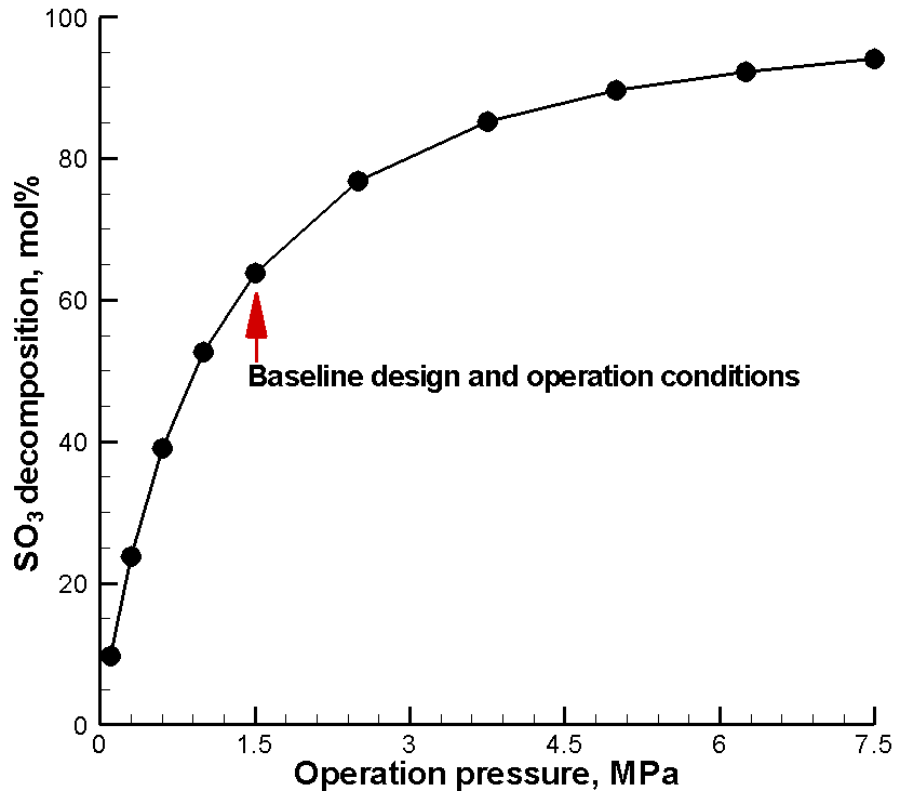


Percentage decomposition of SO₃ versus different mass flow rates in the reacting flow

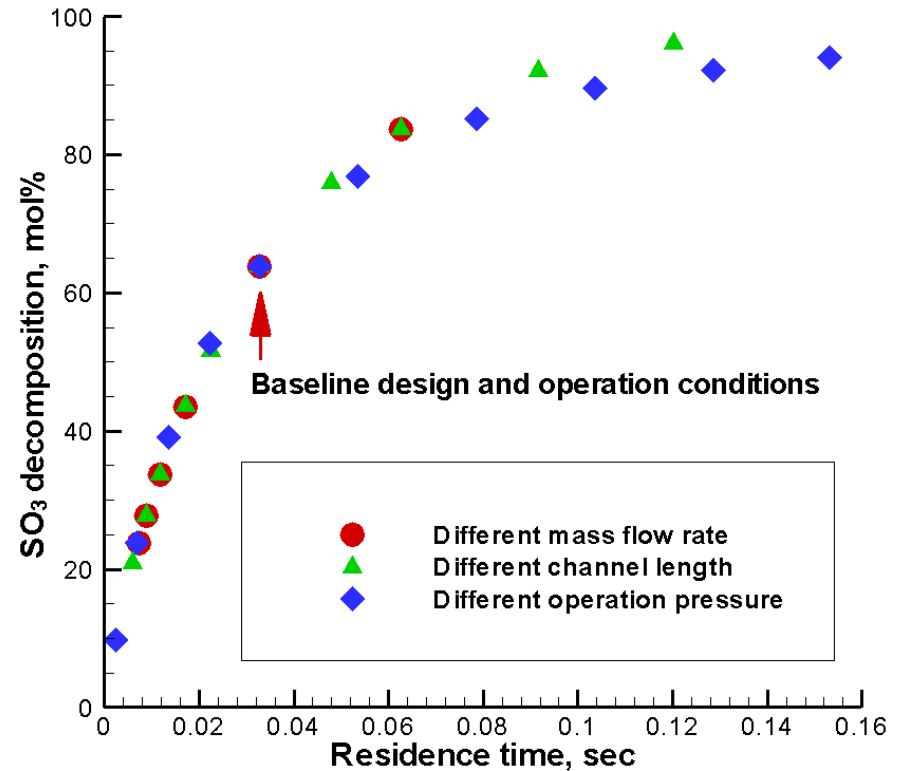


Percentage decomposition of SO₃ versus channel length

Parametric Study of the SI Decomposer Design (Cont.)

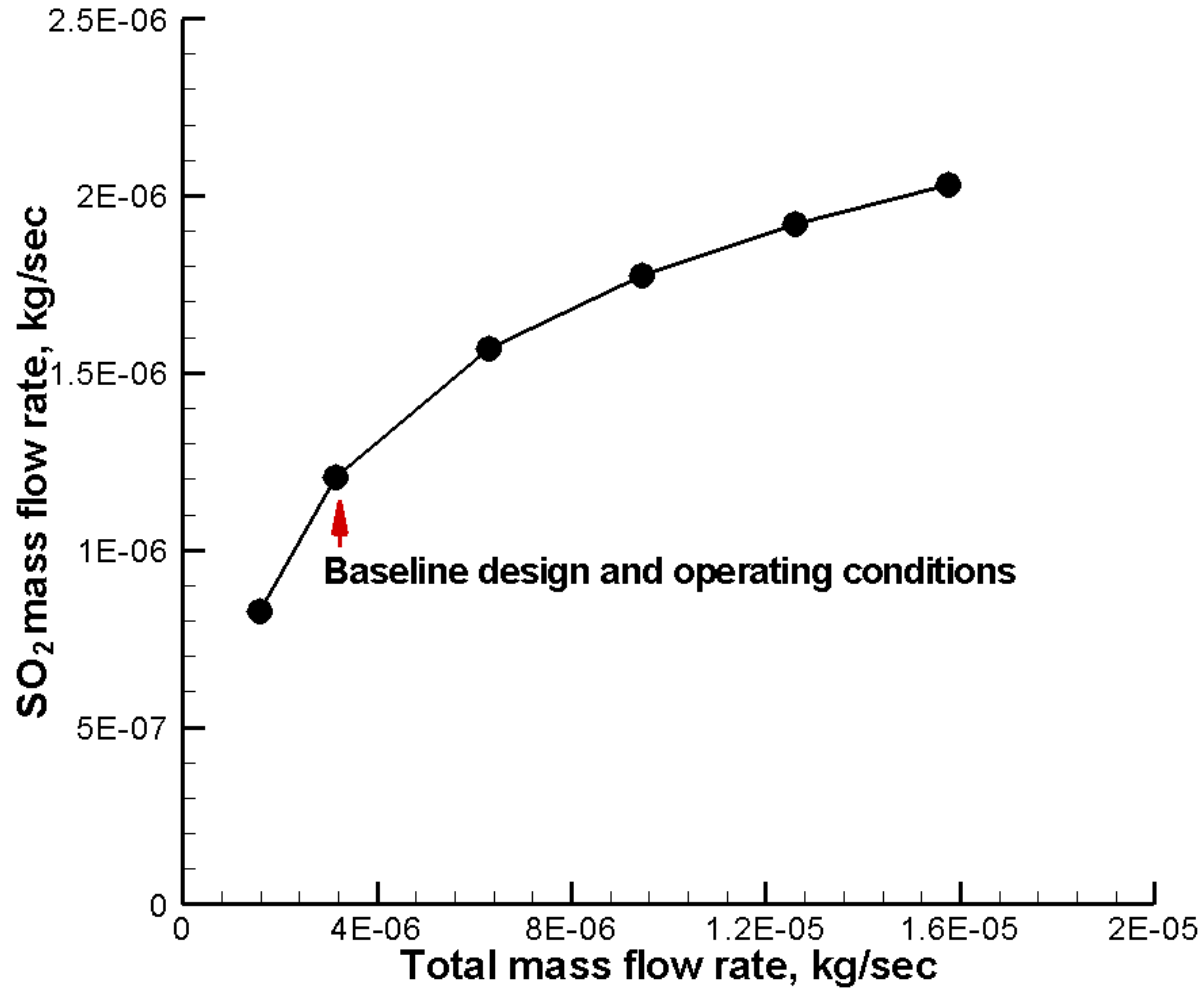


Percentage decomposition of SO₃ versus operation pressure

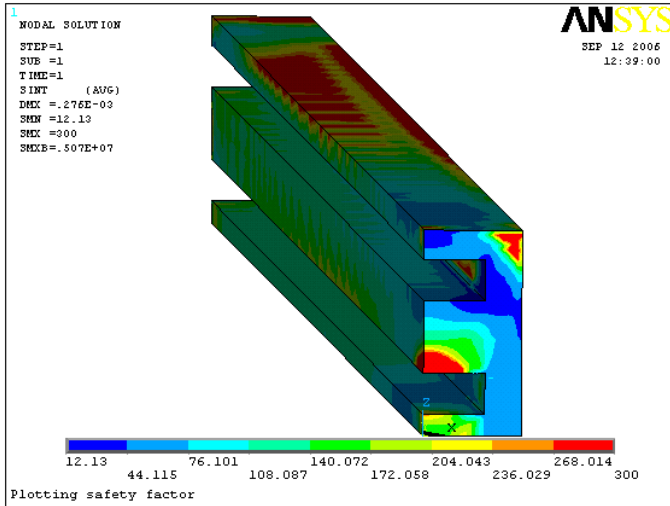


Percentage decomposition of SO₃ versus residence time

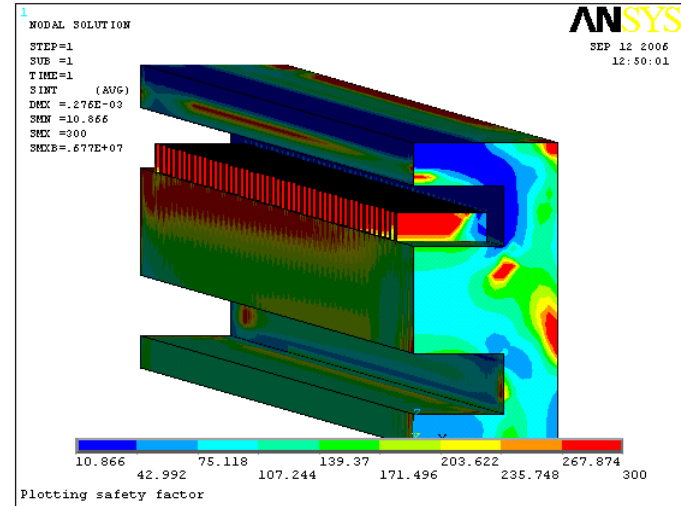
SO₂ Mass Flow Rate at the Output of Reacting Flow Channel (Throughput) vs. Total Reacting Flow Mass Flow Rate



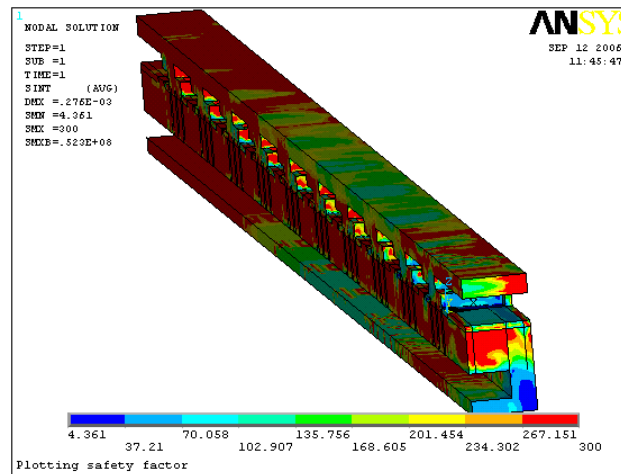
Safety Factor Based on Mohr-Coloumb Criteria



Baseline case

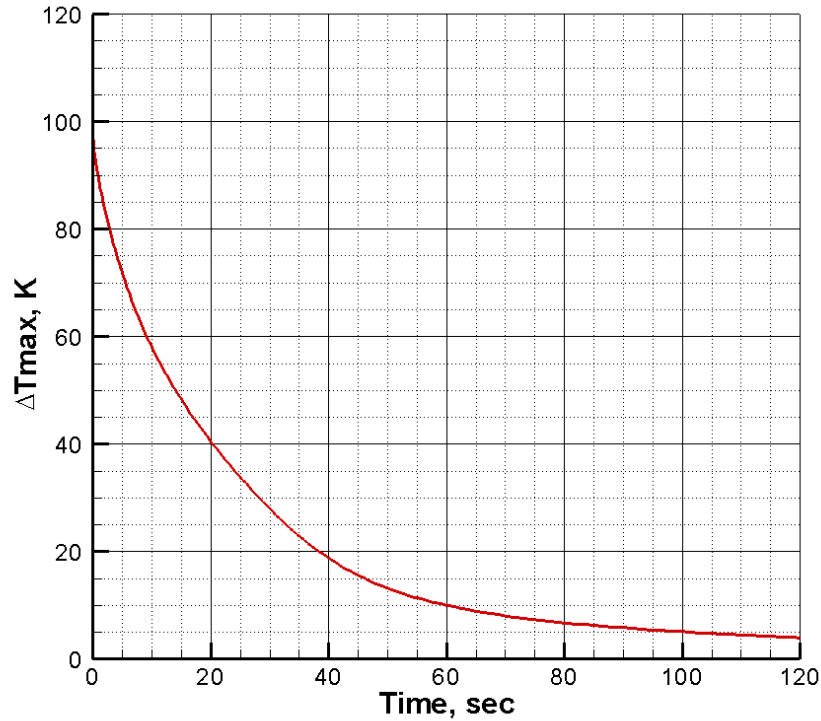


Ribbed channel case

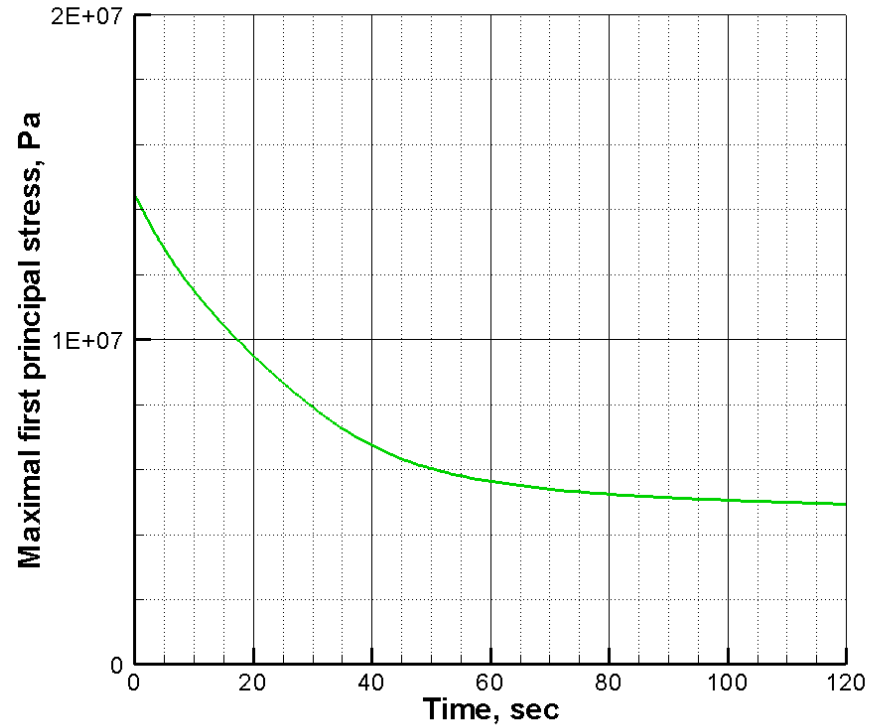


Hexagonal channel case

Stress Analysis of Transient Process (Shutdown Process)



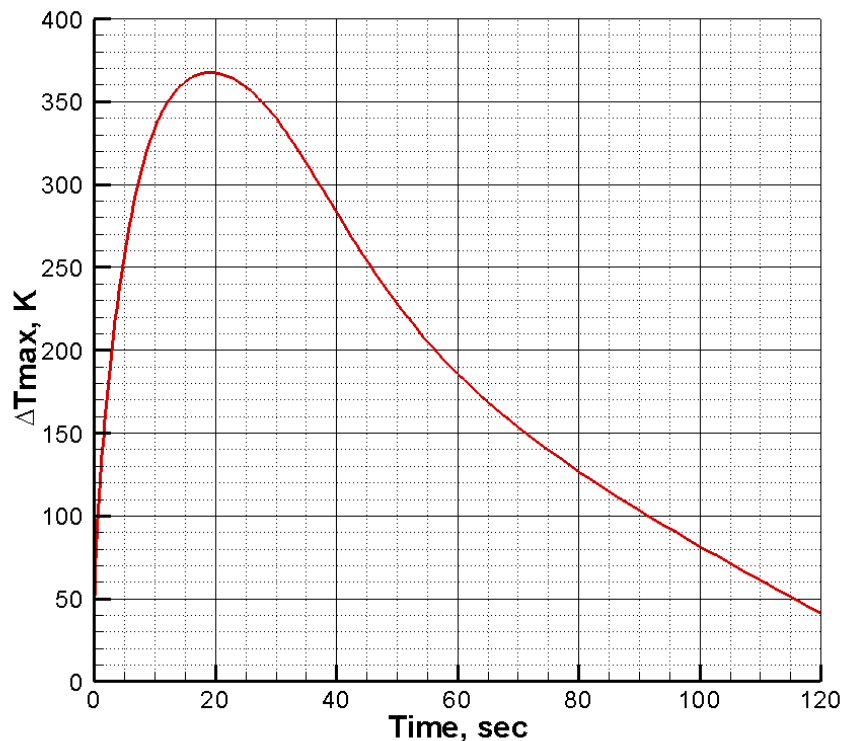
***Maximal temperature difference
in solid part vs. time***



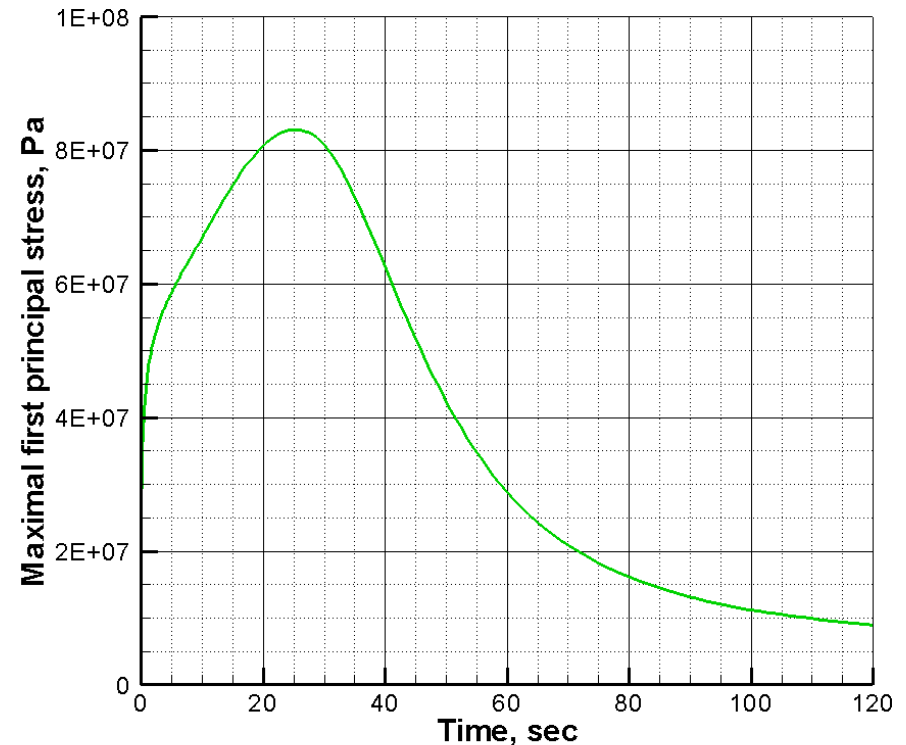
***Maximal first principal stress
in solid part vs. time***

The transient regime started from working condition and suddenly all of the inlets and outlets closed simultaneously

Stress Analysis of Transient Process (Hot Helium Coming to the Decomposer in Room Temperature)



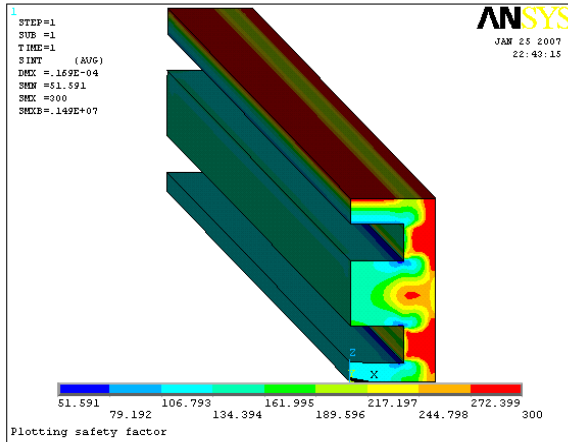
*Maximal temperature difference
in solid part vs. time*



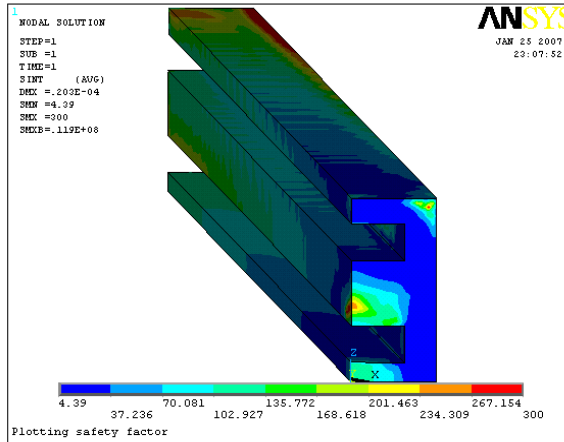
*Maximal first principal stress
in solid part vs. time*

The transient regime started from no flow conditions in room temperature (293.15 K) and suddenly the hot helium with temperature 1223.15 K started to flow in the helium channel

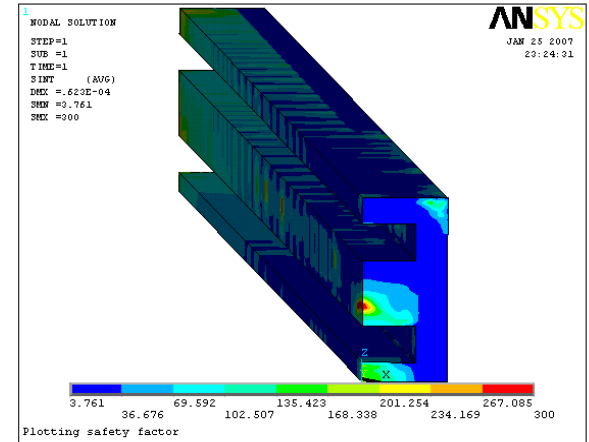
Safety Factor for the Transient Process



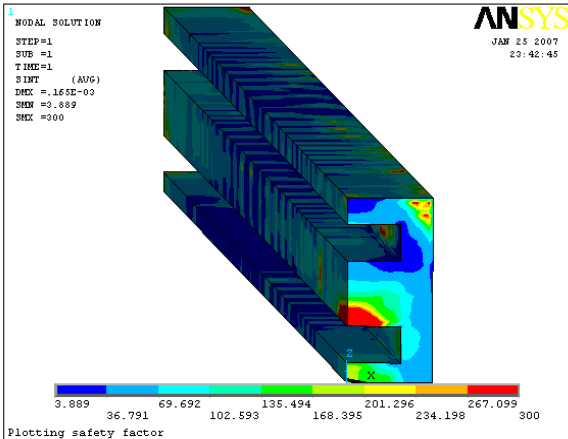
t=0 sec



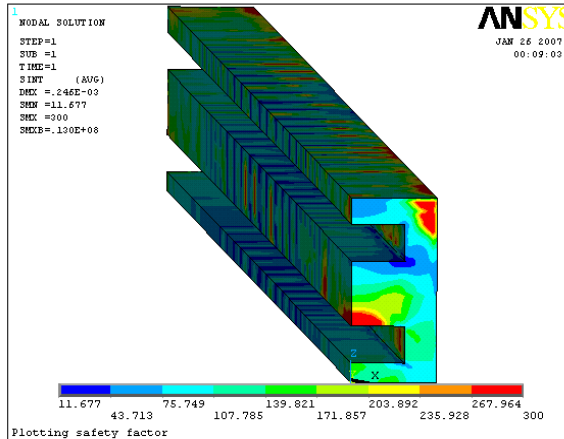
t=1 sec



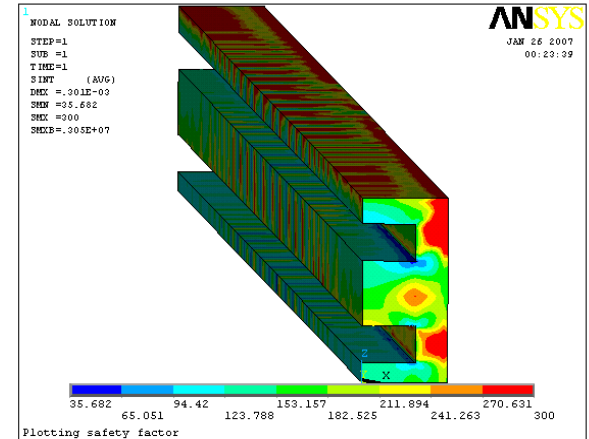
t=10 sec



t=30 sec



t=60 sec



t=120 sec

Results of Calculations for Baseline and Alternative Designs

Name of case	Area of chemical reaction, m ²	Volume of reacting flow, m ³	Area/Volume, m ² /m ³	Percentage of SO ₃ decomposition, %	Pressure drop, Pa
Straightforward channels	$8.864 \cdot 10^{-5}$	$1.409 \cdot 10^{-8}$	6291	63.81	128.7
Ribs - 0.1 mm	$9.320 \cdot 10^{-5}$	$1.319 \cdot 10^{-8}$	7065	64.25	240.8
Ribs - 0.2 mm	$9.756 \cdot 10^{-5}$	$1.234 \cdot 10^{-8}$	7906	65.57	573.2
Hexagons - 50% overlap	$1.330 \cdot 10^{-4}$	$1.903 \cdot 10^{-8}$	6989	76.31	802.4
Hexagons - 100% overlap	$1.359 \cdot 10^{-4}$	$1.903 \cdot 10^{-8}$	7141	77.73	3815.8
Diamonds	$1.480 \cdot 10^{-4}$	$1.736 \cdot 10^{-8}$	8525	79.95	1570.3

Bayonet Heat Exchanger and Decomposer Design

Boiler

Heat H_2SO_4 to 450°C to produce vapor

Superheater

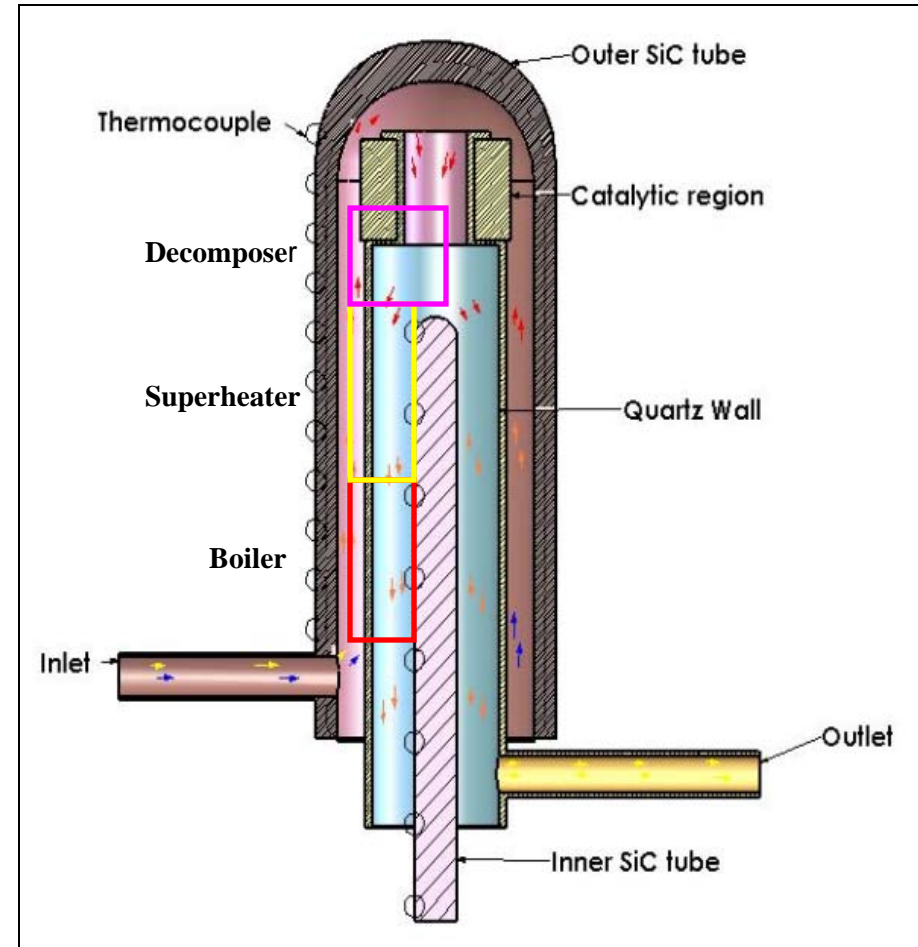
Heat H_2SO_4 vapor from 450°C to 700°C

Decomposer

Heat vapors to maximum operating temp. plus provide heat necessary to dissociate SO_2 & O_2

Recuperator

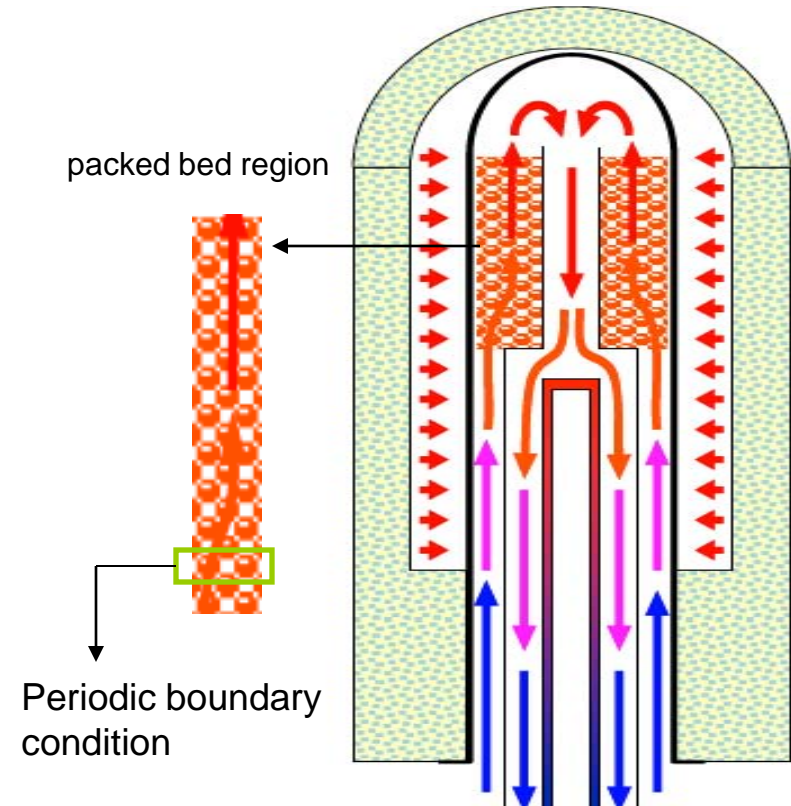
Vapors are recuperated to minimize total required input energy to system



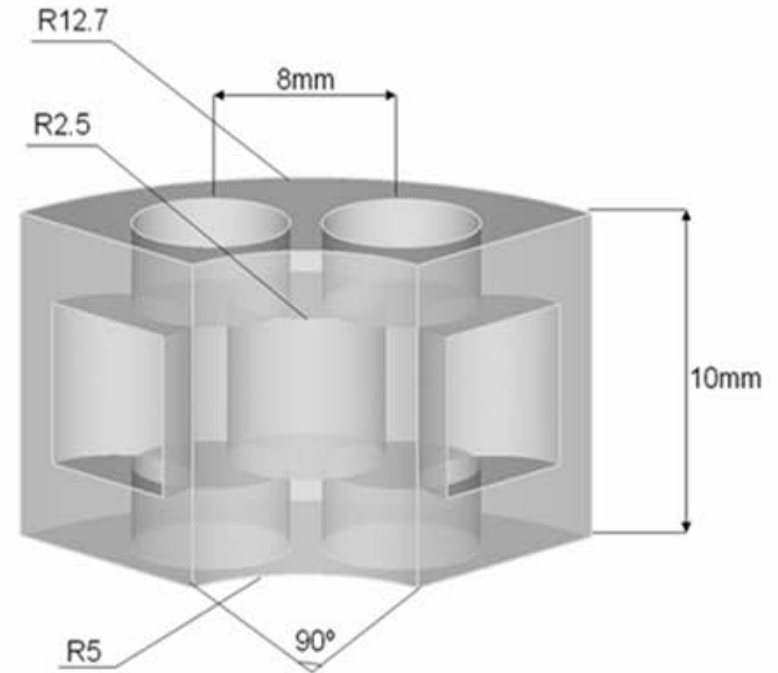
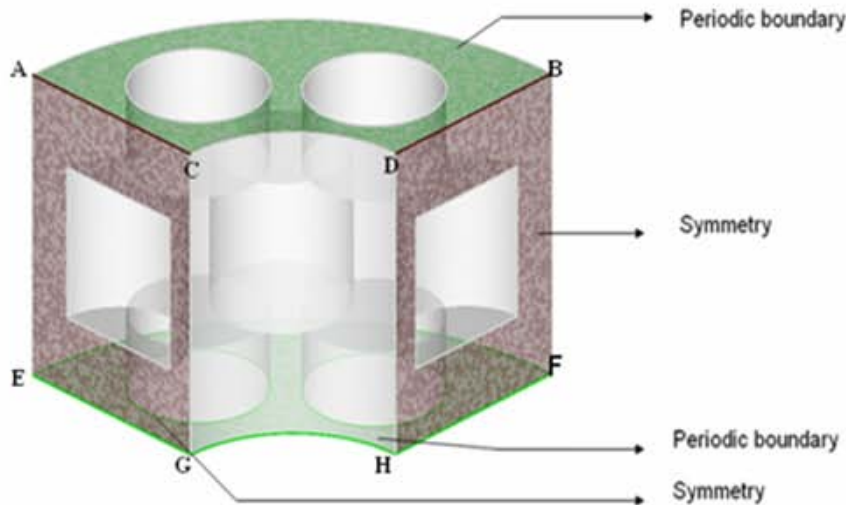
Silicon carbide Integrated Decomposer (SID)

Design of Catalytic Packed Bed Region

- The region locates on the top of heat exchanger and houses pellets
- Cylindrical and spherical pellets are used for modeling in the packed bed region
- Diameter and the height of the pellets is 5mm
- Periodic boundary condition is applied to as the model is symmetric
- The inlet mass flow rate is 0.00043 kg/s and the inlet bulk temperature is 873K



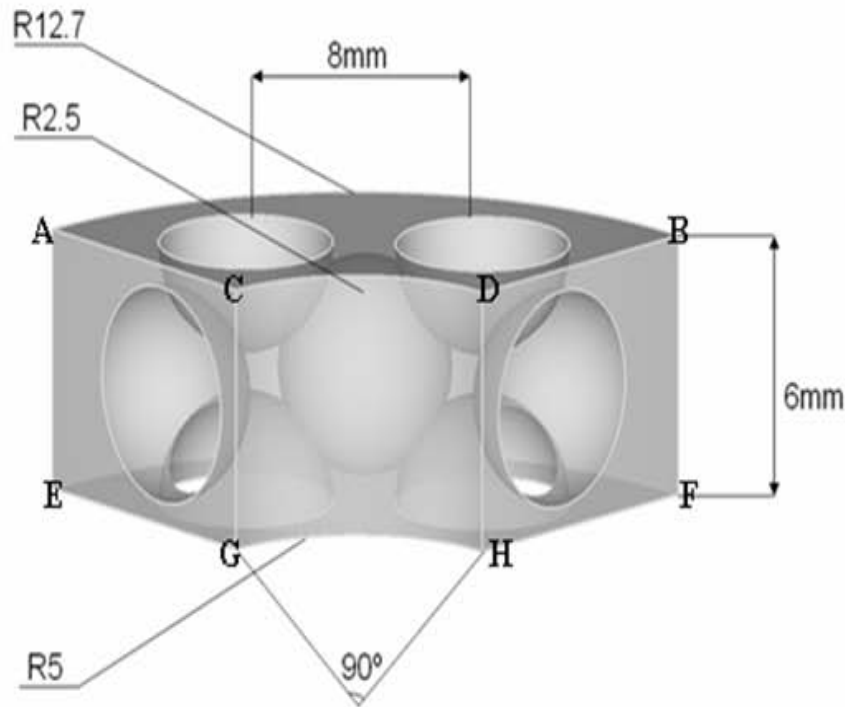
Dimensions and Boundaries of Cylindrical Pellets



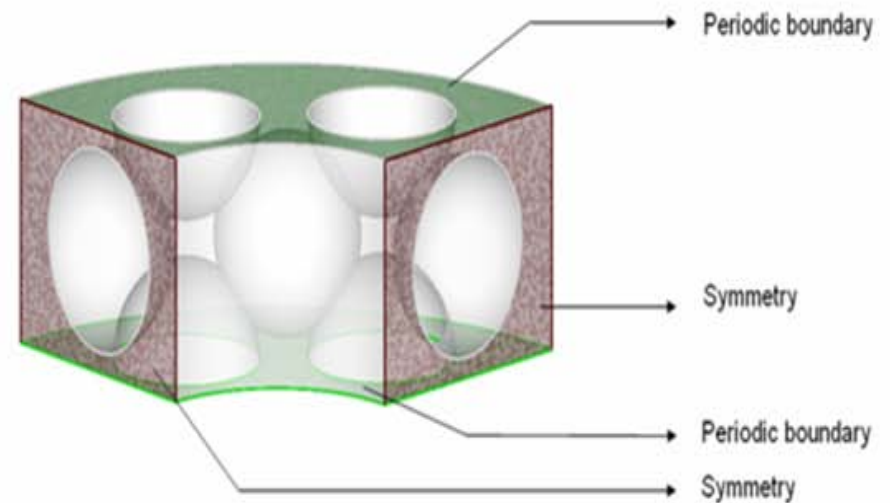
Dimensions of cylindrical pellets

Boundaries of cylindrical pellets

Dimensions and Boundaries of Spherical Pellets

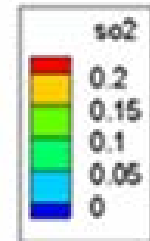
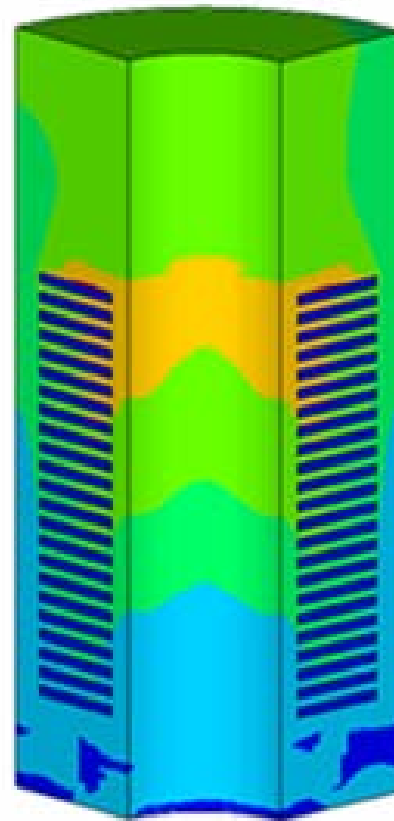
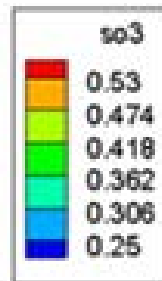
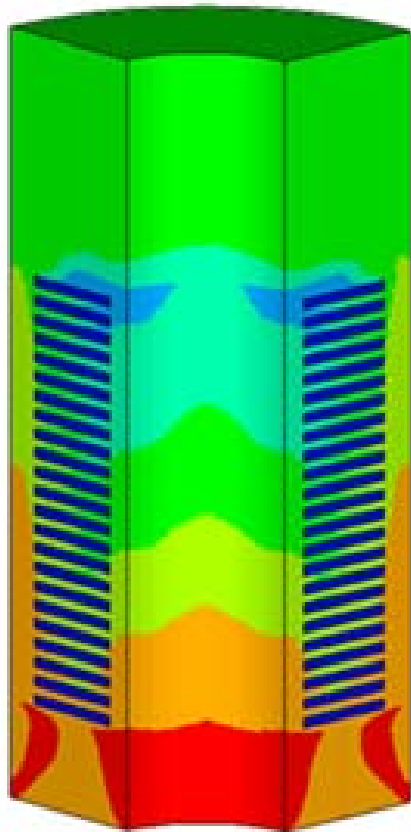


Dimensions of spherical pellets



Boundaries of spherical pellets

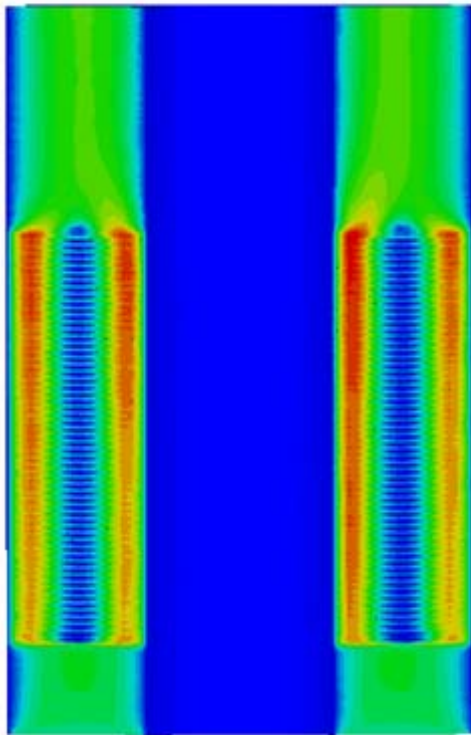
Mass Fractions of SO_3 and SO_2 for Cylindrical Packed Bed Region



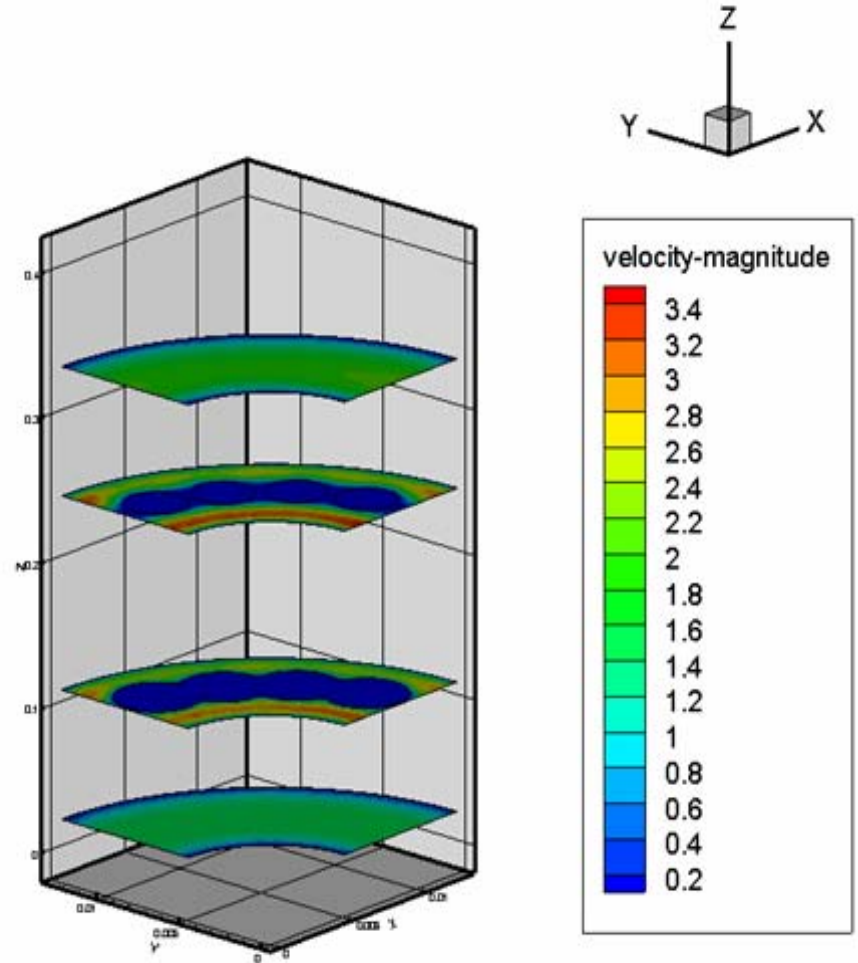
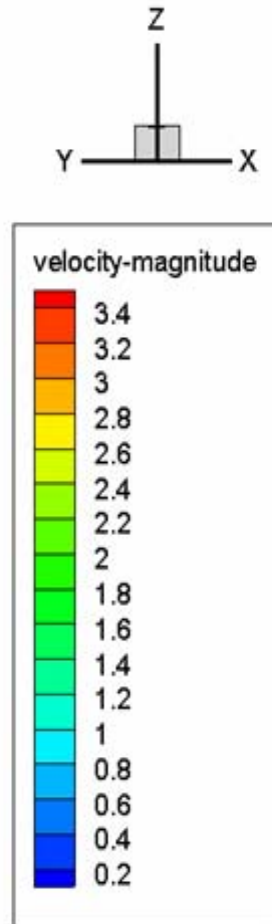
Mass fraction of SO_3

Mass fraction of SO_2

Velocity Magnitude for Spherical Pellets with Regular Packing

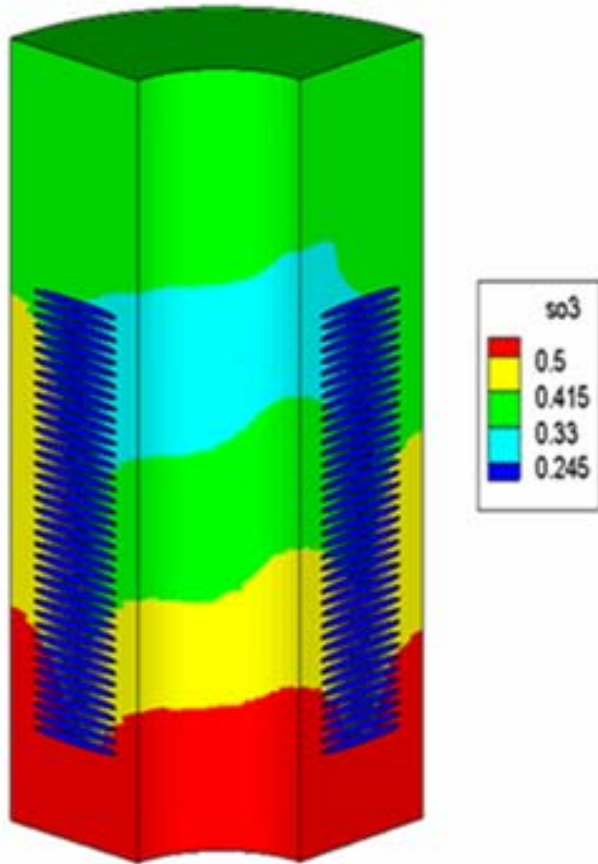


Velocity in m/s

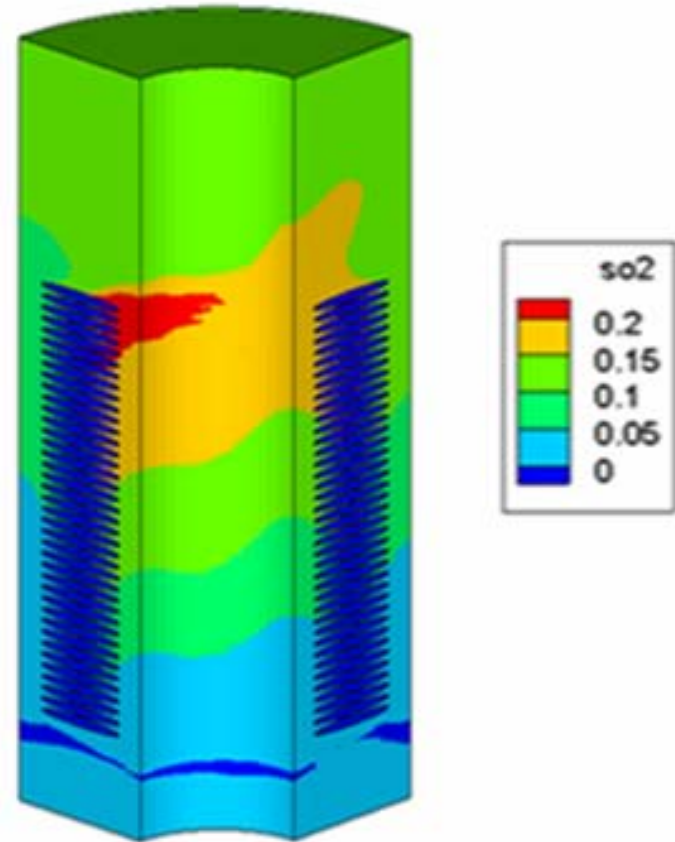


Velocity in m/s

Mass Fractions of SO_3 and SO_2 for Spherical Packed Bed Region



Mass fraction of SO_3



Mass fraction of SO_2

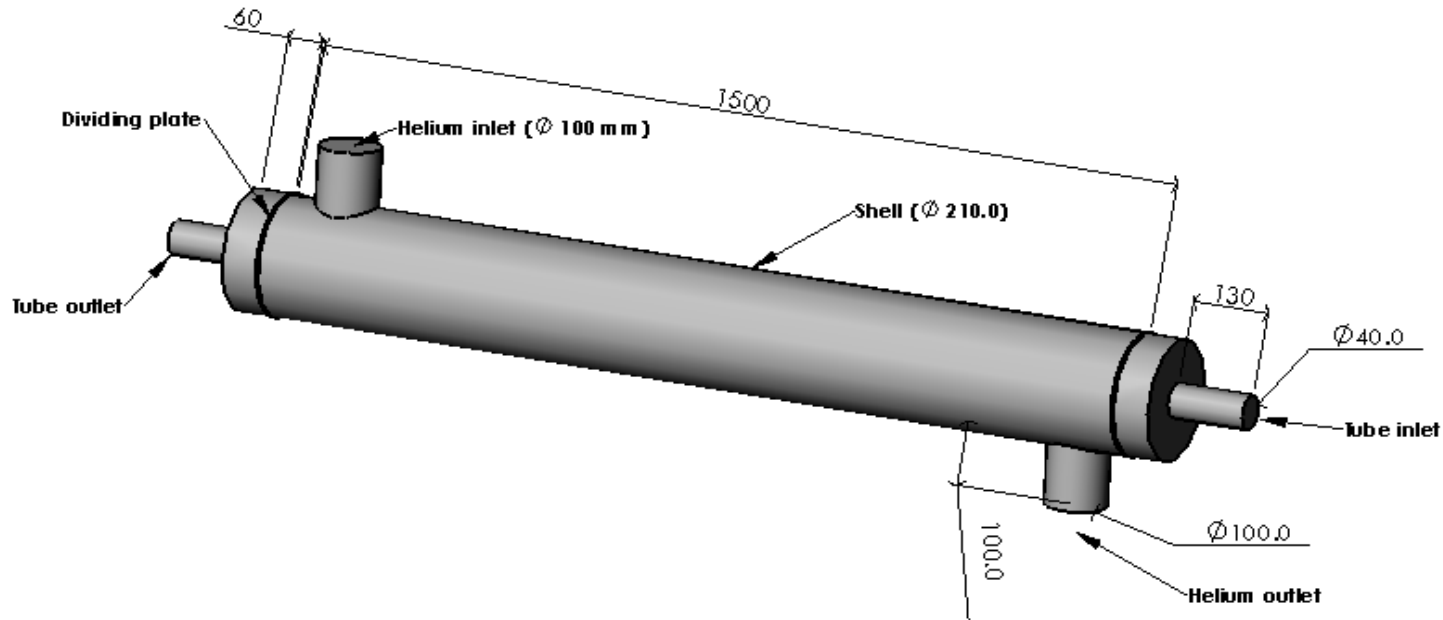
Experimental Results from SNL

Test	Flow Rate (ml/min)	Pressure (atm)	Decomposition Percentage of SO ₃ (%)
SID	5 to 15	1	61
SID and Concentrator	13.4	3 to 5	37

Numerical Results from 3D Model

Packed bed region	Diameter and sides (mm)	Number of pellets	Porosity	Surface-to-volume ratio (m^{-1})	Pressure drop (Pa)	Decomposition % of SO_3 for 15 ml/min flow rate	Decomposition % of SO_3 for 5 ml/min flow rate	Throughput (kg/s)
Cylindrical pellets	5	115	0.73	113.57	20	25.1	56.58	$0.0113 \cdot 10^{-3}$
Spherical pellets staggered packing	5	195	0.70	128.38	32	29.44	60	$0.0130 \cdot 10^{-3}$
Spherical pellets regular packing	5	141	0.78	129.58	26.5	30.47	60.65	$0.0135 \cdot 10^{-3}$
Spherical pellets regular packing	4	232	0.82	136.45	20	34.47	61.26	$0.0148 \cdot 10^{-3}$
Cubical pellets	4	230	0.95	46.27	12	24.12	54.58	$0.010 \cdot 10^{-3}$
Hollow cylindrical pellets	OD-5, ID-4	230	0.81	825.30	20	39.6	70.5	$0.018 \cdot 10^{-3}$

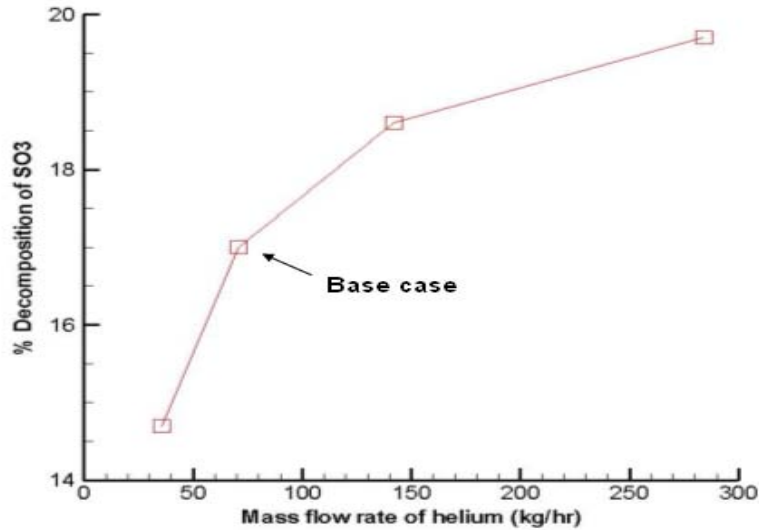
Conceptual Design of Shell and Tube Heat Exchanger and Chemical Decomposer



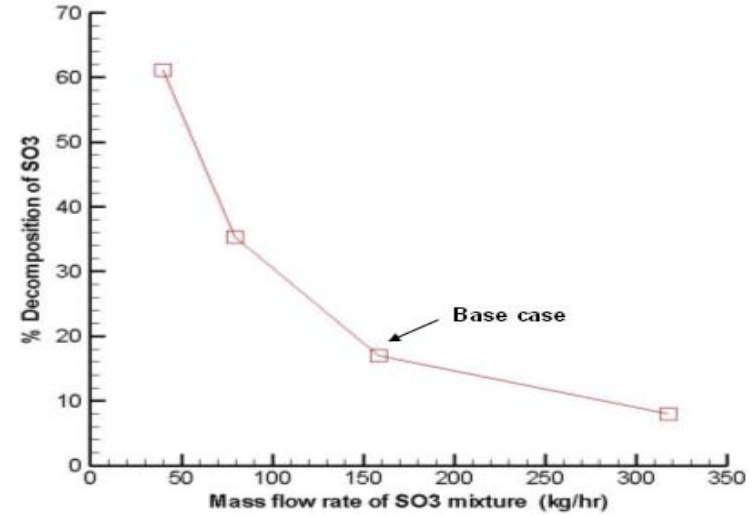
Tube diameter: 16 mm
Shell diameter: 210 mm
Dividing plate: 4 mm
Tube thickness: 4 mm
Tube material: SiC ($k=120$ W/m-K)
Dividing plate material: silicon carbide
Number of tubes: 24
Tube pitch: 31.75 mm

Mixture mass flow rate: 158.66 kg/hr
Helium mass flow rate: 71 kg/hr
Helium inlet temperature: 1223 K
Mixture inlet temperature: 973 K
Reynolds Number at the helium entrance: 12,469
Reynolds number at the tube entrance: 60,841
Shell wall: adiabatic
Operating pressure: 1.5 atm

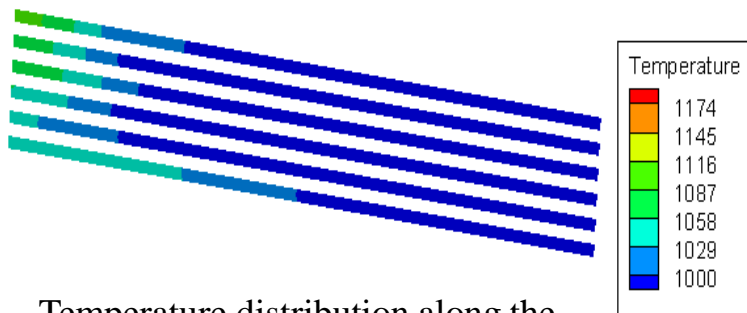
Parametric Study of Different Mass Flow Rates of He and SO₃



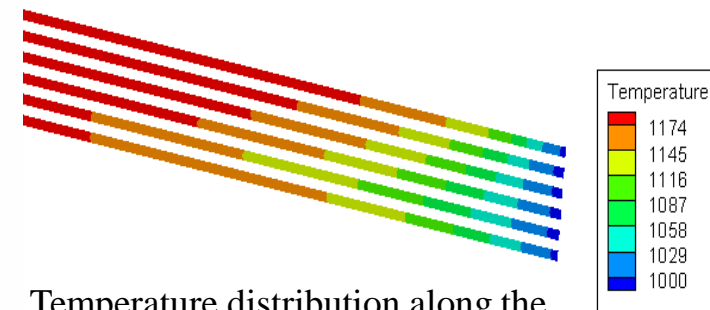
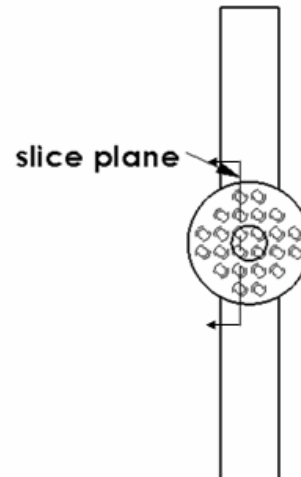
Mass flow rate of He vs. decomposition percentage



Mass flow rate of SO₃ mixture vs. decomposition percentage

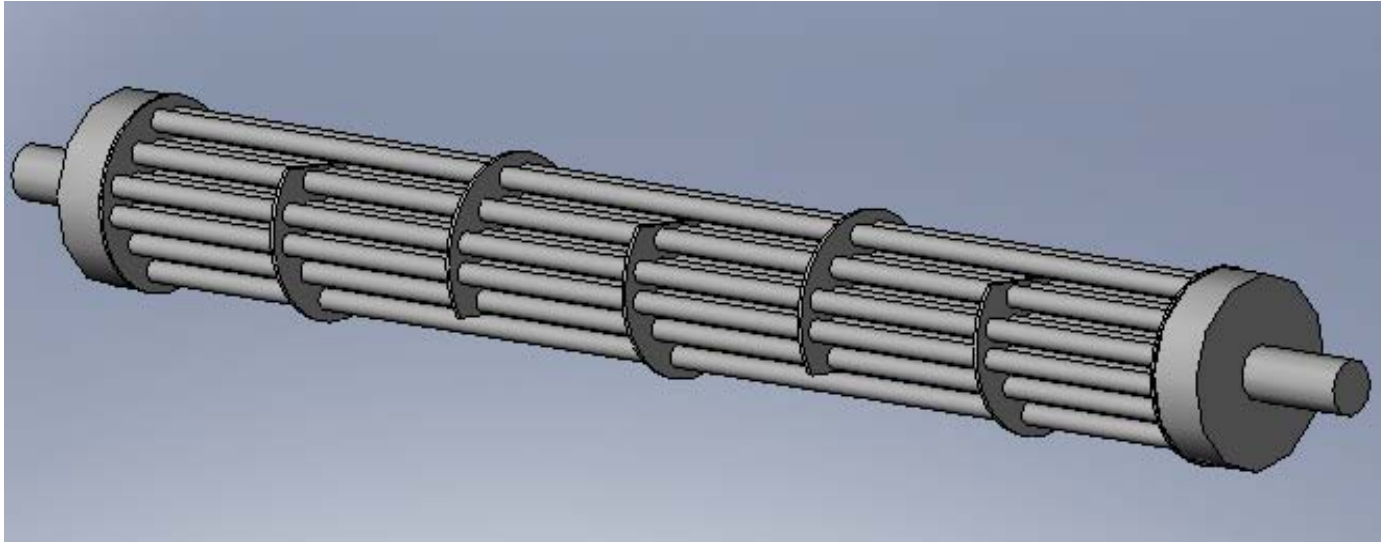


Temperature distribution along the tubes cross section for low m_{He} (K)

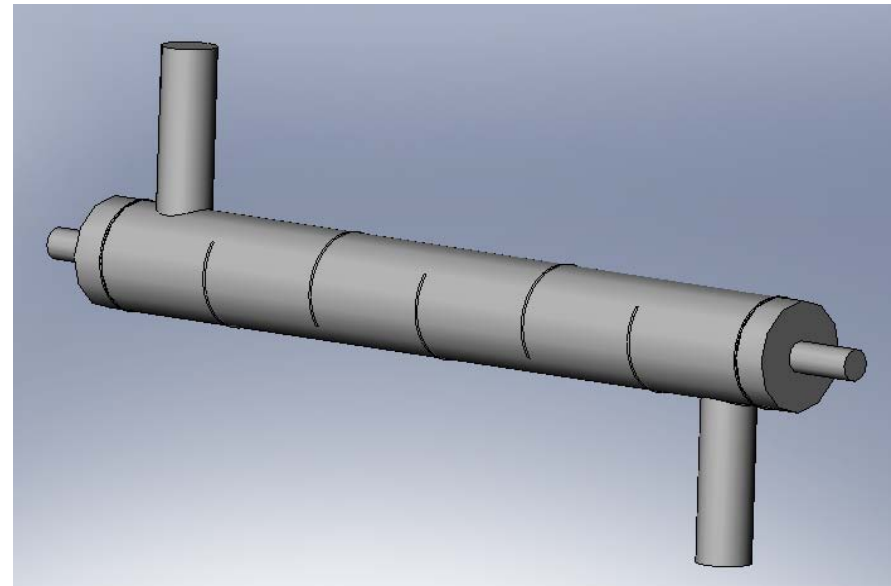


Temperature distribution along the tubes cross section for high m_{He} (K)

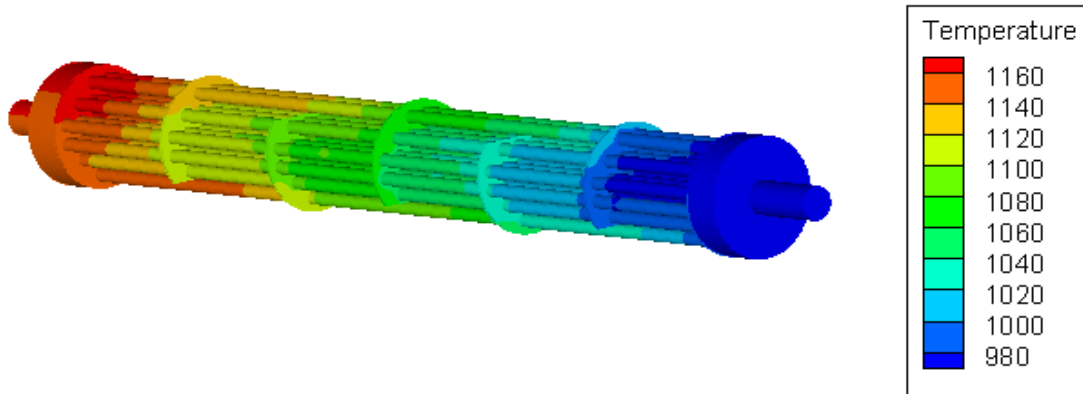
Design of Shell and Tube Heat Exchanger and Decomposer with Baffles



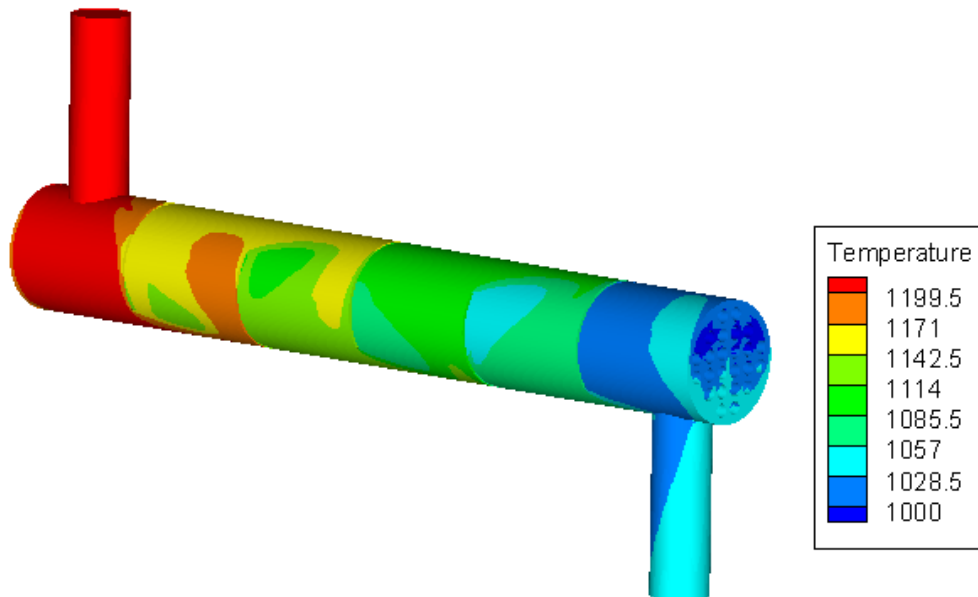
Thickness of the baffle : 5.0 mm
Baffle cut : 20%
Baffle to baffle spacing : 245.0 mm
Baffle type: segmental



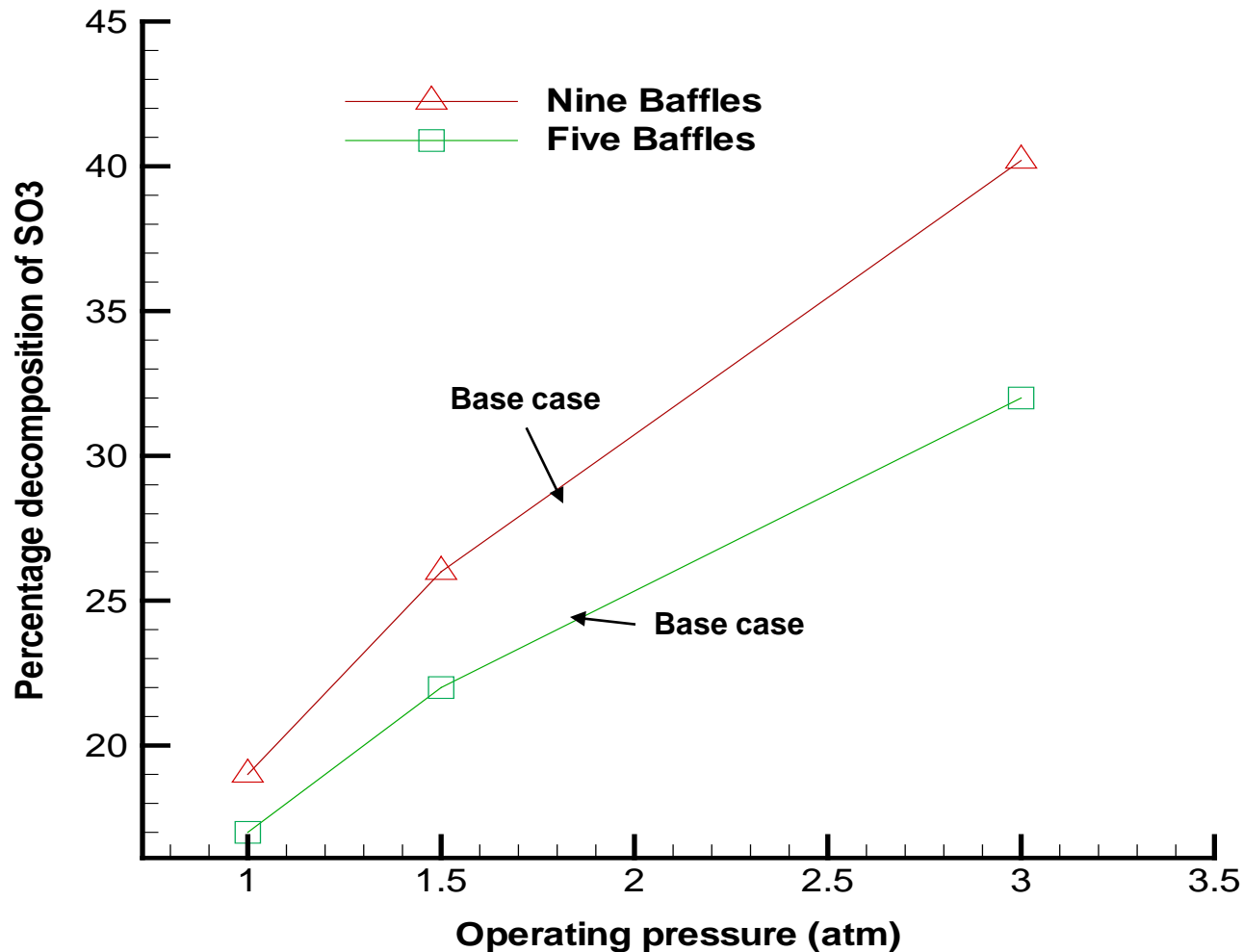
Numerical Results (Five Baffles)



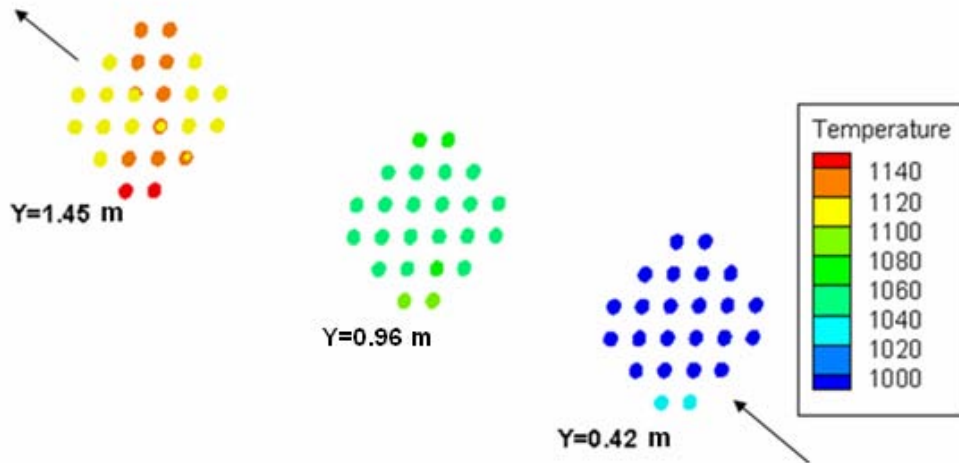
- Decomposition percentage of SO_3 : 20 %
- Effectiveness of the heat exchanger : 0.70
- Throughput of SO_2 : 25.2 kg/hr



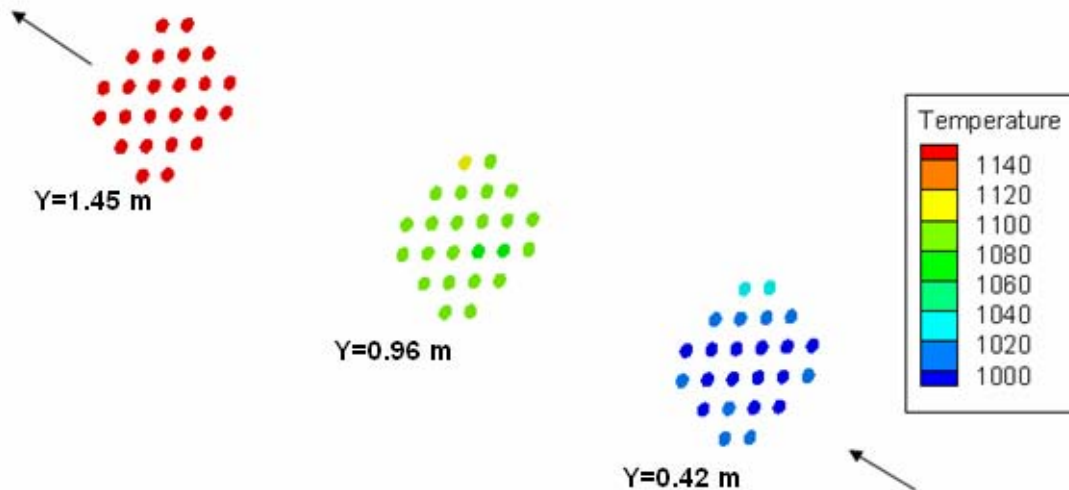
Parametric Study of Heat Exchanger with Nine and Five Baffles



Comparison of Heat Exchanger with Five and Nine Baffles

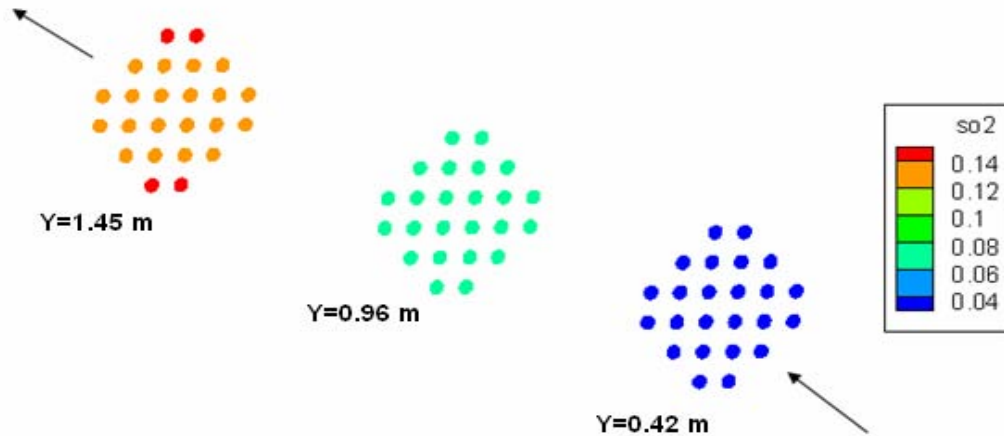


Temperature distribution along slices with five baffles (K)

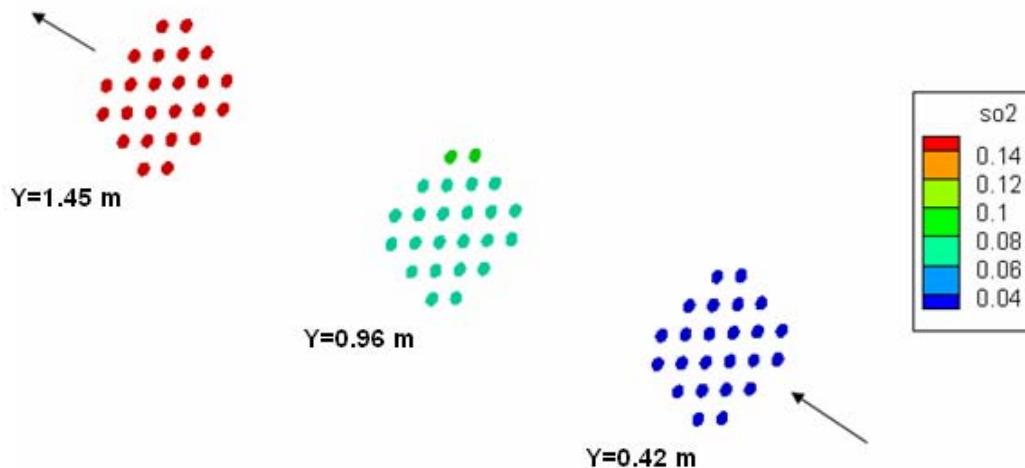


Temperature distribution along slices with nine baffles (K)

Comparison of Heat Exchanger with Five and Nine Baffles (Cont.)



Average mass fraction of SO₂ along slices with five baffles



Average mass fraction of SO₂ along slices with nine baffles

Solar Production of Hydrogen is an Appealing Goal

- **Solar receivers can deliver high temperature**
 - NREL/U of Colorado demonstrated 51% collection efficiency at 2000°C in the process fluid for thermal cracking of methane
- **Solar diurnal cycle is a real limitation**
 - ~ 8 hours of useful energy per day
 - $8/24 = 33\%$ duty cycle
 - Capital equipment only earning revenue 1/3 of time
 - Hydrogen unit cost increased 3 x
- **Solar can deliver higher temperatures than nuclear --can we use it effectively to off-set the low duty cycle?**



Preliminary Estimates of Solar Thermochemical Hydrogen Production are Encouraging

- **Start with nuclear-matched S-I cycle coupled to solar receiver**
 - NREL heliostat/collector: 1 kW/m², 51% capture, \$130/m², 8 hr/day
 - **Lower capital cost than nuclear, but low duty cycle hurts**
- **Increase temperature to maximum S-I can use – 1100°C**
 - NREL advanced heliostat/collector: \$75/m²
 - Better – but doesn't use the full temperature potential of solar
- **Assume hypothetical thermochemical cycle at 2000°C**
 - Assume same 79% of Carnot efficiency as S-I → 65% heat to H₂ efficiency
 - Assume same \$/kWt capital cost as S-I
- **While the assumptions are unproven, the result is interesting**

Process	Nuclear S-I	Solar S-I	Solar Hi T S-I	V Hi T Cycle
Temperature °C	900	900	1100	2000
Efficiency - Heat to H ₂	52%	52%	56%	65%
Hydrogen cost, \$/kg	1.42	3.45	2.50	2.15

Evaluation of Solar Water-splitting is Needed

- **We have proposed to do serious investigation of solar thermochemical cycles**
 - **Update and search our database for cycles well-suited to solar:**
- **Develop solar screening criteria**
- **Higher temperature cycles possible for higher efficiency**
- **Match receiver characteristics to chemical reactions**
- **Search for diurnal accommodation to improve capital utilization**
 - **Do conceptual designs for interesting cycles and systems**
 - **Build and test prototype solar receivers/chemical reactors**



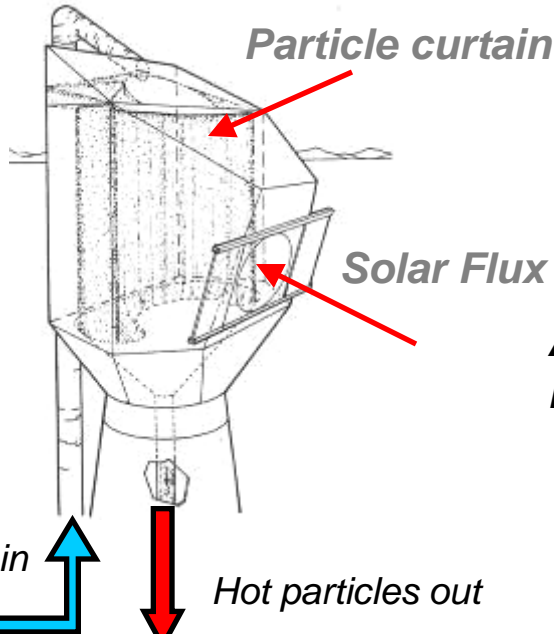
Ref.: SNL Solar Power Tower

U.S. Solar Thermochemical Hydrogen (STCH) Participants

- **UNLV** – *Solar particle receiver (SPR) design and experiment, numerical modeling, database design and management, chemical kinetics study for possible cycles, cadmium quenching modeling*
- **SNL** – *Solar tower design, process HX design, heliostat design and cost evaluation, H₂A analysis, Ferrite cycles evaluation*
- **GA** – *Cadmium cycle evaluation, material testing, process analysis and design, screening criteria*
- **ANL** – *Cu-Cl cycles evaluation*
- **CU-Boulder** – *Zinc and manganese cycles evaluation, fluid water reactor design, high temperature cavity receiver design*
- **NREL** – *high temperature cavity receiver design, solar furnace design*

Solar fuels process diagram

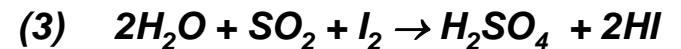
Solid Particle Receiver (SPR)



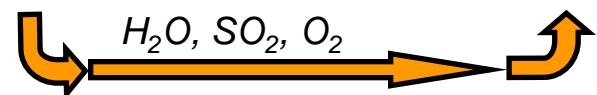
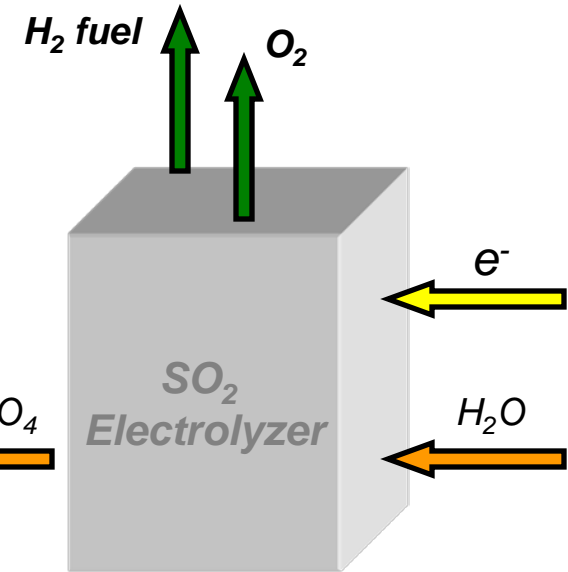
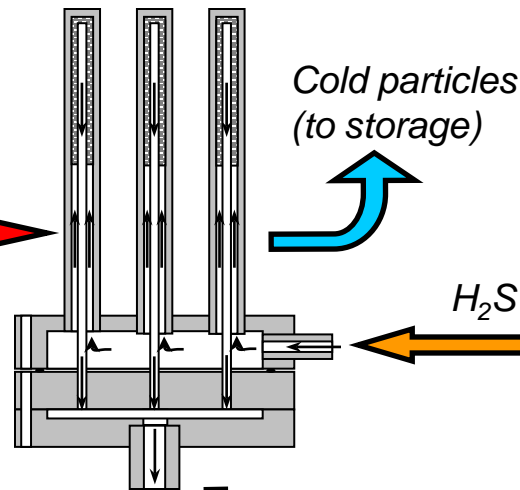
Hybrid-Sulfur Process



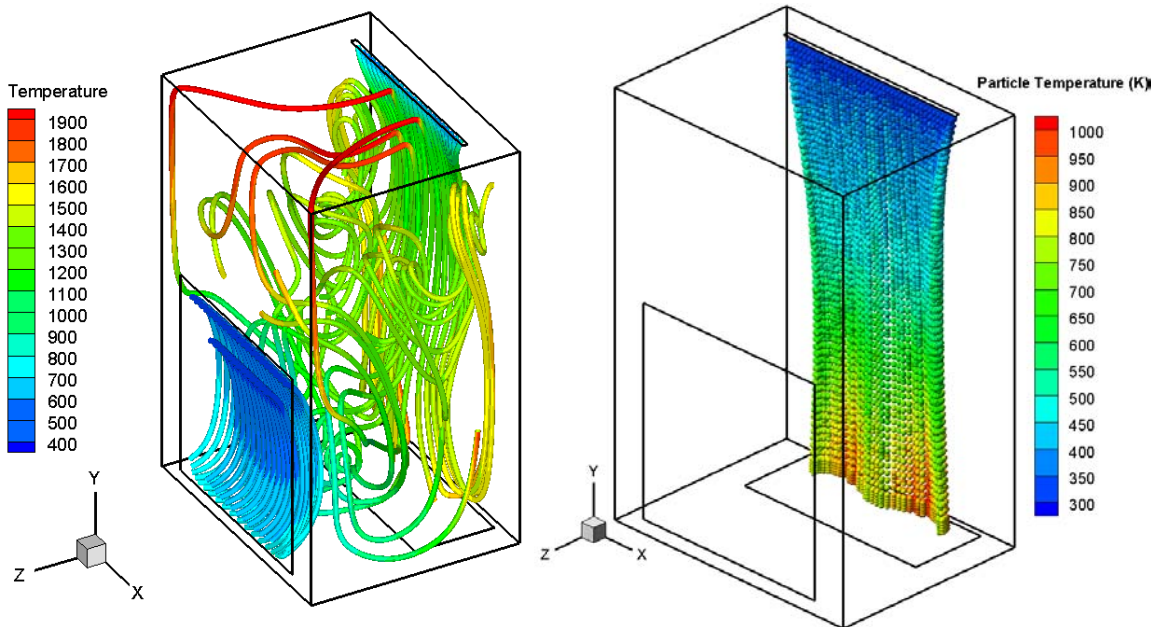
Sulfur-Iodine Process



Acid decomposer Bayonet heat exchanger



SPR Design Accomplishments in the Past



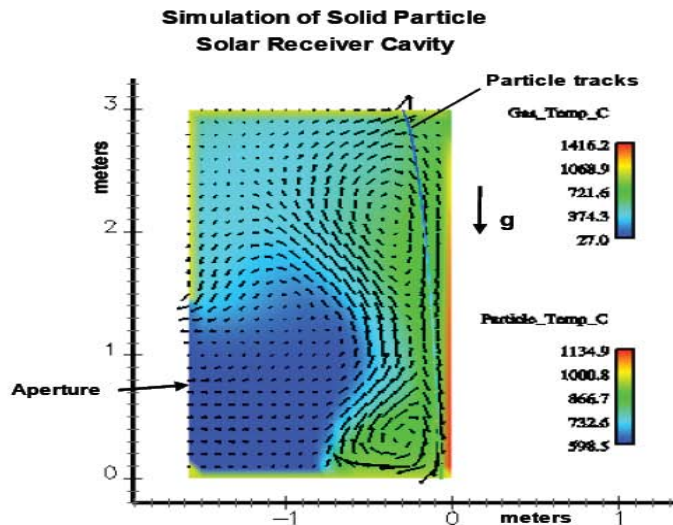
Entrained air flow path lines (left) and particle tracks. The path line is colored by gas temperature (K). Particle size is 600 micron. Mass flow rate is 1.5 kg/s.

- Creation of cold gas-particle flow model;
- Establishment of numerical modeling of SPR with/without catch hopper;
- Parametric CFD study to find the optimum operating condition;
- Initial optimum geometry design with CFD analysis

- According to the previous study, the cavity efficiency is relatively low (<65%) while it approaches around 80% obtained from the 2-D PSI-Cell numerical results done by SNL.

Possible Reason for the Different Cavity Efficiencies

Model of solid particle solar receiver for use in hydrogen production.



• Summary of simulation inputs

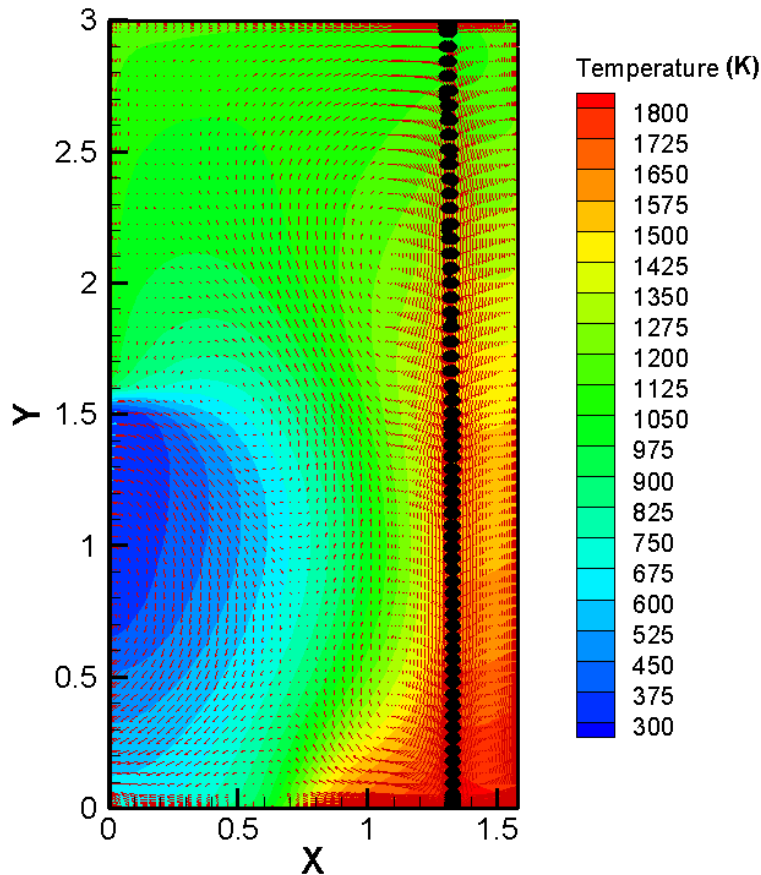
- Cavity Height = 3.0 m
- Cavity Depth = 1.58 m
- Aperture Opening = 1.5 m
- Solar flux = 800 sun = $8.0 \times 10^5 \text{ W/m}^2$
- Particle Flowrate = 5 Kg/sec
- Particle Inlet Velocity = 8.8 cm/sec
- Particle Diameter = 0.65 mm
- Particle Inlet Temperature = 600 C
- Particle Density = 3.2 g/cm³

• Summary of simulation outputs

- Cavity efficiency = 81.5%
- Particle temp. at exit (front of curtain) = 1135 C
- Particle temp. at exit (back of curtain) = 841 C
- Ave. temp. cavity top wall = 971 C
- Ave. temp. cavity bottom wall = 934 C
- Ave. temp. cavity upper front wall = 1025 C
- Ave. temp. cavity lower front wall = 995 C
- Approx. cavity back wall temp. at top = 740 C
- Approx. cavity back wall temp. at bottom = 1423 C

- Possible reason for the different cavity efficiencies:
 - Solar load model
 - Current model: the incoming solar ray can penetrate the particle curtain and bounce back from back wall to outside (big radiation loss)
 - PSI-cell model: The solar irradiation is uniformly loaded at the front of curtain (small radiation loss)

An Improved Numerical Model with the Uniform Irradiation Source (2-D)

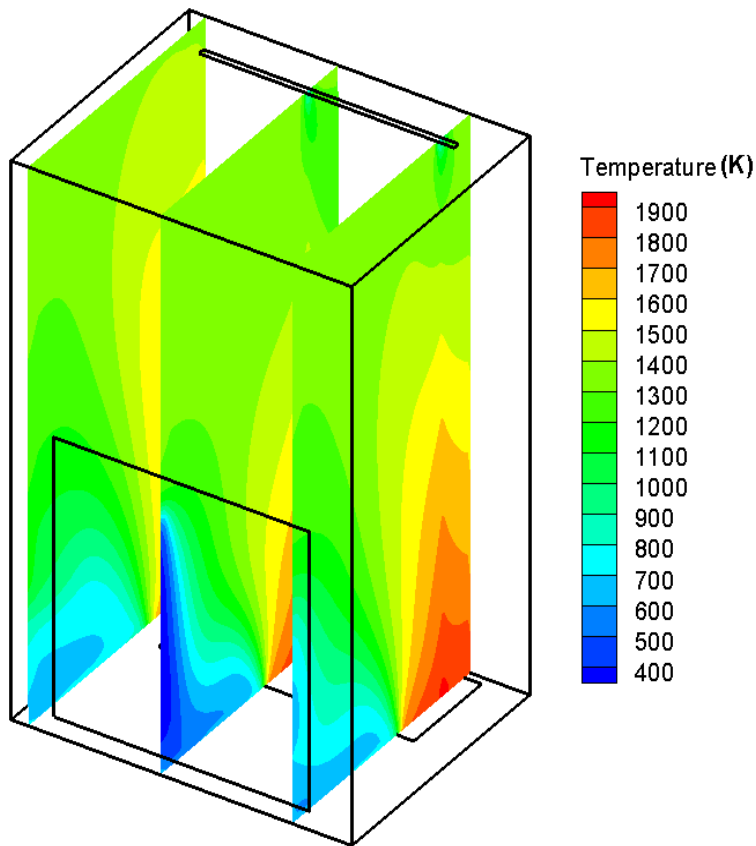


Improved modeling on solid particle receiver.
Solar flux is 800 suns

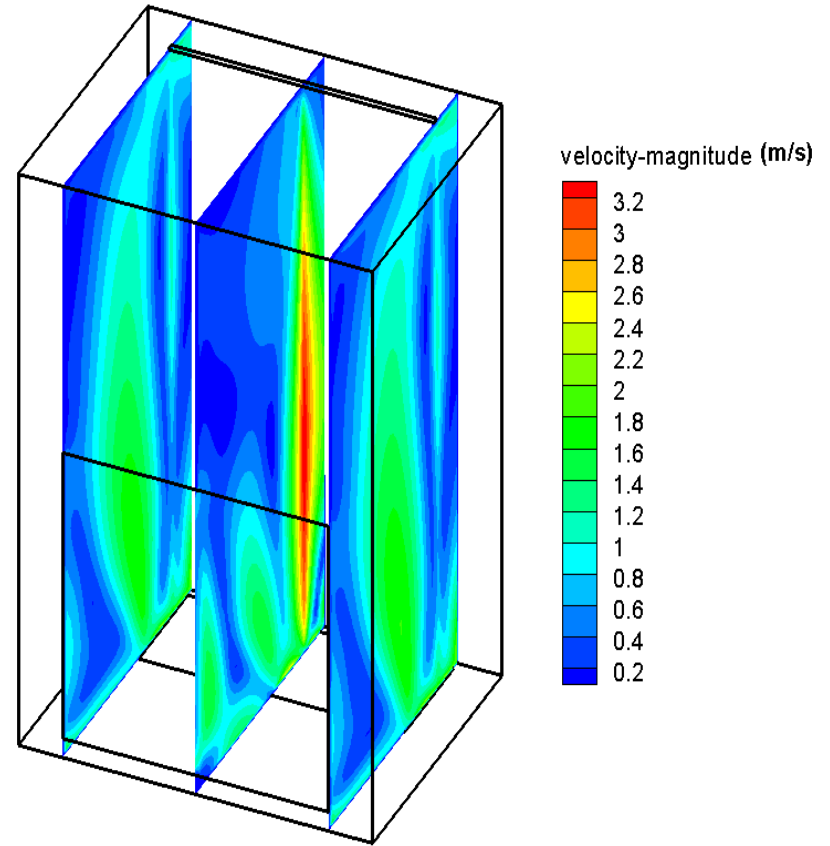
- **Gas phase**
 - Operating pressure: 10,100 Pa
 - Air outlet condition: Pressure outlet
 - Inlet air temperature: 300 K
 - Temperature boundary condition: Adiabatic
- **Solid phase**
 - Particle density: 3,200 kg/m³
 - Heat capacity C_p : 1,285 J/ kg-K
 - Thermal conductivity: 6.67 W/m-K
 - Particle inlet velocity: 0.088 m/s
 - Particle diameter: 650 micron
 - Particle inlet temperature: 873 K
 - Particle total mass flow rate: 5 kg/s

- It is assumed that the solar irradiation on particle is considered as a uniform heat source
- The calculated particle exit temperature is 1,289 K
- The calculated cavity efficiency is around 79%

An Improved Numerical Model with the Uniform Irradiation Source (3-D)

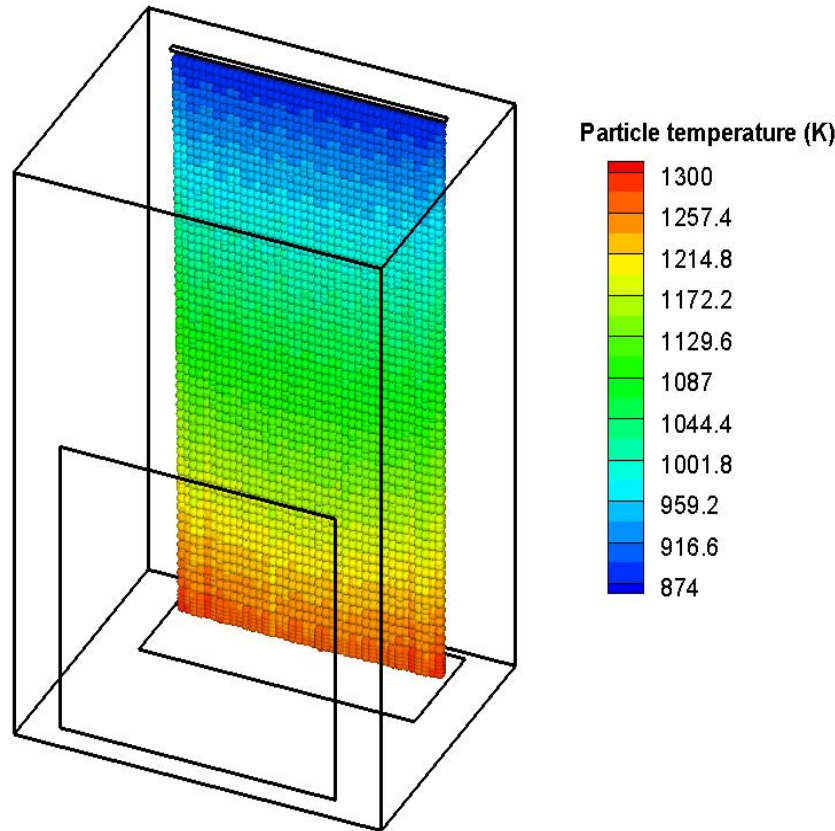


Gas temperature (K) contour at different slices



Air flow velocity magnitude (m/s) at different slices

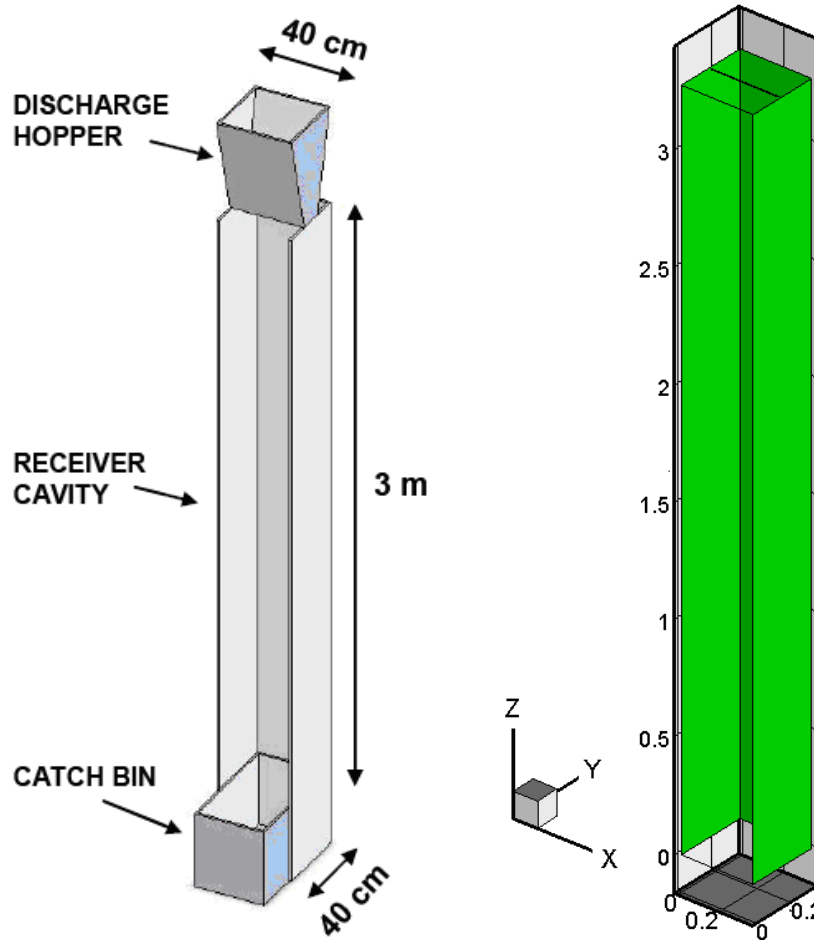
An Improved Numerical Model with the Uniform Irradiation Source (3-D) (Cont.)



- The average particle temperature is around 1,296 K
- The cavity efficiency is about 77%
- The radiation loss is much larger than convection loss and the convection loss is about 20% radiation loss

Particle tracks released from inlet on the top wall. The path tracks are colored by particle temperature (K). Total 400 particle point sources are tracked.

Benchmark with the Experimental Data Provided by SNL



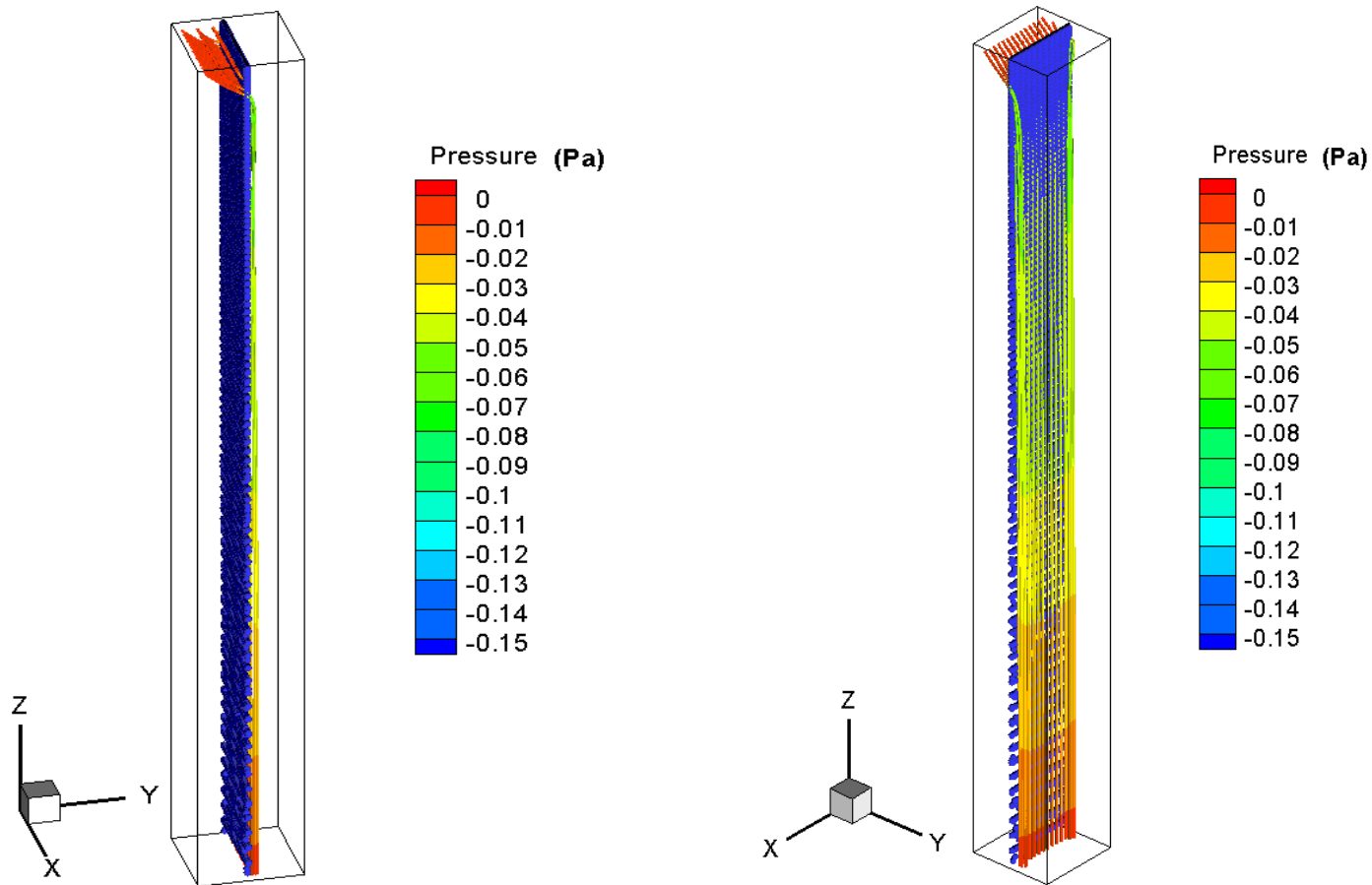
Schematic of drop test platform and computational domain

Simulation conditions

Input information for solid particle:

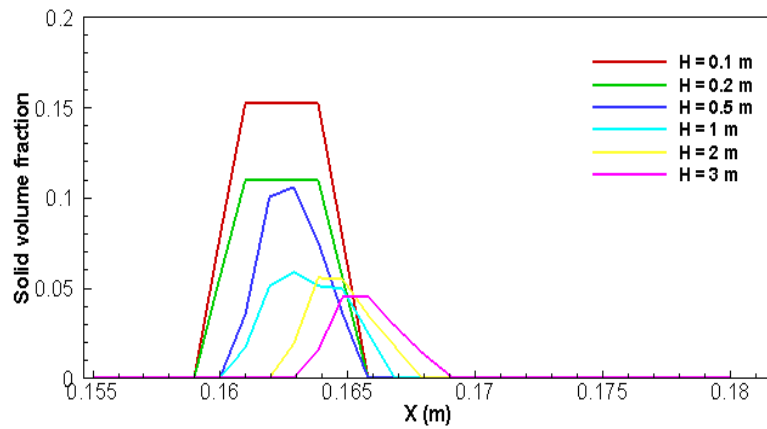
Particle density: 3,560 kg/m³
 Particle sphericity: 0.9
 Particle inlet velocity: 0.4 m/s
 Particle angle: 8.53° (Case A),
 5.71° (Case B), -2.29° (Case C)
 Particle discharge slot width: 4.88
 mm (Case A), 9.5 mm (Case B),
 12.7 mm (Case C)
 Particle bulk density (packed bed):
 2,000 kg/m³
 Particle diameter: 697 micron
 Particle total mass flow rate: 1.2
 kg/s (Case A), 4.5 kg/s (Case B),
 6.7 kg/s (Case C)
 Particle diameter distribution:
 uniform

Benchmark with the Experimental Data Provided by SNL (Cont.)

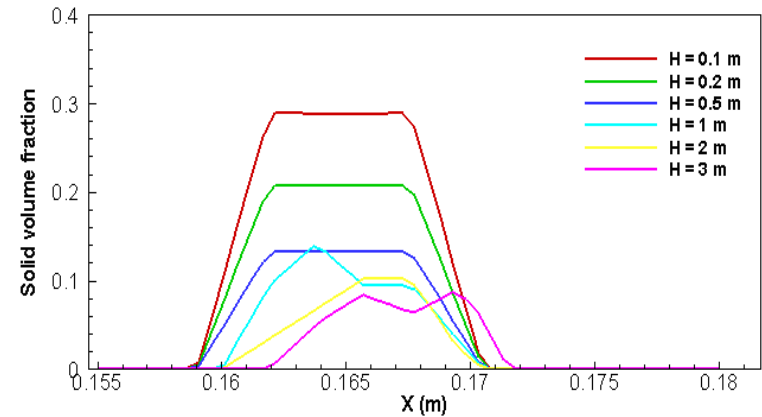


Particle tracks and path lines (released from top surface) for Case A.
Total 400 particle sources are tracked

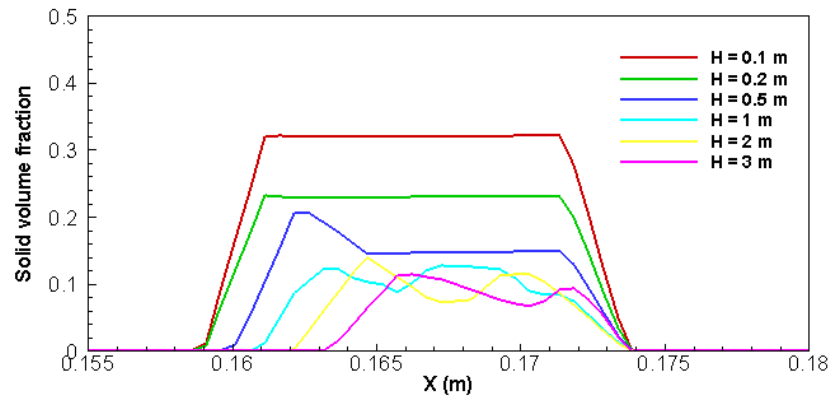
Benchmark with the Experimental Data Provided by SNL (Cont.)



(a) 1.2 kg/s



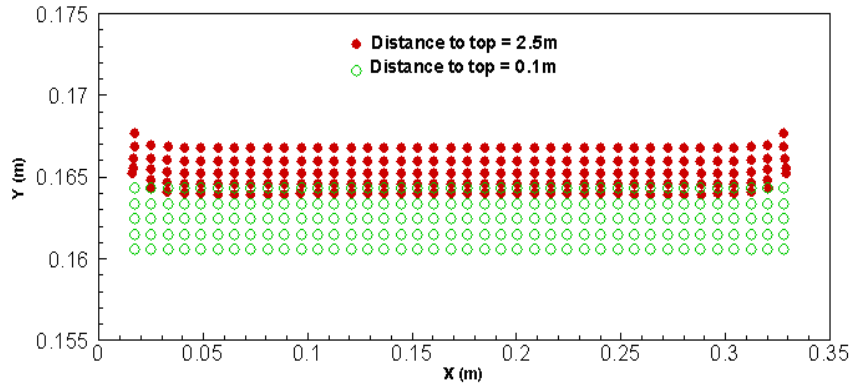
(b) 4.5 kg/s



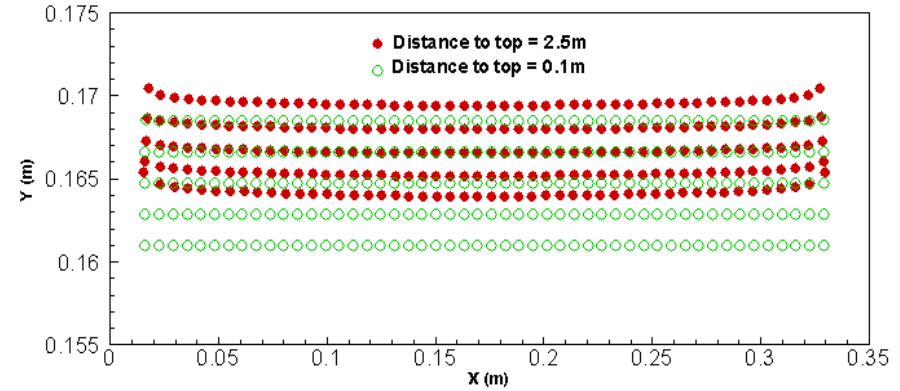
(c) 6.7 kg/s

Solid volume fractions as a function of X coordinate in the center plane. H is the distance to top inlet

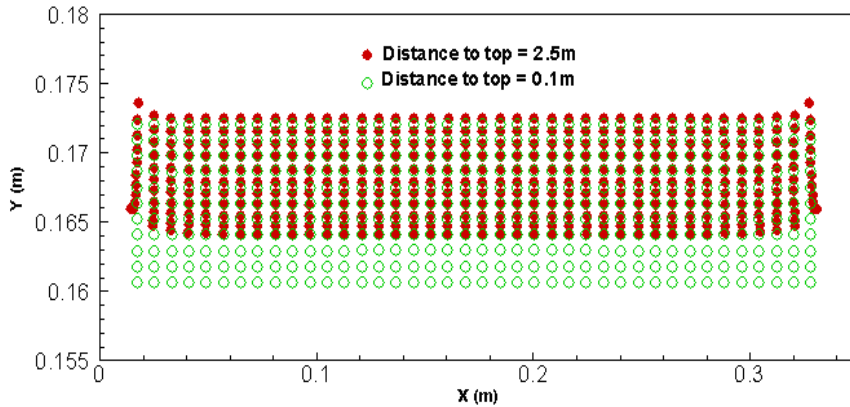
Benchmark with the Experimental Data Provided by SNL (Cont.)



(a) 1.2 kg/s

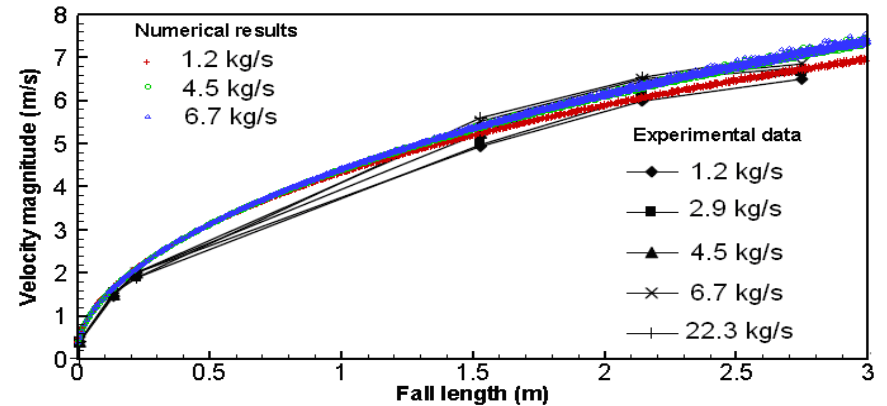


(b) 4.5 kg/s



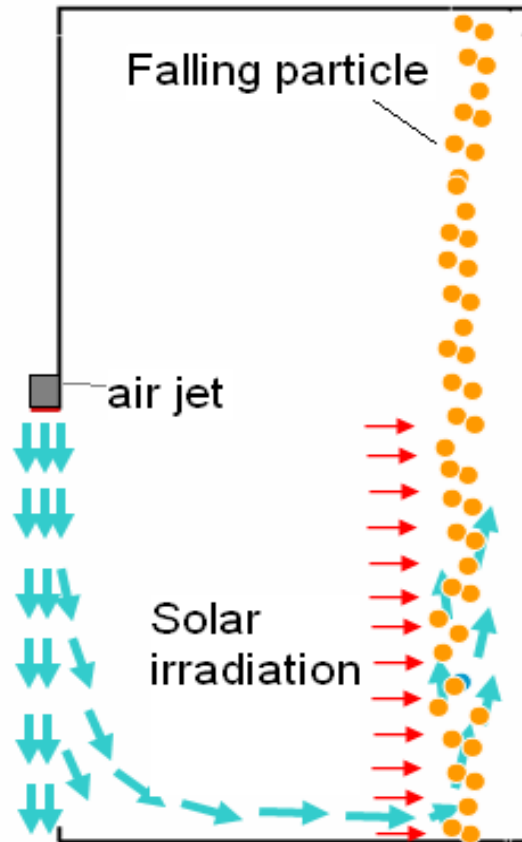
(c) 6.7 kg/s

Solid particle distribution at different planes



Comparisons of numerical results with experimental data

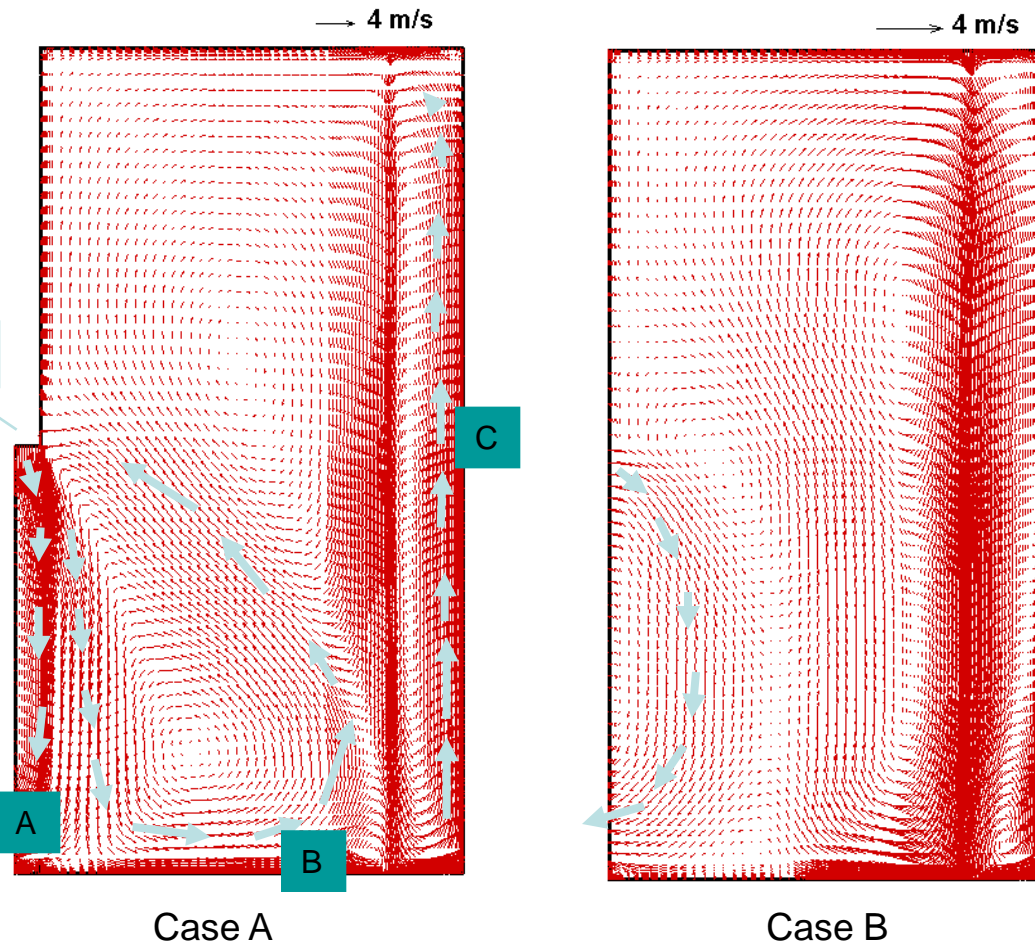
The Effect of Air Jet



Schematic of solar irradiation of solid particle receiver with air jet

- Investigation on the effect of air jet on solid particle receiver performance:
 - Air jet was placed on the top of side aperture
 - Reducing heat loss
 - Isolating the interiors of solid particle receiver
 - The direct solar irradiation (800W/m^2) keeps as the constant for all the cases and it is assumed as a uniform heat source on particles
 - The velocity magnitude of air jet varies from 0 -10 m/s
 - The particle size is taken as 650 micron for all the cases
 - The mass flow rate for the solid particle is taken as 5 kg/s

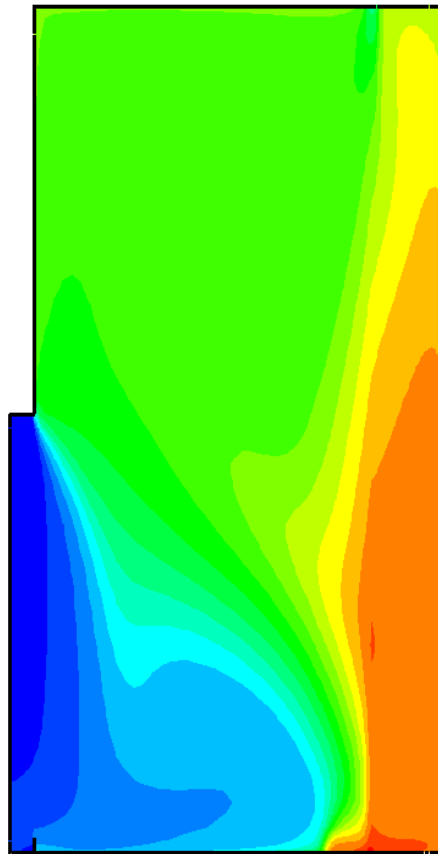
The Effect of Air Jet : 2-D Modeling



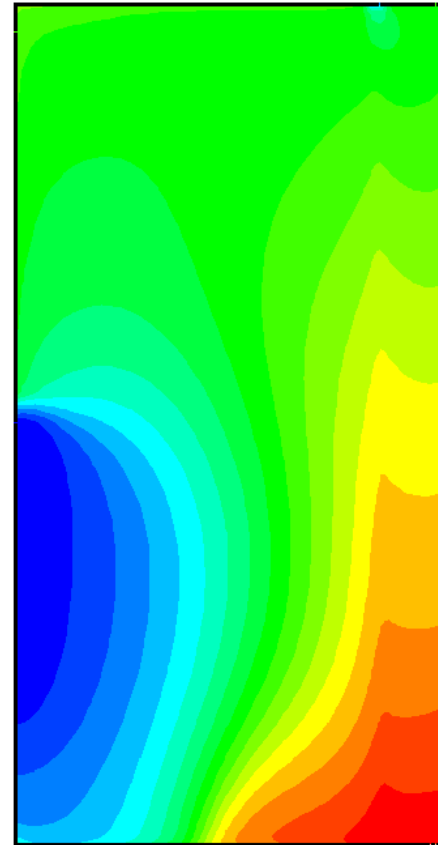
- The air flow from the air jet (Case A) can be divided into two parts
 - Part A: Air curtain, isolating the interior of SPR, reducing the convection loss;
 - Part B: dragged counter clockwise rotating vortex, constituting a mixing loss while increasing particle residence time in receiver;
- The upward buoyancy flow (marked by C) in Case A can also enhance the particle residence time

Velocity vector graph for the cases with (Case A, 5 m/s) / without (Case B) air jet

The Effect of Air Jet : 2-D Modeling (Cont.)



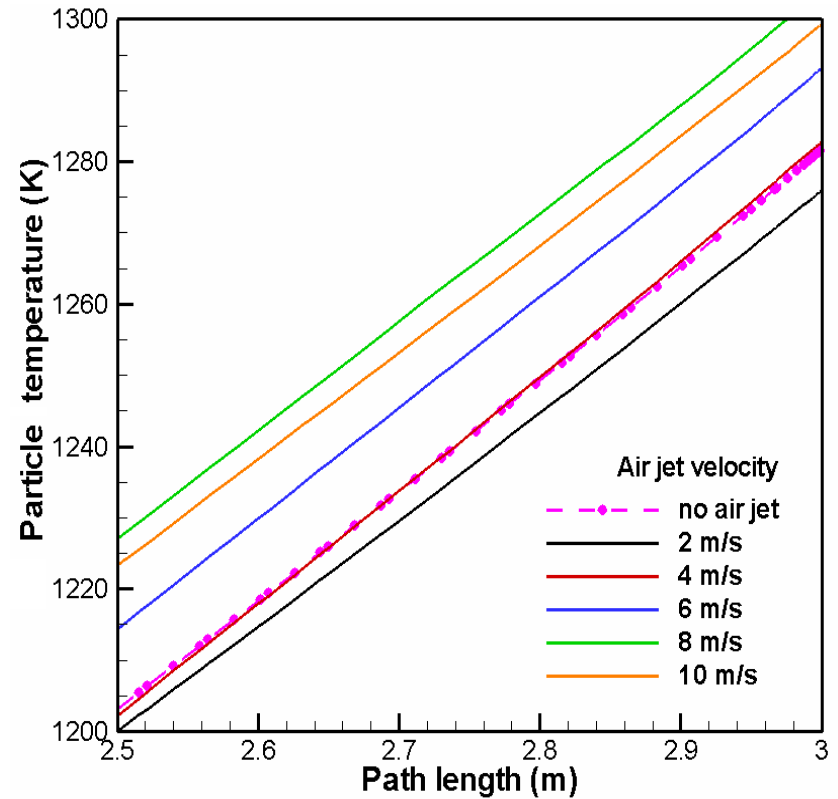
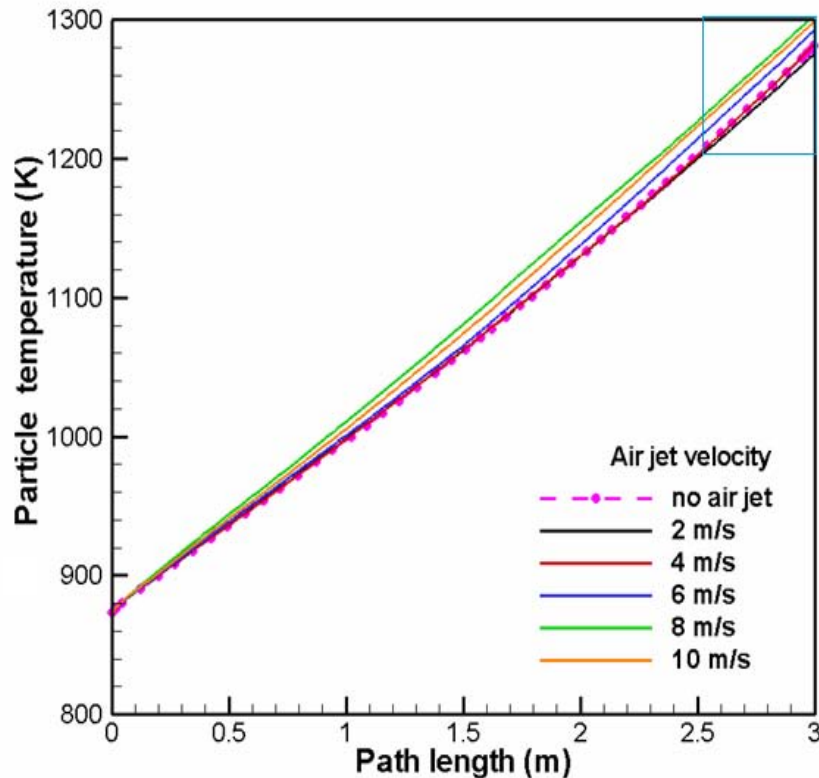
Case A



Case B

Temperature distributions for the cases with (Case A, 5 m/s) / without (Case B) air jet

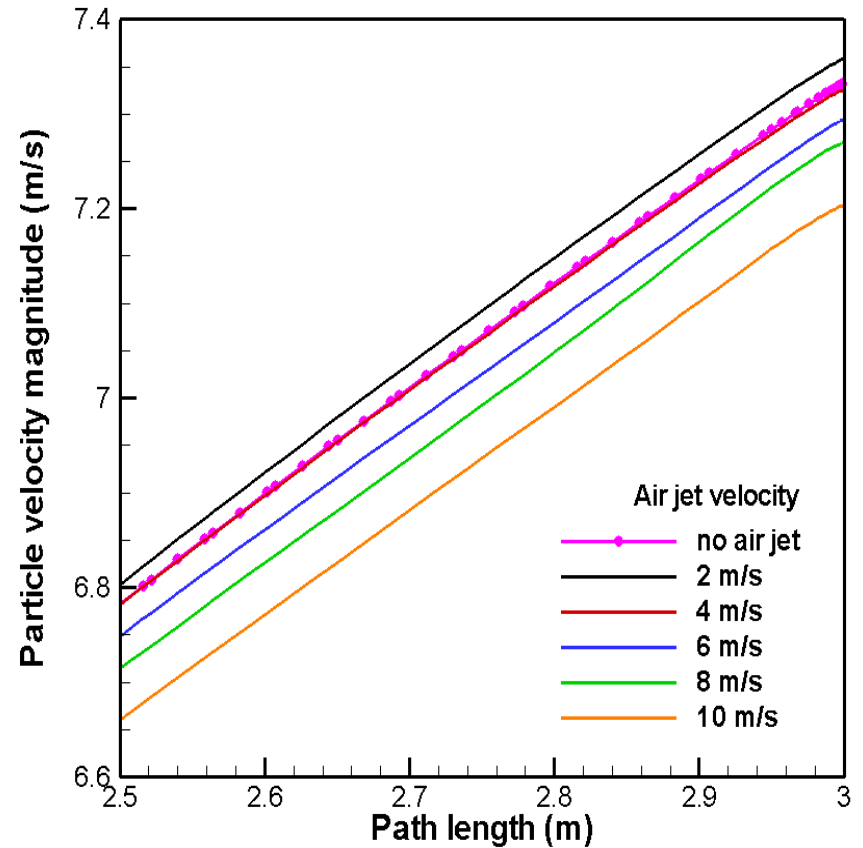
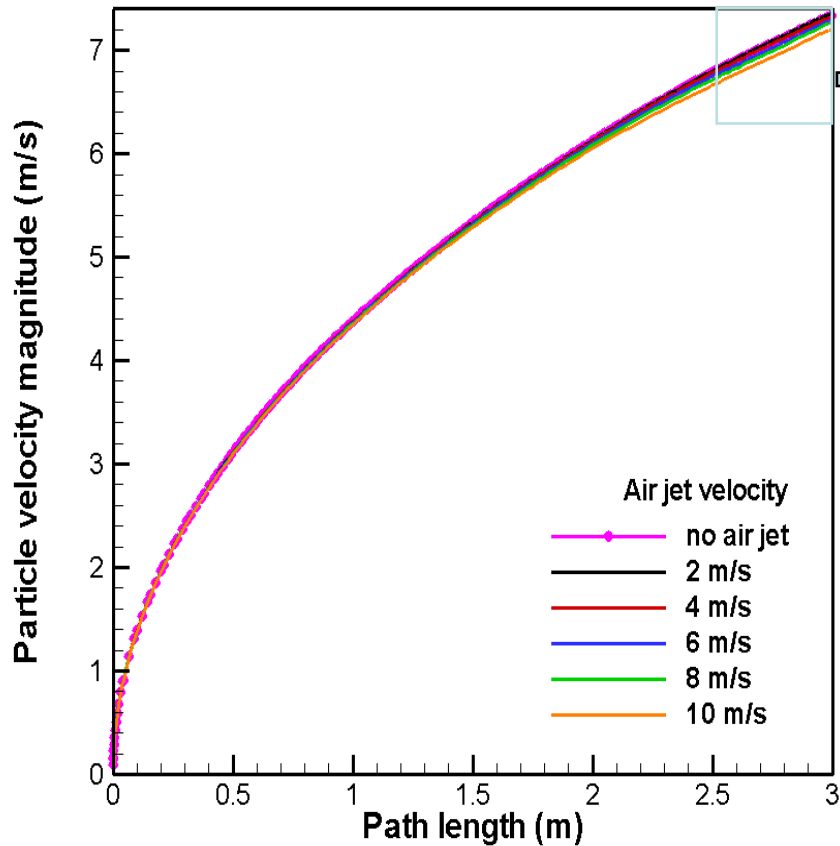
The Effect of Air Jet : 2-D Modeling (Cont.)



Particle temperature as a function of path length for different air jet velocities

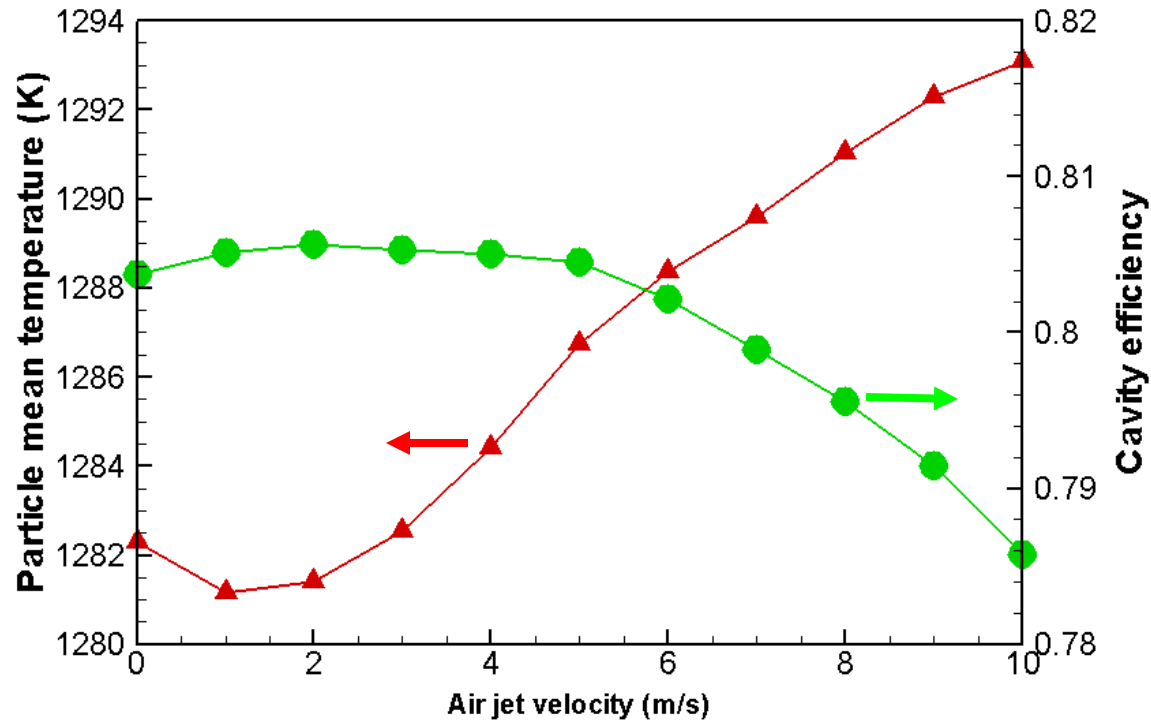
- Particle exit temperature firstly decreases (<2m/s) as air jet velocity increases and then increases (>2 m/s)

The Effect of Air Jet : 2-D Modeling (Cont.)



Particle temperature as a function of path length for different air jet velocities

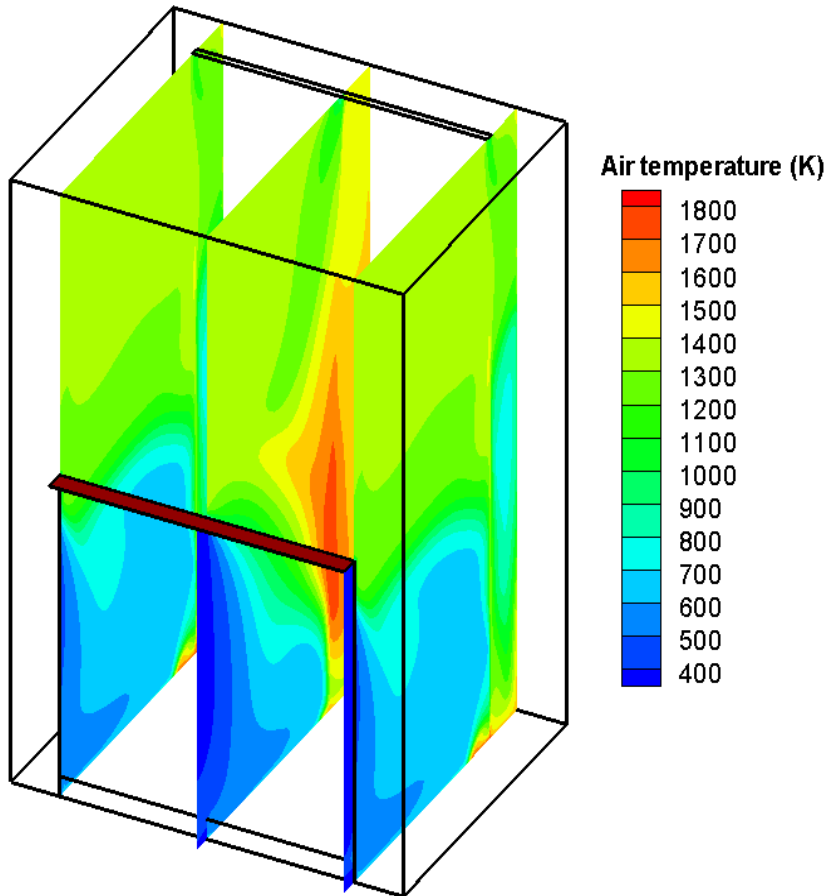
The Effect of Air Jet : 2-D Modeling (Cont.)



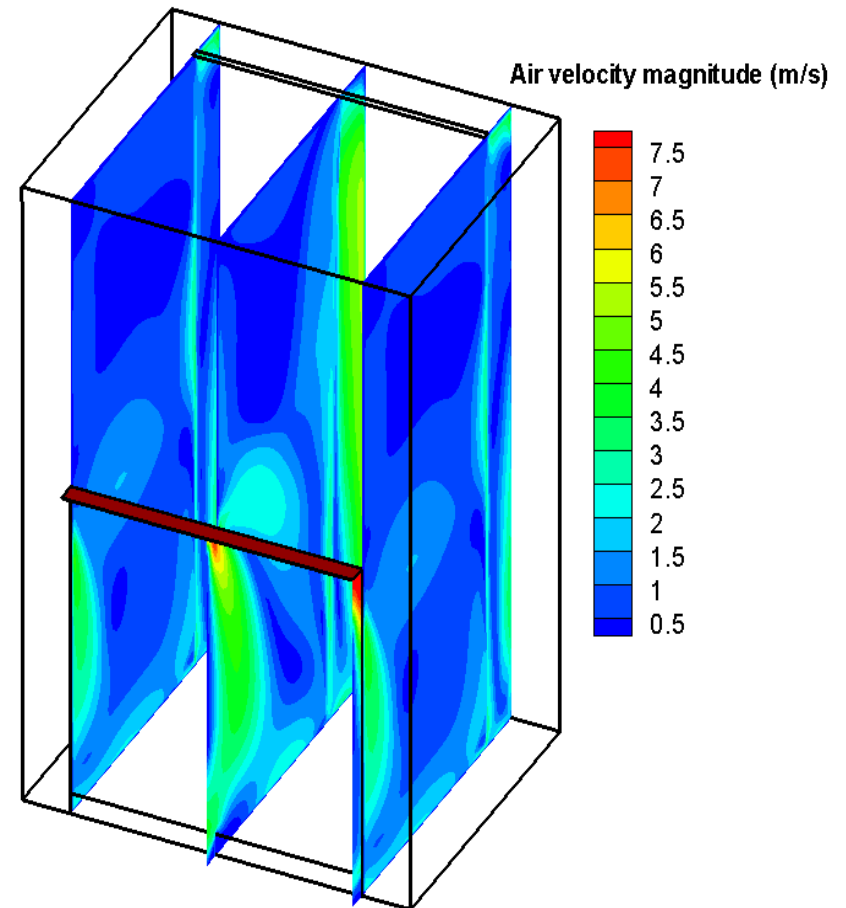
Particle mean exit temperature (left) and cavity efficiency (right) as a function of air jet velocity

- Particle mean exit temperature increases as air jet velocity increases (>2 m/s) while the cavity efficiencies approximately keep as 80%

The Effect of Air Jet (8 m/s): 3-D Modeling

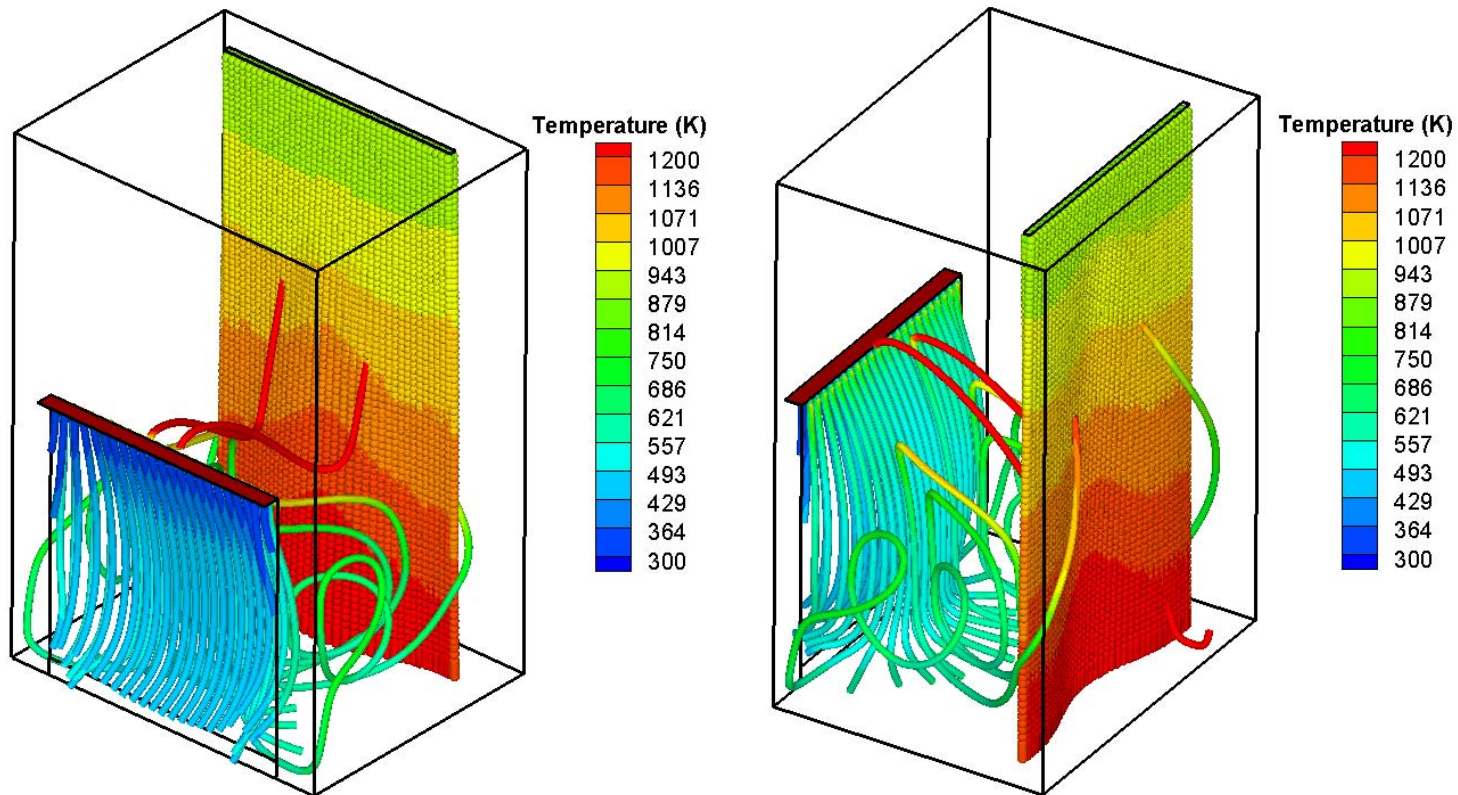


Temperature (K) contour for gas phase



Velocity magnitude (m/s) contour for gas phase

The Effect of Air Jet (8 m/s): 3-D Modeling (Cont.)



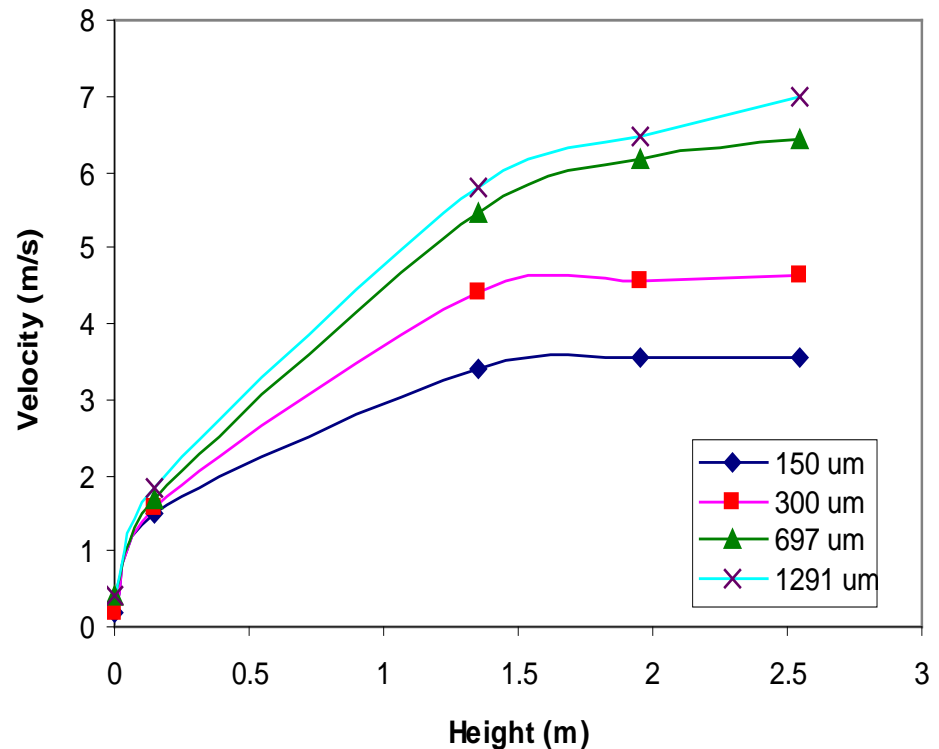
Path lines released from air jet and particle tracks released from inlet on the top. Both of the path lines and particle tracks are colored by temperature (K). Total 400 particles are tracked.

- The average particle temperature is around 1278 K and the cavity efficiency is about 78%

Solid Particle Receiver Cold Flow Testing

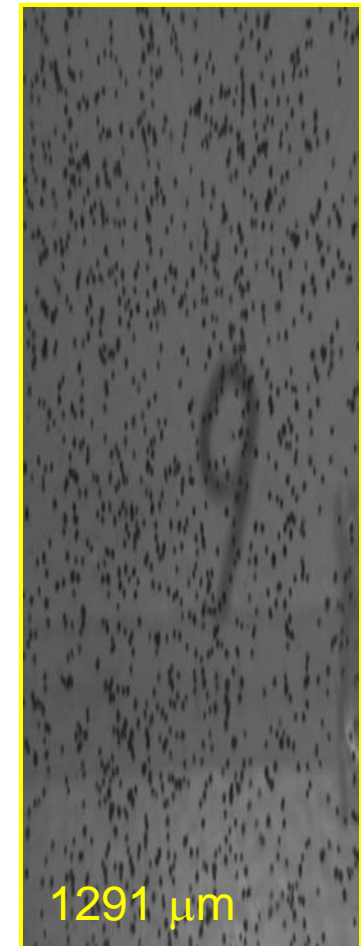
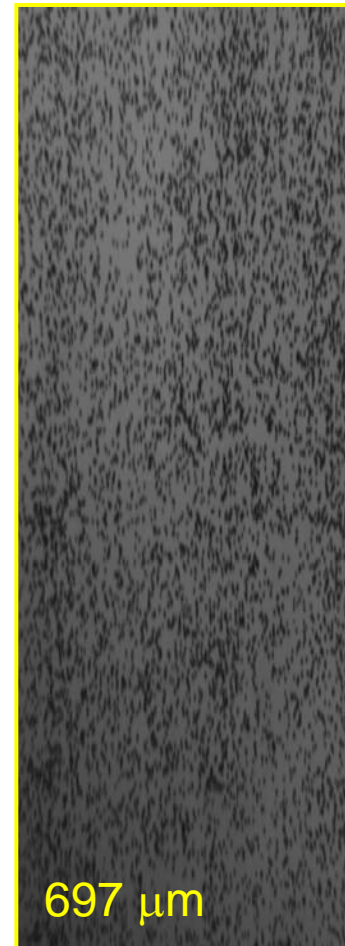
- Images were taken at different positions from the exit of the hopper up to 2.7 m
- A fixed slot opening has been used for different mass flow rates which are dependent on particle size
- Determined velocity distribution for 4 different size particles
- The smaller the particle size, the longer the residence time and better heat transfer rate, but worse flow stability by wind

Experimental data of Falling Velocity



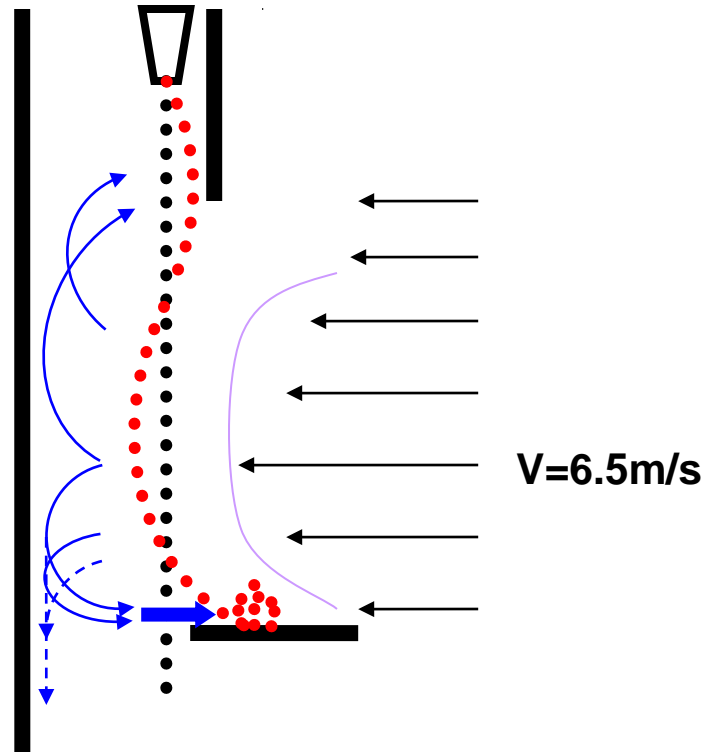
Note that fewer particles were used to extract particle velocities except the case for the particle size of 697 μm

Solid Particle Receiver Cold Flow Testing (Cont.)



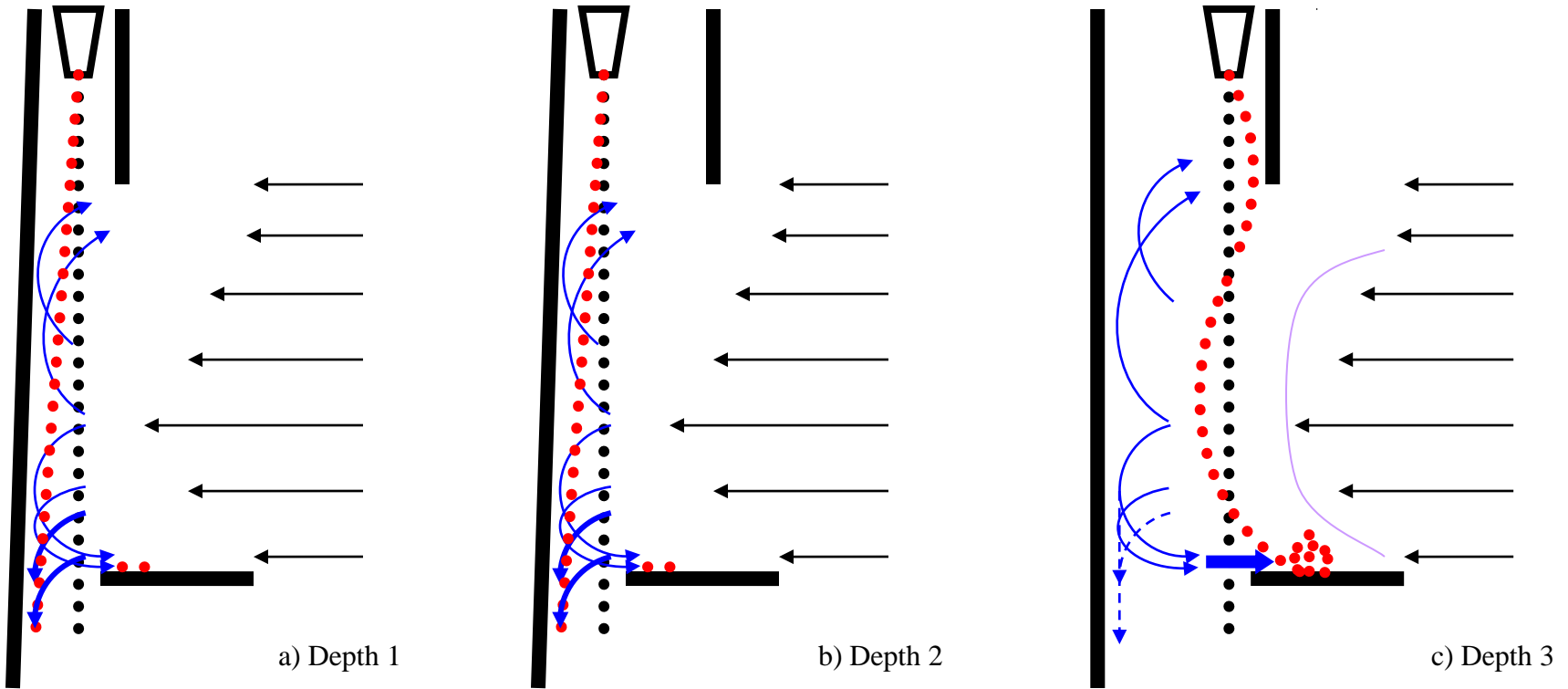
Particle Flow Testing with Ambient Wind

- Wind may affect particle flow stability during receiver operation.
- Qualitative studies indicate that the internal receiver geometry plays an important role.
- Particle loss may occur under extreme conditions.
- A wind-flow straightener was constructed to reduce variability in wind-effects testing



Qualitative results from wind studies. Particle flow path due to wind interaction is shown in red, streamlines in blue.

Wind Enters Perpendicular to the Back Wall (90 degree)



a) Depth 1

b) Depth 2

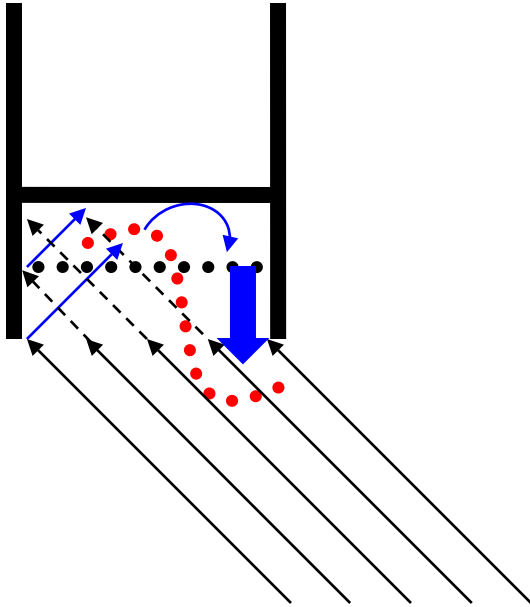
c) Depth 3

Particle Loss (%)

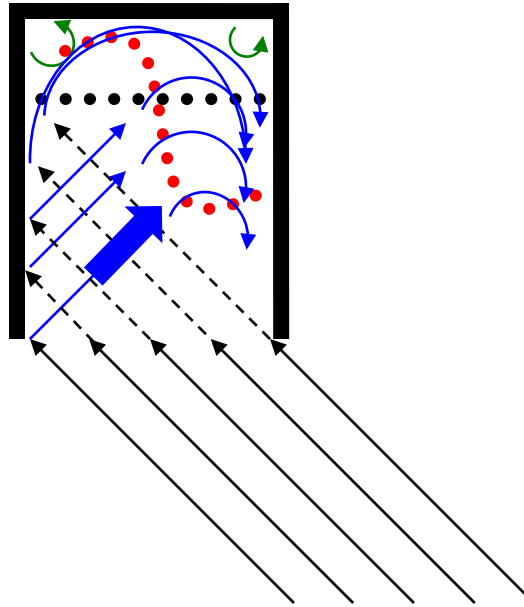
Velocity \ Depth	5.5 m/s	6.5 m/s
Depth 1	-	1.76
Depth 2	1.13	0.77
Depth 3	-	>5

- Compared to the cases a) and b), noticeable amount of particle loss was observed in the case c)
- Lesson?? – To reduce particle loss keep curtain close to back wall

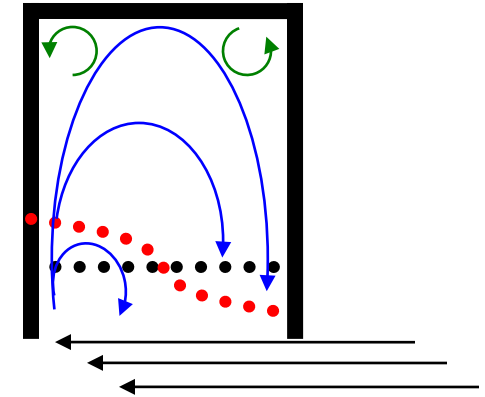
45 degree and Parallel to the Back Wall (0 degree)



a) Depth 1 with 45° angle



b) Depth 2 with 45° angle



c) Depth 3 with 0° angle

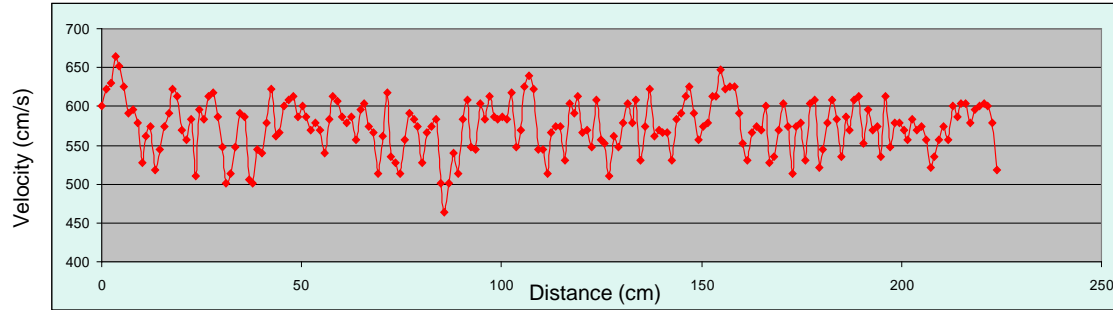
Particle Loss (%) for 45°

Velocity \ Depth	5.5 m/s	6.5 m/s
Depth 1	-	11.5
Depth 2	1.21	1.8
Depth 3	-	>5

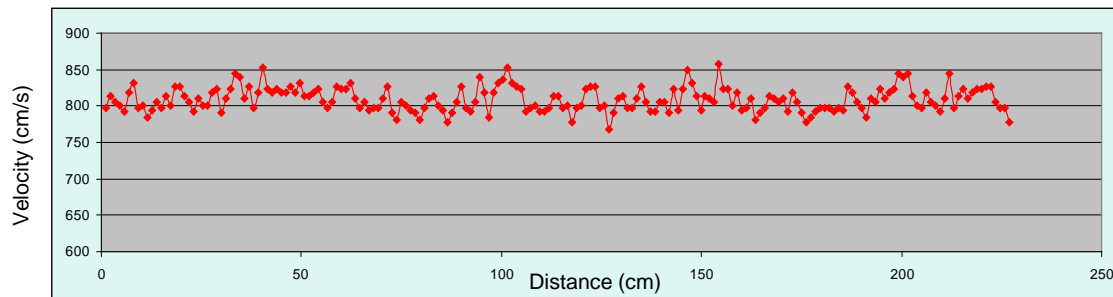
Particle Loss (%) for 0°

Velocity \ Depth	5.5 m/s	6.5 m/s
Depth 1	-	15.33
Depth 2	-	6.02
Depth 3	-	<5

A Wind-flow Straightener was Constructed to Reduce Variability in Wind-effects Testing



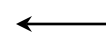
**Without
Straightener
6% Wind
Speed
Variance**



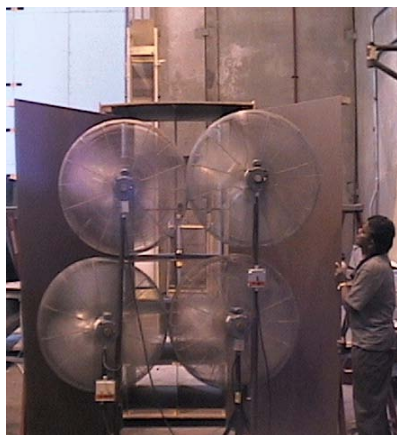
**With
Straightener
2% Wind
Speed
Variance**



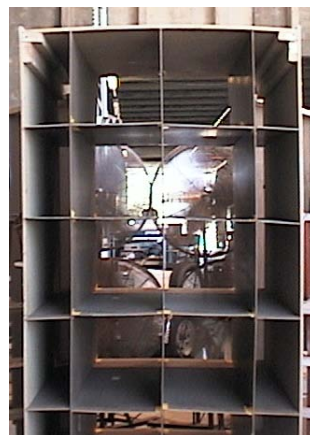
Particle Curtain



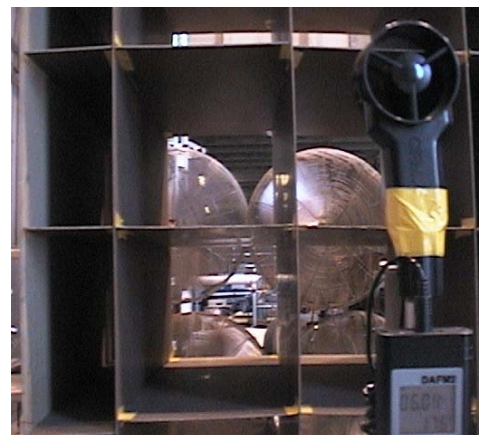
Wind Source



Back



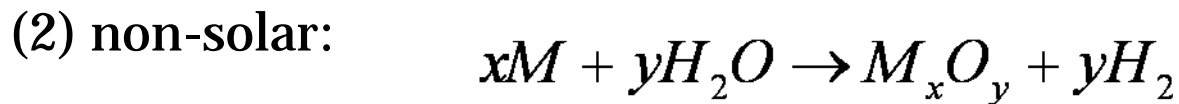
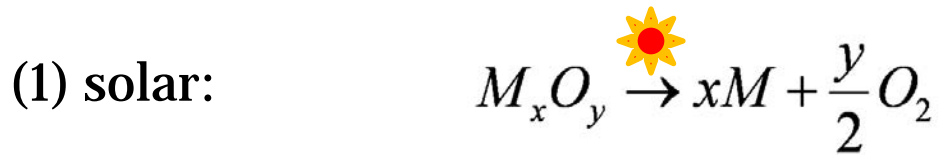
Front



Velocity Measurement

Solar Thermochemical Cycles of Using Metal Oxide

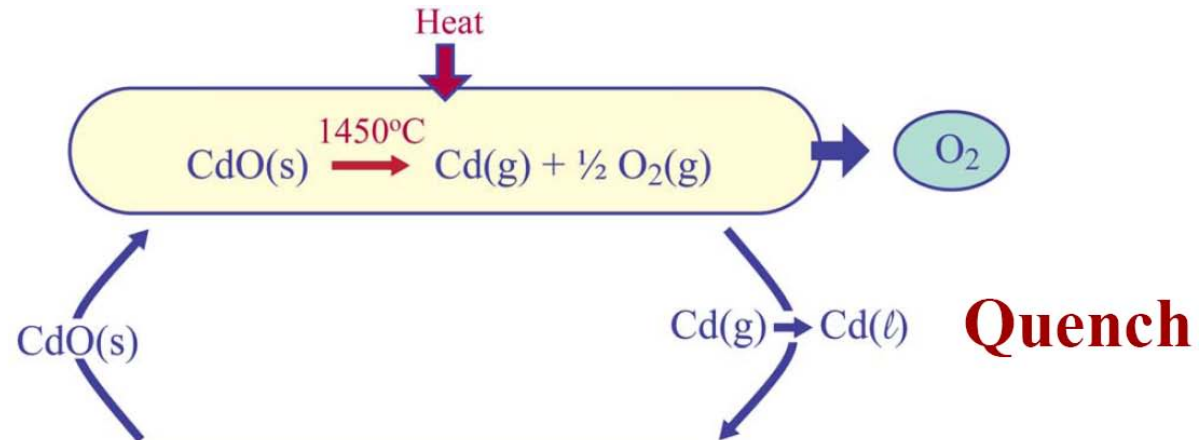
- There exist many multistep thermochemical cycles for splitting water (Norman et al., 1982; O’Keefe et al., 1982; Serpone et al., 1992; Steinfeld et al., 1998; Funk, 2001; and others).
- Two-step thermochemical cycles using metal oxide redox reactions can be expressed as (Bilgen et al., 1977):



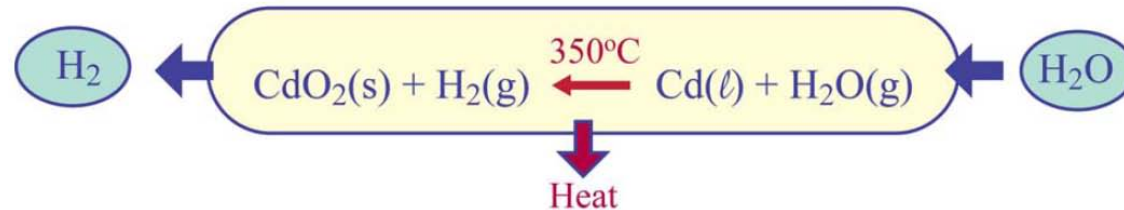
- Equation (1) is an endothermic step, where solar energy decomposes the metal oxide to the metal and oxide.
- Equation (2) is a non-solar, exothermic step, where the hydrolysis of the metal occurs to form hydrogen and the metal oxide.

Cd/CdO Two-step Cycle

Step 1



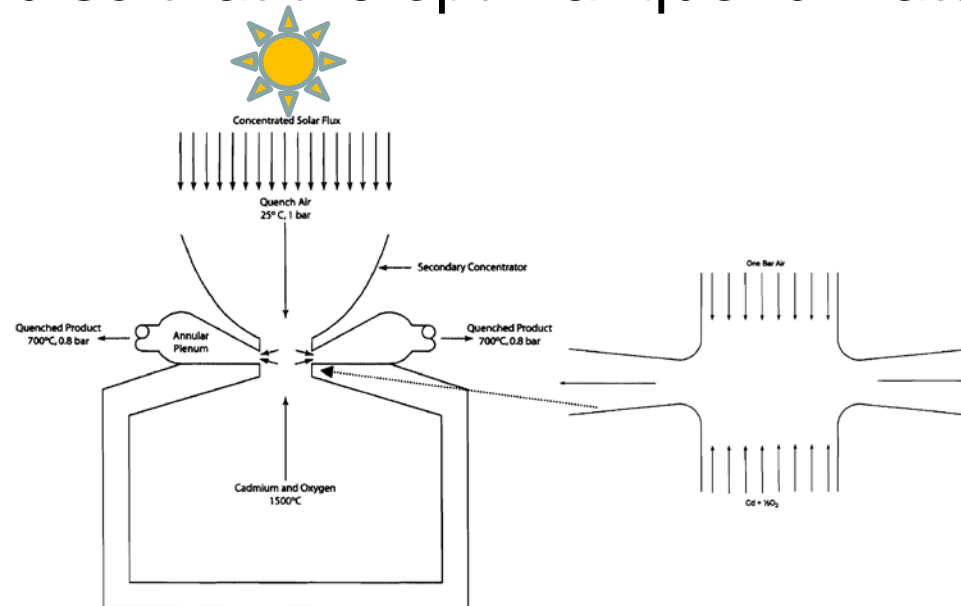
Step 2



- It is necessary to quench the products in order to avoid re-oxidation (Steinfeld et al., 1999).
- In order to effectively guide the design of decomposer and vapor quencher receiver, it is of critical importance to understand the mechanisms of transport phenomena inside them.

CdO Decomposer Conceptual Design

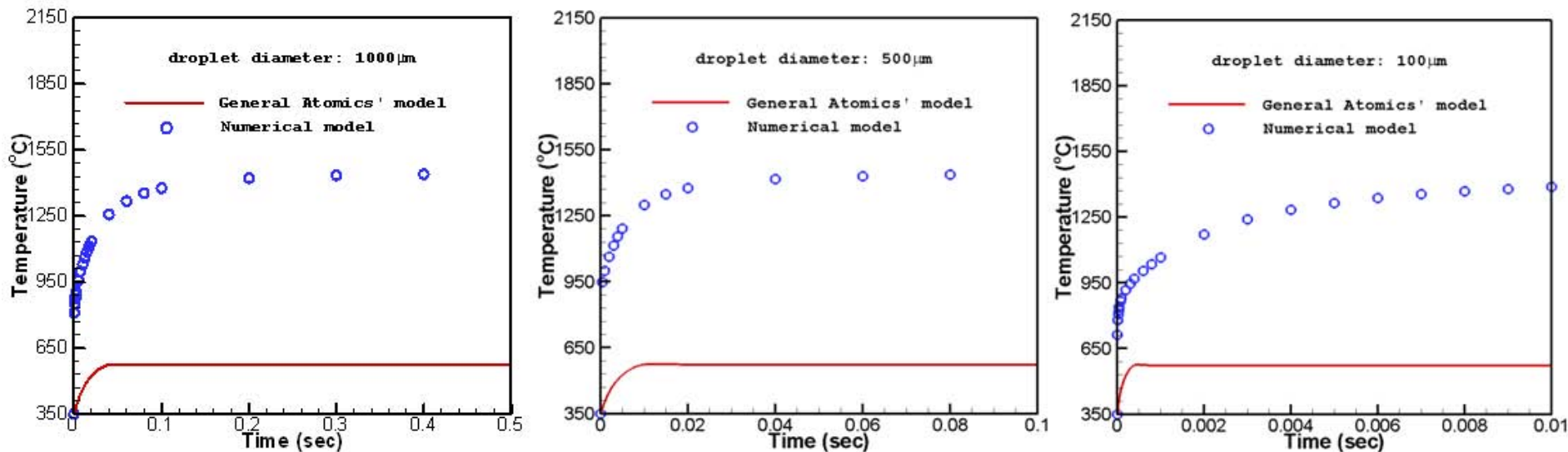
- Very little work (for example, for the cadmium quenching process) has been reported about vapor condensation mechanisms of metal.
- This work was aimed to defining a baseline condensation-quench model for cadmium vapor.
- Effects of various parameters on the quench set up will be investigated so that the optimal quench rate can be determined.



CdO decomposer: windowless (Brown et al., 2007)

Comparison between 2-D Numerical and 1-D Analytical Results

- Change of the average droplet temperature for different droplet sizes

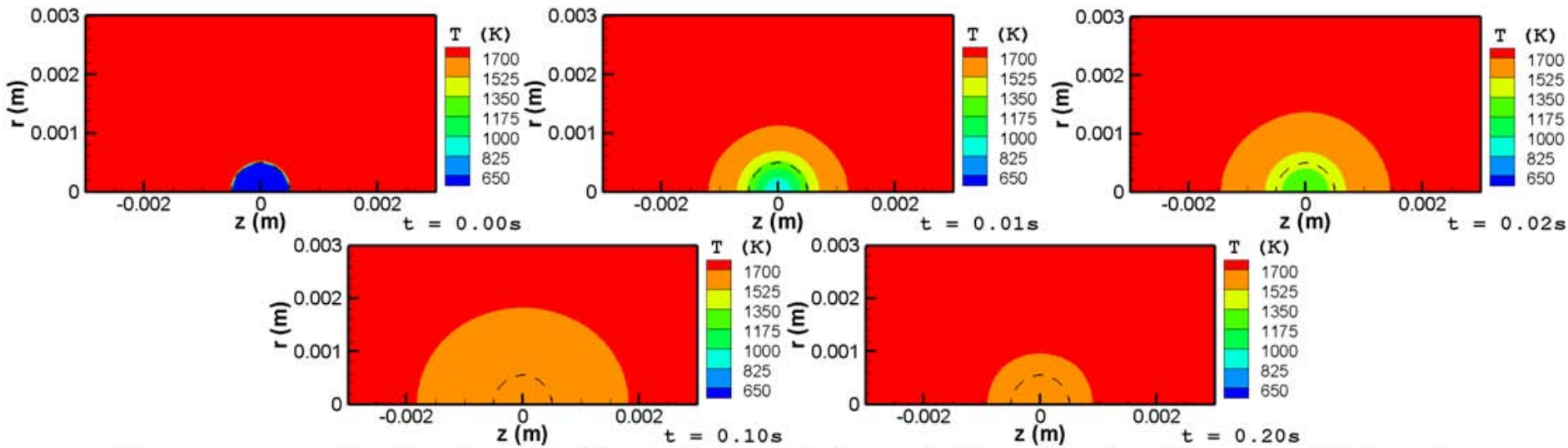


The droplet temperature increases as time increases, and asymptotically approaches the equilibrium temperature. The required time to vaporize decreases as the droplet size becomes smaller.

Numerical Model Assumptions

- The predicted kinetic time to reach the equilibrium temperature from the present model compares very well with the result from the General Atomics' model.
 - Some different parameters and assumptions were used than those in the General Atomics' model.
- (1) the cadmium droplet is immersed in the moving mixture of cadmium vapor and oxygen gas, even though the velocity is very low; and (2) temperature of the mixture of cadmium vapor and oxygen gas, which is 1450°C, does not significantly decrease because of the cadmium droplet.

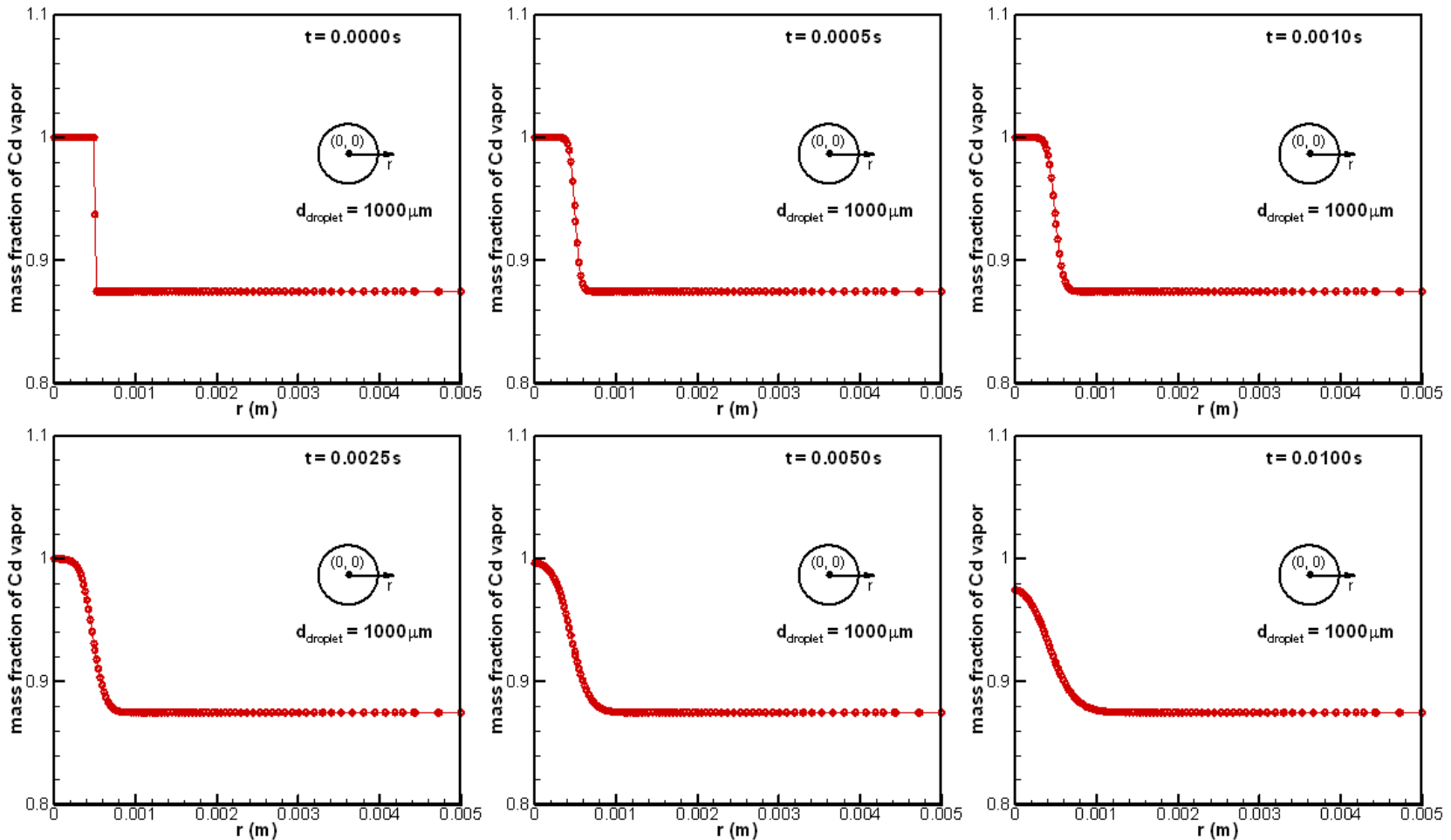
Temperature Distributions and Around the Cadmium Droplet



Temperature distributions inside and around the cadmium droplet ($d_{\text{droplet}} = 1000 \mu\text{m}$)

- It can be seen that temperature inside the “droplet” region does not change very much as t is greater than 0.1 s any more.
- The dashed line represents the domain of the original droplet at $t = 0$ s.

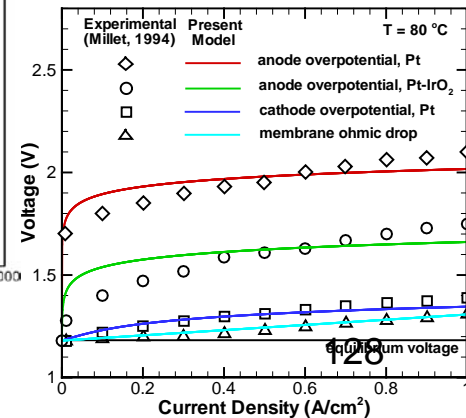
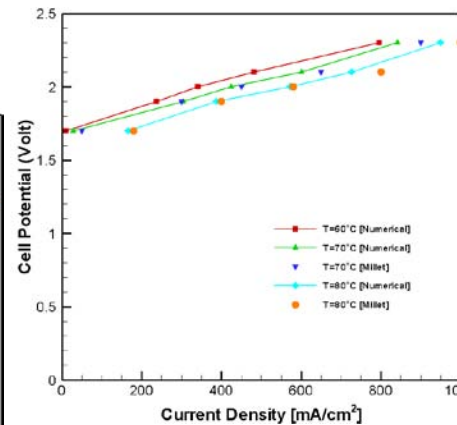
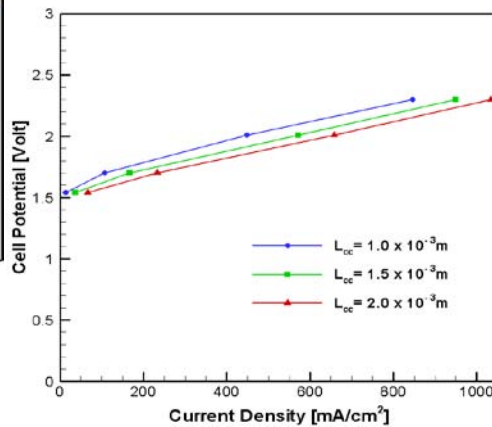
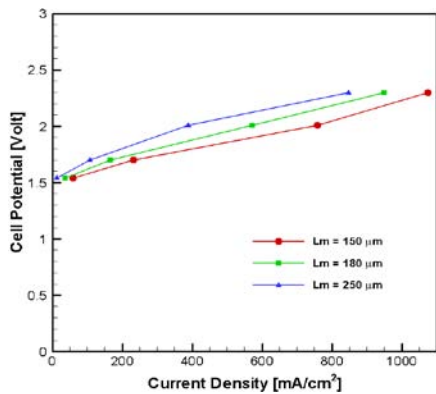
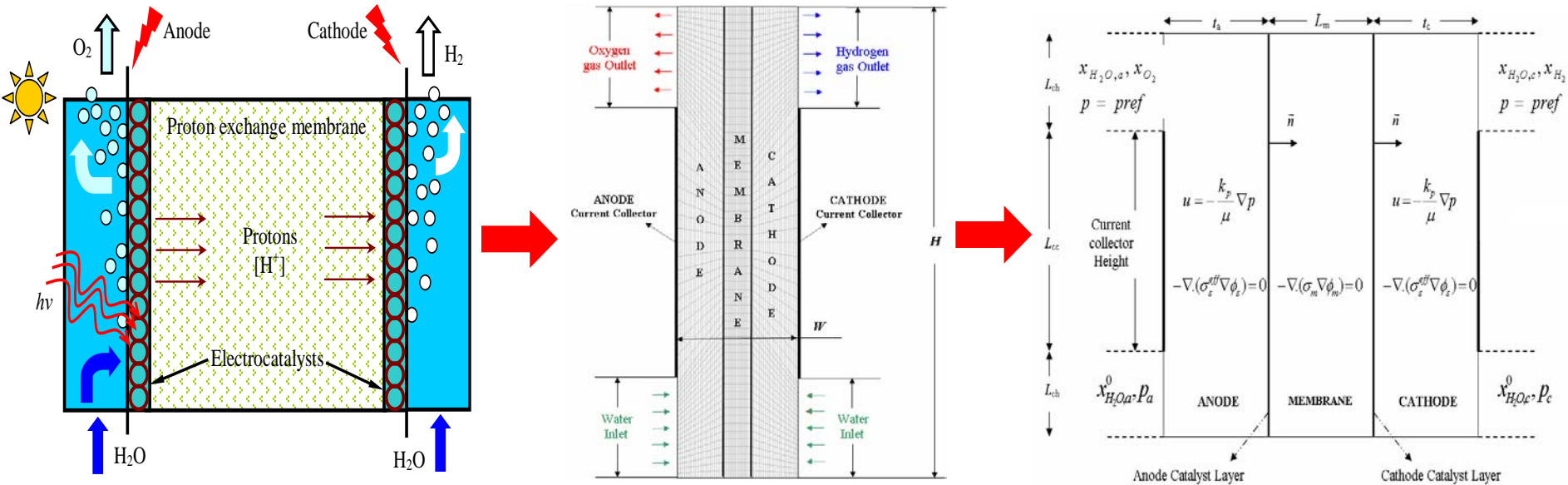
Distribution of Mass Fraction of Cadmium Vapor



Distributions of mass fraction of cadmium vapor

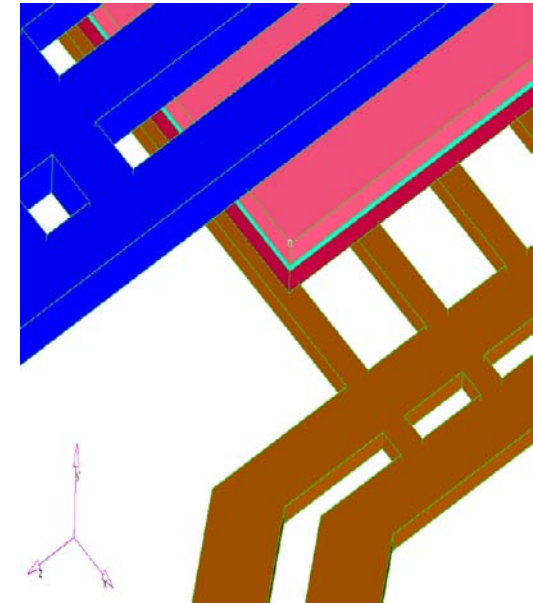
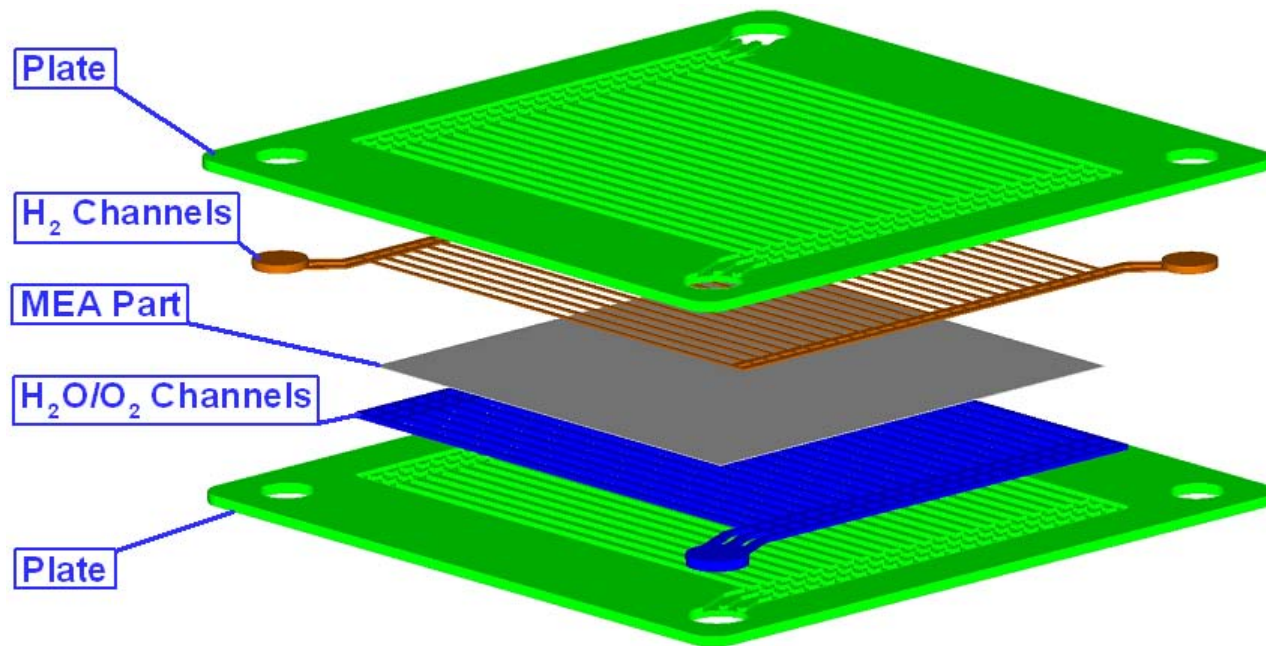
- As time becomes greater, this liquid-vapor zone becomes wider.

Numerical Modeling of PEM Water Electrolyzer



Bipolar Plate Electrolysis Cell

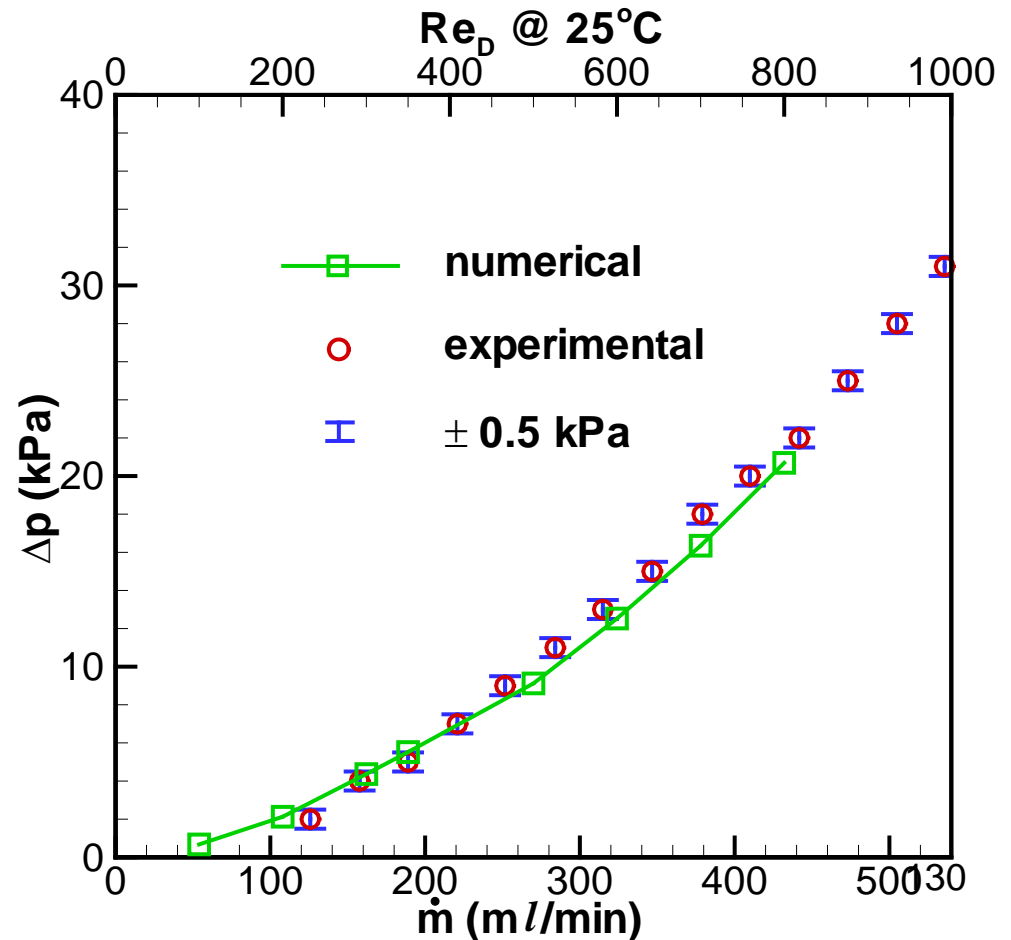
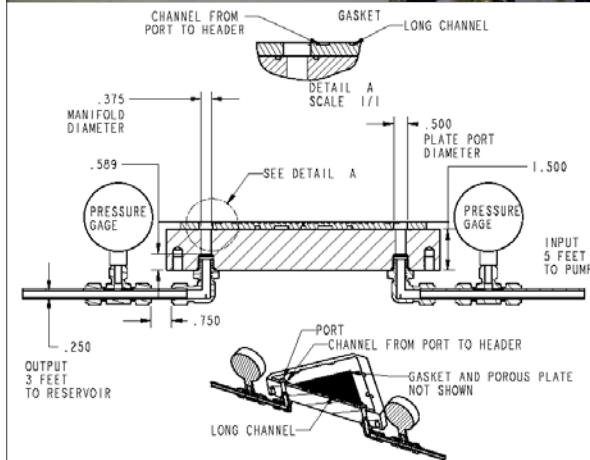
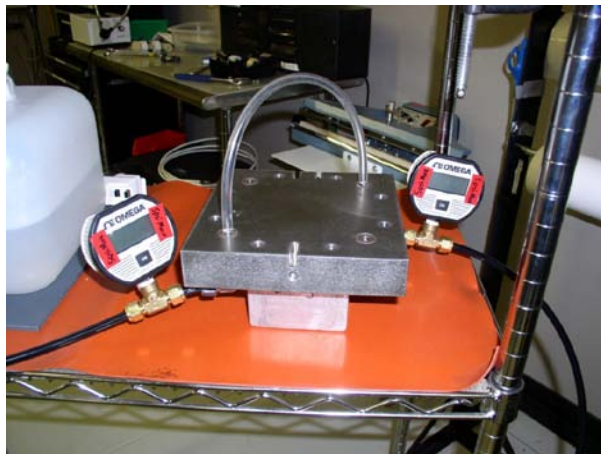
- Bipolar plate is one of the key components in proton exchange membrane (PEM) electrolysis cell
- It functions as reactant supply, current collector and mechanical support to MEA.



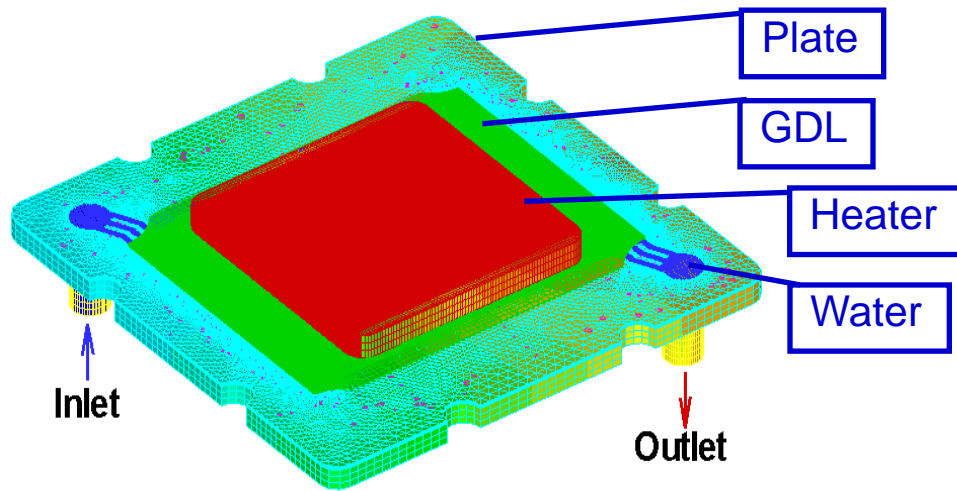
- Objective: uniform/homogenous flow

Code Validation: Fluid Dynamics

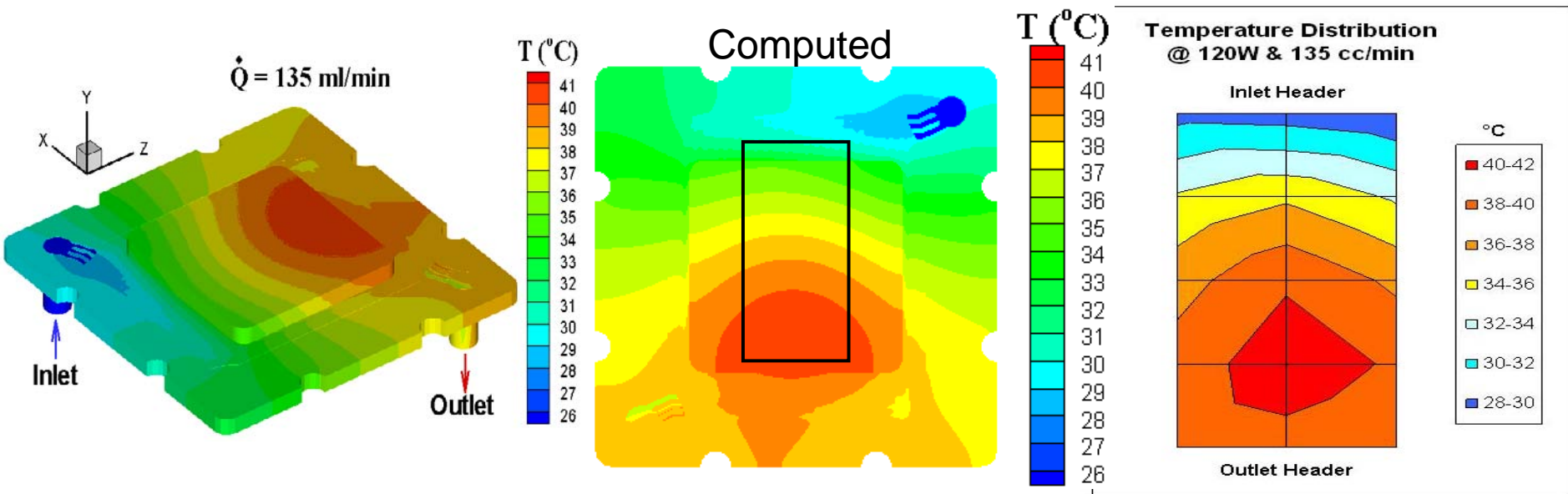
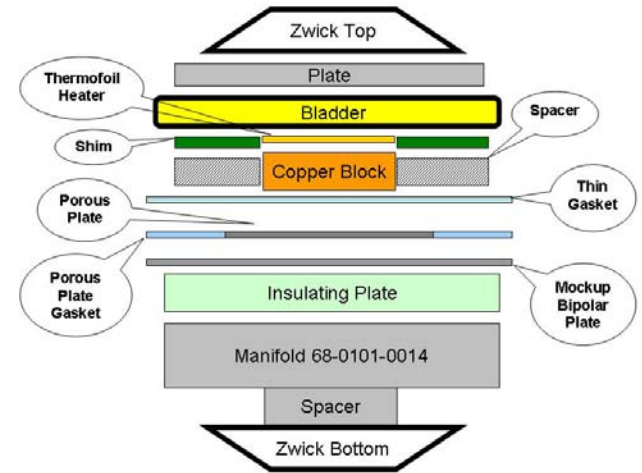
- 1,360,000 elements are used through 10 sets of grids
- Computed pressure drops agree very well with measurements



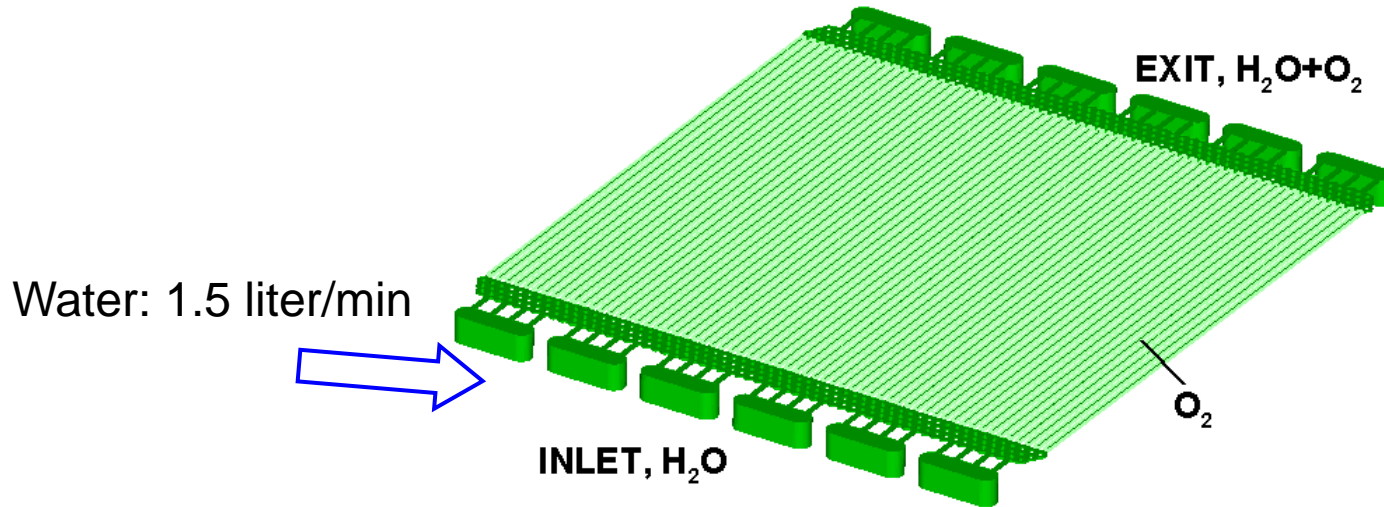
Code Validation: Coupled Heat Transfer



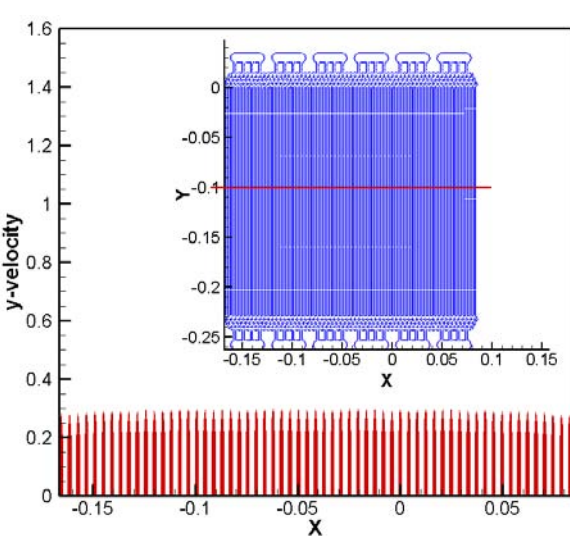
Temperature Testing Fixture Configuration



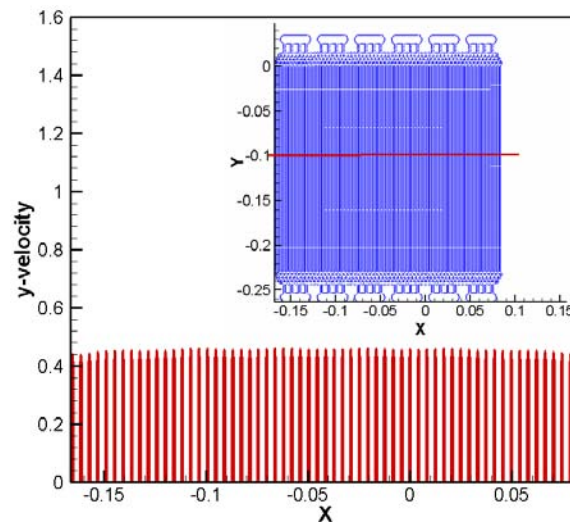
Channel Velocity Distributions for Two-phase Flow



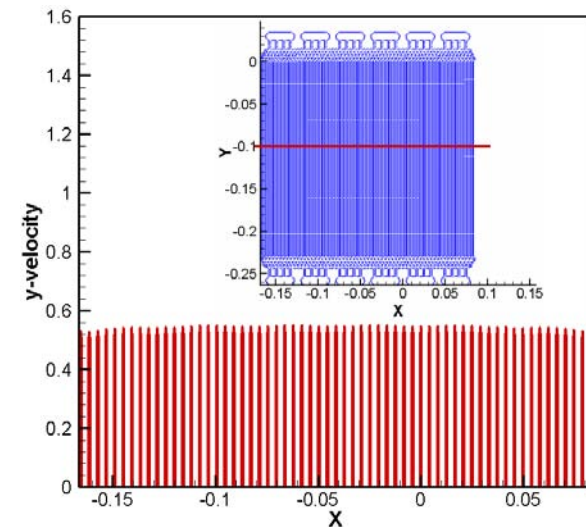
UNIFORM



Oxygen: 0 g/s

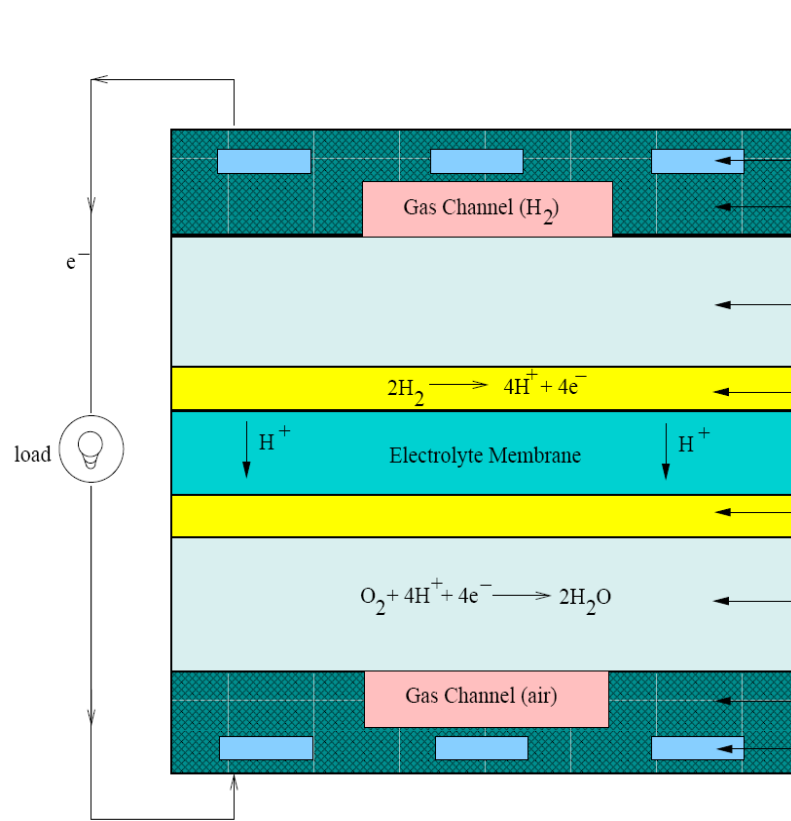


Oxygen: 0.060 g/s

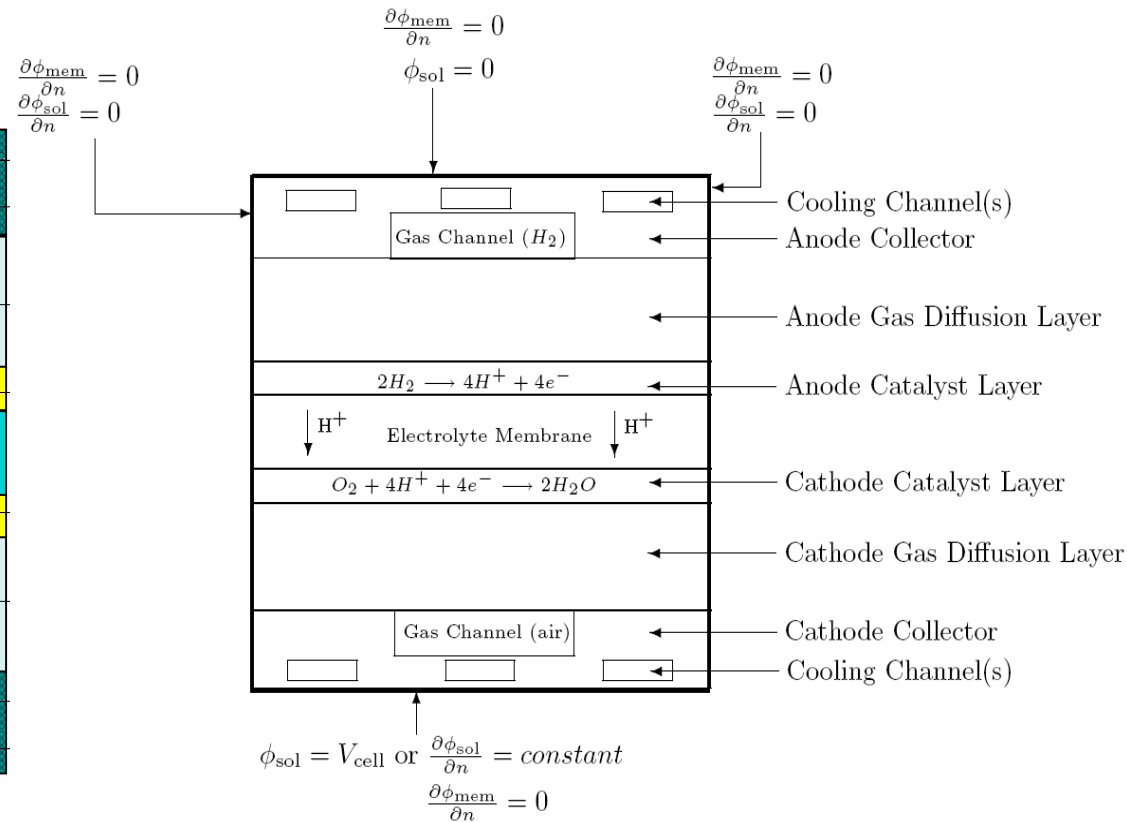


Oxygen: 0.086 g/s

Electrochemistry Modeling for PEM Fuel Cell

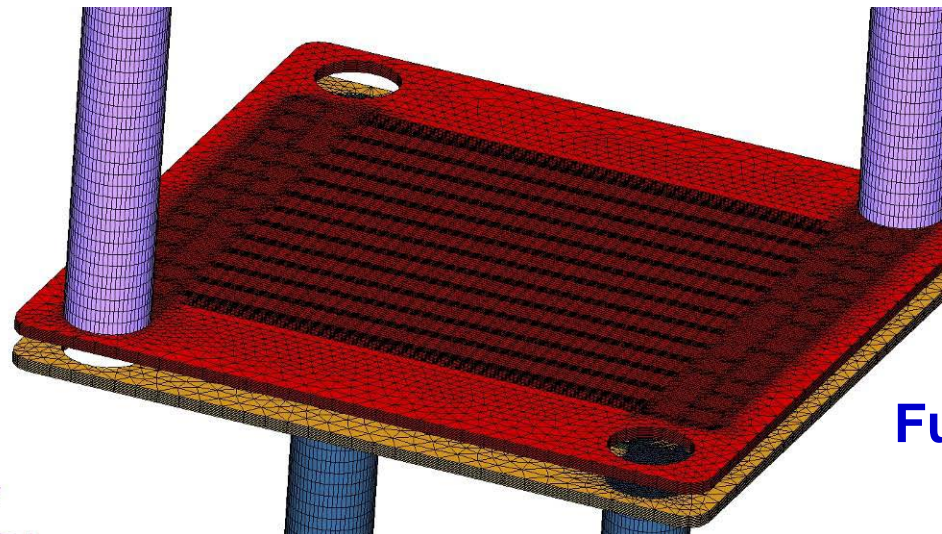
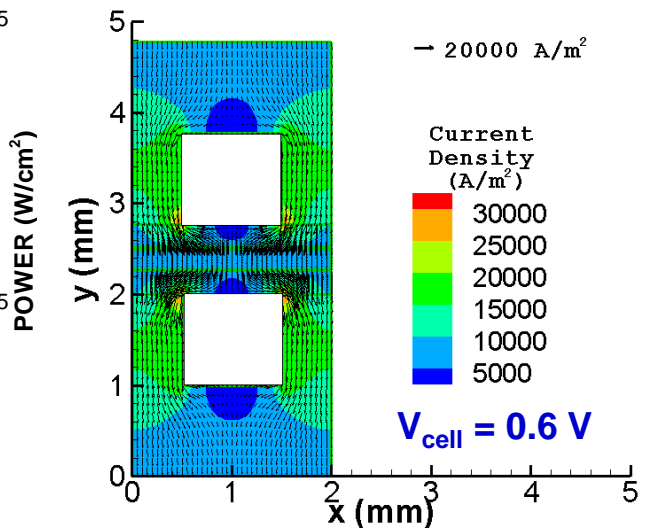
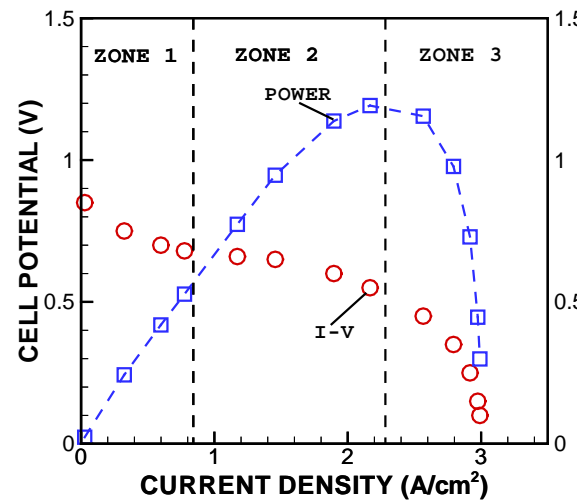
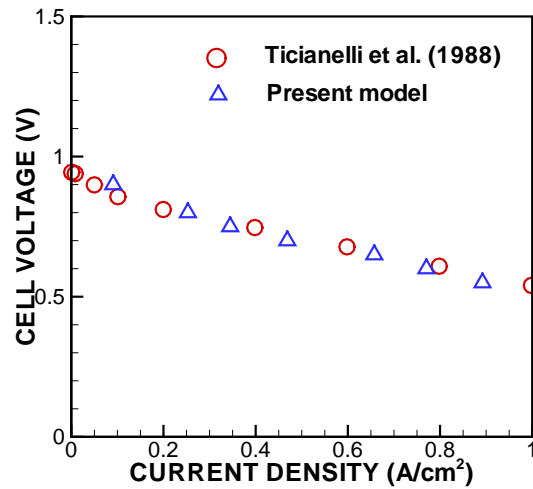


PEM fuel cell model



Boundary conditions

PEM Fuel Cells: Validations



Fuel cell with new design

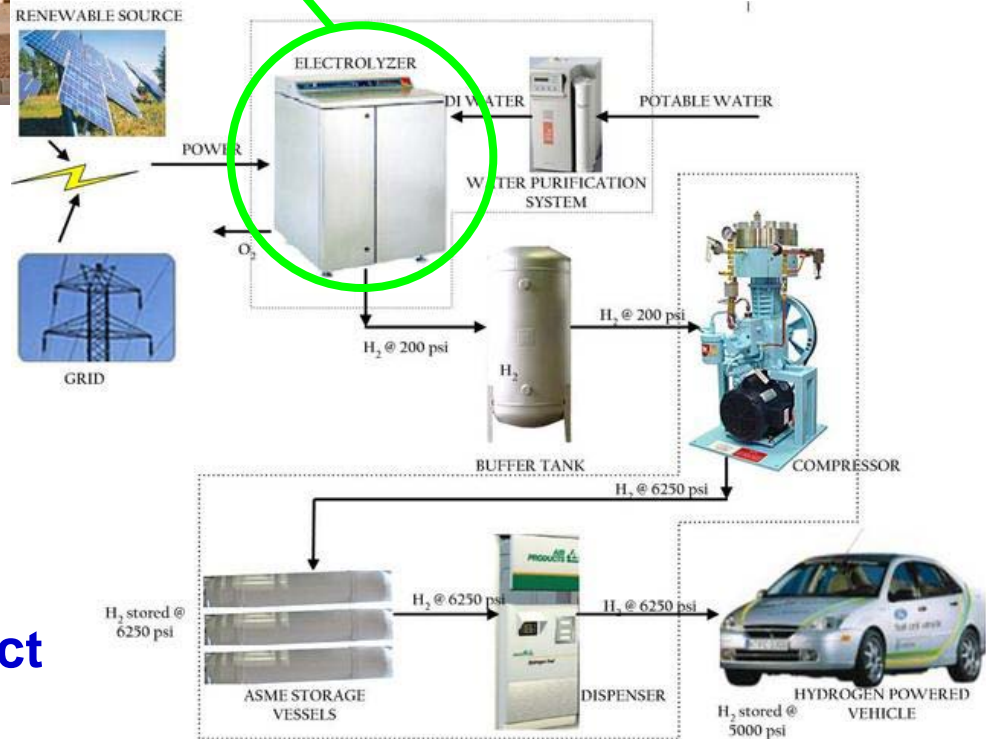
Hydrogen Filling Station



Electrolysis cell stack

Sponsor:
Department of Energy

Participants:
UNLV
Proton Energy Systems
(now, Distributed Energy)
Air Products Inc.
Las Vegas Valley Water District



Database Management

SOLAR HYDROGEN GENERATION RESEARCH

- Sponsored by Department of Energy -

UNLV

[Home](#) | [About Us](#) | [Projects](#) | [Contact Us](#) | [Reports](#) | [Partners/Links](#) |

 Search

Friday, April 27, 2007

...: Home ...

[Register](#) [Login](#)

Welcome to SHGR project home page

The Solar Hydrogen Generation Research (SHGR) project, led by the University of Nevada Las Vegas Research Foundation, will define economically feasible concepts for solar-powered production of hydrogen from water, consistent with the cost and schedule goals outlined by the Department of Energy (DOE). The SHGR project integrates efforts that cross the program boundaries of two Department of Energy activities: the Hydrogen Fuel Cells and Infrastructure Technology Program (HFCIT) responsible for research and development of hydrogen production technologies and the Solar Energy Technology Program (SET) responsible for collection and utilization of solar thermal and photolytic energy.



Quick Links

[Google](#)

[University of Nevada, Las Vegas \(UNLV\)](#)



Announcements

**Annual Review Meeting -
Friday, March 31, 2006**

Annual SHGR review meeting
will be held in Washington
DC in May 06.

[URL: http://shgr.unlv.edu](http://shgr.unlv.edu)

Database Management (Cont.)

SOLAR HYDROGEN GENERATION RESEARCH
- Sponsored by Department of Energy -

UNLV

Home | About Us | Projects | Contact Us | Reports | Tools | Partners/Links | Search

Thursday, April 26, 2007

SHGR_Member Logout

Welcome to SHGR project home page

The Solar Hydrogen Generation Research (SHGR) project, led by the University of Nevada Research Foundation, will define economically feasible concepts for solar-powered production of hydrogen from water, consistent with the cost and schedule goals outlined by the Department of Energy (DOE). The SHGR project integrates efforts that cross the program boundaries of two Department of Energy activities: the Hydrogen Fuel Cells and Infrastructure Technology Program (HFCIT) responsible for research and development of hydrogen production technologies and the Solar Energy Technology Program (SET) responsible for collection and utilization of solar thermal and photolytic energy.

- Automatic scoring system,
- Cycle information search
- Experimental data

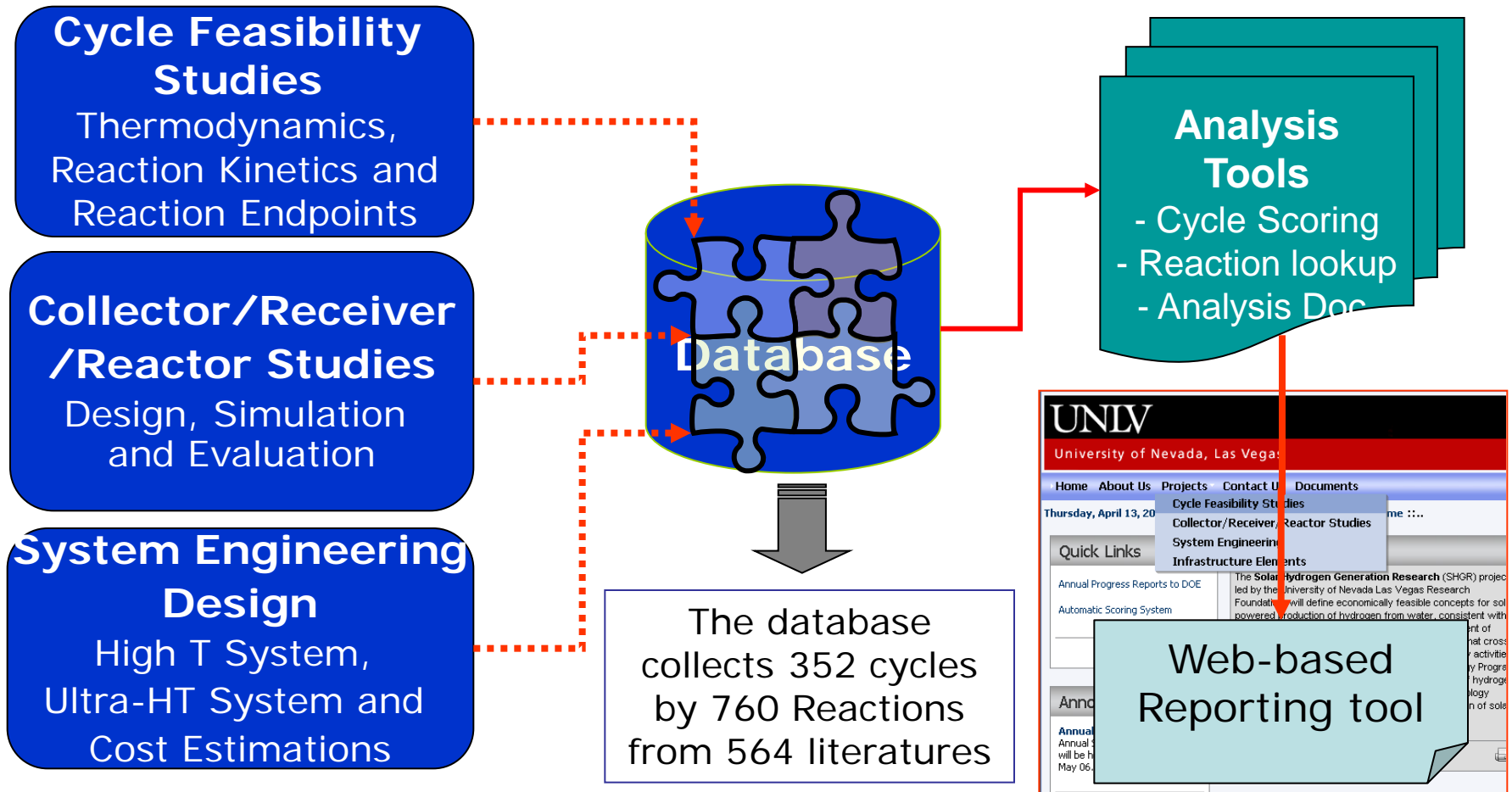
Thermochemical Cycle Scoring
Cycle Search
Experimental Data
Edit Experimental Data
Upload Experimental Data

University of Nevada, Las Vegas (UNLV)

Announcements

Annual Review Meeting - Friday, March 31, 2006
Annual SHGR review meeting will be held in Washington DC in May 06.

Management System Layout



Barriers to Nuclear Thermochemical Water-splitting and Research Opportunities

• **BARRIERS**

Reactor

- Public antipathy to nuclear energy
- Development and demonstration of MHR is needed
 - Demonstrate cost and performance
 - Mitigate investment risk

S-I Process

- Demonstration of S-I cycle
 - Demonstrate cost and performance

System economics

- Fossil fuels with no environmental costs dominate the market

• **OPPORTUNITIES**

- Study of public perceptions and public education

- Development and demonstration

- Fuel fabrication and testing
- Detailed reactor design
- Construction of a Demo plant

- S-I Process validation

- Measure chemical data
- Demonstrate process
- Verify materials

- Study cost/value of CO₂ Cap&Seq

- Can sustainable sources of H₂ compete? When?

Barriers to Solar Thermochemical Water-splitting and Research Opportunities

• **BARRIERS**

Solar collector

– Need low cost & high efficiency

- High collection efficiency
- High energy retention
- Low maintenance, high reliability

Process

– Need solar-matched process

- High temperature/efficiency
- Match to solar receiver geometry?
- Diurnal accommodation
- Demonstrate cost and performance

System economics

– Economics of high temperature solar are challenging

• **OPPORTUNITIES**

– **Develop efficient, effective collectors**

- Selective filters, tailored emissivities
- “Smart” systems for alignment
- Value engineering of system

– **Process selection and validation**

- Identify and select solar-matched cycle
- Measure chemical data
- Demonstrate process
- Verify materials

– **Study system economics**

- Can renewable sources of H₂ compete? When?

Questions?



Thank You